AD-A050 563 NAVAL RESEARCH LAB WASHINGTON D C F/G 20/1
THEORETICAL MODELS AND NUMERICAL ESTIMATES OF ACOUSTIC SIGNALS --ETC(U)
DEC 77 S HANISH
UNCLASSIFIED NRL-8150 SBIE-AD-E000 111 NL

1 OF 1
AD
A050563

END
DATE
FILMED
4-78
DDC

[illegible] Models and Numerical Estimates of Acoustic Signals of High-Energy Cosmic Particles in the Ocean

[illegible] 15, 1977

SECURITY CLASSIFICATION OF THIS PAGE (When Data Entered)

REPORT DOCUMENTATION PAGE

READ INSTRUCTIONS BEFORE COMPLETING FORM

1. REPORT NUMBER: NRL Report 8150	2. GOVT ACCESSION NO.
3. RECIPIENT'S CATALOG NUMBER	
4. TITLE (and Subtitle): THEORETICAL MODELS AND NUMERICAL ESTIMATES OF ACOUSTIC SIGNALS OF HIGH-ENERGY COSMIC PARTICLES IN THE OCEAN.	5. TYPE OF REPORT & PERIOD COVERED: Survey report.
	6. PERFORMING ORG. REPORT NUMBER
7. AUTHOR(s): Dr. Sam Hanish	8. CONTRACT OR GRANT NUMBER(s)
9. PERFORMING ORGANIZATION NAME AND ADDRESS: Naval Research Laboratory, Washington, D.C. 20375	10. PROGRAM ELEMENT, PROJECT, TASK AREA & WORK UNIT NUMBERS: None
11. CONTROLLING OFFICE NAME AND ADDRESS: Office of Naval Research, Arlington, Va. 22217	12. REPORT DATE: 15 December 1977
	13. NUMBER OF PAGES: 83 (12) 83 p.
14. MONITORING AGENCY NAME & ADDRESS (if different from Controlling Office): (16) SBIE (19) AD-E000 111	15. SECURITY CLASS. (of this report): Unclassified
	15a. DECLASSIFICATION/DOWNGRADING SCHEDULE

16. DISTRIBUTION STATEMENT (of this Report)

Approved for public release; distribution unlimited

DDC RECEIVED MAR 1 1978 B

17. DISTRIBUTION STATEMENT (of the abstract entered in Block 20, if different from Report)

18. SUPPLEMENTARY NOTES

19. KEY WORDS (Continue on reverse side if necessary and identify by block number)

Heat sources of sound; spot, bubble, explosion and diffusion models of cosmic particles are heat sources in liquids; numerical predictions of acoustic noise generated by muons and neutrinos in the ocean.

20. ABSTRACT (Continue on reverse side if necessary and identify by block number)

The generation of acoustic noise by deceleration of high-energy elementary particles in liquids has been documented in several publications by various groups of physicists, who have also provided tentative models for understanding and prediction. In this report several theoretical models are re-derived, assembled, and compared, and further development is undertaken on a selected few. Numerical calculations are made in the specific cases of muons and neutrinos and conclusions are drawn as to the conditions under which the noise of cosmic particles in the ocean can be detected by hydrophones.

DD FORM 1 JAN 73 1473 EDITION OF 1 NOV 65 IS OBSOLETE
S/N 0102-LF-014-6601

SECURITY CLASSIFICATION OF THIS PAGE (When Data Entered)

251 950 JCB

CONTENTS

PREFACE

In a summer 1976 workshop at the University of Hawaii an international group met under the auspices of the Deep Underwater Muon and Neutrino Detection Committee (DUMAND) to discuss the detection of cosmic particles and their interaction byproducts by listening through hydrophones to the noises they make in the ocean. A full proceedings of their work was published in early 1977 (cited as Ref. 1 in this report). Of particular interest were the conclusions of the Acoustics Panel, which examined the acoustic aspects of DUMAND and developed several acoustic models to serve as prediction tools. Although the models are accessible to advanced students of acoustics theory, they were not given in sufficient detail to allow appreciation of their content. The purpose of this survey report is to place the models in perspective by showing their origin, derivation, and limits of validity.

The conclusions of the DUMAND Acoustics Panel covered many features of the acoustic problem. Points most pertinent to this survey are briefly as follows:

- The cosmic particle deposits energy in the ocean as it decelerates. The spatial distribution of this energy along the path of the resultant conical cascade is roughly Gaussian. The length of track varies from 1 to 10 m, depending on the energy E_0 of the incoming particle and on the nature of the cascade. For hadronic (massive-particle) plus electromagnetic showers the full width at half maximum (FWHM) of the Gaussian distribution in the direction of the shower is about 3.8 m at $10^{12} eV$ to 6.4 m at 10^{16} eV. The lateral distribution (across the shower) is not specified but is expected to be similar to purely electromagnetic cascades. For purely electromagnetic cascades the FWHM is 3.2 m at $10^{12} eV$ to 4.5 m at 10^{16} eV. In the cross section the fraction (F_E) of total energy deposition between r ($r = 0$ is the axis of the cascade) and r_1 (Moliere length, which equals 10 cm in deep sea) is $F_E \simeq 2.5\ r/r_1$ if $r << r_1$.

- The ambient noise in the ocean is a minimum at 25 kHz, making it a good choice for a listening frequency. At 25 kHz the ambient noise power (in SI units) is proportional to $(10\ \mu N/m^2)^2$ in a 1-Hz band. Since a bandwidth of some 10 kHz is needed to resolve the expected transients due to the acoustic pulses of the cosmic particles, the noise power in the receiver is at best proportional to $(10\mu N/m^2)^2 10^4$, so that the noise pressure spectrum level is $\sqrt{(10\mu N/m)^2 10^4} = 10^{-3}(N/m^2) = 10^{-2}(\text{dyne/cm}^2)$. This is taken as the lowest DUMAND signal that can be detected in the band 15 to 25 kHz say.

- The mass of ocean water required to detect neutrinos must be very large because of the extremely small scattering cross section of neutrinos. It is estimated that a volume of 10 by 10 by 1 km^3 is needed to detect 100 neutrino related events per day, each event having an energy averaged over many of 10^{13} eV. The number of hydrophones needed to make this detection over the prescribed volume is estimated at 10^5.

One gathers from the DUMAND report that further progress in the prediction of noise pulses from the deceleration of high-energy particles in the ocean must await more detailed experimental data, specially designed to display the impulse nature of the physical event and give reasonable estimates of time duration and magnitude of heat generation. Although it has been verified in the laboratory that high energy particles do make noise when they are decelerated in liquids, the lack of good experimental data precludes any decision on which model is most nearly correct.

THEORETICAL MODELS AND NUMERICAL ESTIMATES OF ACOUSTIC SIGNALS OF HIGH-ENERGY COSMIC PARTICLES IN THE OCEAN

EXECUTIVE SUMMARY

High-energy physicists in the field of cosmic rays are faced with a difficult problem that is blocking advance. They wish to clarify their understanding of the universe by probing into the origin of neutrinos which reach the earth from outer space. In particular they wish to construct a *neutrino telescope* that will pinpoint the angular distribution of these particles in the heavens, and chart their temporal and spatial fluctuations. To date they have been unable to do this in any practical way, because the scattering cross sections of neutrinos are extremely small, even at high energies. Groups of scientists interested in this problem have assembled themselves into a committee with the name DUMAND (Deep Underwater Muon and Neutrino Detection) and have met in the last few years at annual intervals to discuss advances toward solution of their problem. The most recent meeting was at the U. of Hawaii, in the Summer of 1976. They conclude the following in their report: immense masses of matter will be needed to detect these muons and neutrinos at some usable (practical) rate, say a few tens or hundreds of events per day. This mass must essentially be free to all at no cost. Clearly the only practical resort to get great mass is the ocean. Hence they visualize the neutrino telescope to be an underwater detector. Furthermore, to avoid too many non-muon and non-neutrino events per unit time, which could cause saturation in the detector they conceive the underwater detector to be deep in the ocean. Thus an immense structure of hydrophones and photodetectors estimated to be some 5 to 10 km square and 1 kilometer high is proposed, eventually at a depth of 5 kilometers, in some favorable ocean far away from man-made activities which create underwater noise.

The theory of the neutrino telescope is this: High-energy particles entering seawater give birth to cascades of ionized collision products. These cascades can be detected by two effects: they create a bow wave of light (Cerenkov effect) (similar to a surface "bow wave" caused by a ship) which is visible as a flash of light, and they generate an acoustic shock pulse, theoretically detectable with hydrophones. The source of the energy in the acoustic effect is thought to be the ionization energy loss caused by charged particles colliding with water molecules. The energy ultimately appears as nearly instantaneous local heating of the water, in a time of about 1 μs to 0.01 *ns*, over a volume of water at the largest of radius 10 nm but generally of the dimensions of a few molecules. The efficiency of conversion of kinetic energy of cosmic particle into acoustic energy is estimated to be 10^{-11} or less.

From the point of view of the acoustician the problem is posed as follows. Coming in from the atmosphere, and ultimately from outer space, is a continuous shower of high-energy particles, charged and uncharged, which collide with molecules of air to generate cascades of

Manuscript submitted July 20, 1977.

collision products, ionized molecules, etc. In particular a large flux of massless, chargeless neutrinos enter the seas, where they in turn collide with water molecules and create additional cascades. At the instant these cascades are formed, they radiate transient pulses of sound. Thus the acoustician sees a volume of space randomly illuminated with bursts of sound (firefly effect). The problem posed then is to create a mathematical model of this effect.

Several models of single cascades were initially made under the auspices of DUMAND. These can be grouped into thermoelastic models and bubble models. In the group of thermoelastic models are a heated-rod model, a heated-spot model, and a heated-filament model. In the heated-rod model the cascade is considered to be a cylinder of water typically 3 to 10 m long and 1 to 12 cm in diameter, heated in a time of 1 μs to 1 ns, and coherently radiating a transient whose spectrum is roughly from 25 kHz to several hundred kilohertz. The radiation pattern is thought to be pancake shaped, that is, sharply narrow broadside to the axis of the cylinder. In the heated spot model a spherical volume of water of radius 10 nm or smaller is heated in 0.1 ns to 0.01 ps., radiating a spherical shock wave followed by a tail thought to be due to a heat diffusion effect. In the heated-filament model the local heating is confined to a large number of fine filaments approximately 1 μm in diam. Each filament radiates a separate acoustic wave, but all the filaments are considered to radiate coherently. In the group of bubble models the principle effect is modeled as local boiling of the fluid medium into bubbles, with subsequent collapse of these bubbles giving rise to acoustic transients. Not too different are models which treat the phenomenon as local explosions, as if made of TNT, the equivalent weight being 0.01 μg of TNT or less.

Both the thermoelastic models and the bubble models have been widely discussed. They are reviewed in detail in the body of this report, and a number of calculations have been made to illustrate the character of the predictions that can be made with their use.

Experiments conducted to date in laboratory mockups [1] show that the transient acoustic pulse due to high-energy particles partakes of the nature of a wave called a *bipolar*, with an initial compression wave followed by a final rarefraction, as shown in the following sketch:

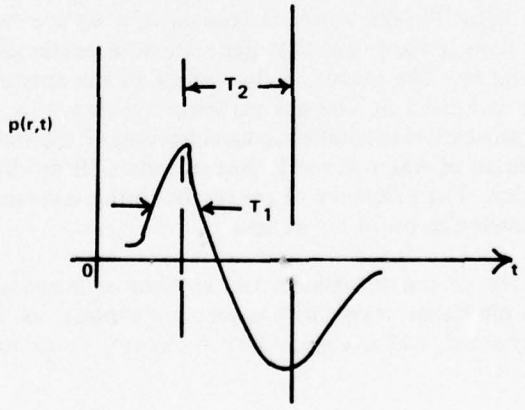

This type of acoustic signal is predicted by a generalized thermoelastic model developed in the body of this report. The model is obtained by solving the linear acoustic wave equation driven by a heat source, namely,

$$\nabla^2 p - \frac{1}{c^2}\frac{\partial^2 p}{\partial t^2} = -\frac{\beta}{C_p}\frac{\partial H}{\partial t},$$

where H is the heat flux. A typical transient solution of this equation has a form

$$p(r,t) = \frac{E_o}{T_1 T_2} \times \text{const.} \times f(t),$$

in which E_o is the cosmic particle energy, T_1 is essentially the time of heat expansion, and T_2 is the interval between the peak of compression and the "peak" of rarefaction. When the generalized model applied to specific cases, the differences between these specific models is found to rest on choices of T_1 and T_2. Actually, E_o/T_1 determines the magnitude of the peak compression, and T_2 determines the dominant portion of the frequency spectrum of the radiated wave. Measurements in laboratory experiments show T_2 to be 10 to 1 μs, leading to the conclusion that the significant spectrum of $p(r,t)$ begins somewhere near 25 kHz and extends thereafter upward.

A crucial question is the range limit of detectability of these bursts of sound. Local noise, frequency content of signal, incident cosmic particle energy, propagation attenuation, etc. all must be considered in determining the limit of "audibility". Rough approximates have been made in the body of this report. For example, if the pressure pulse is processed in a filter centered at 25 kHz and 10 kHz wide, then the limit of range in units of meters per electron-volt at which the transient signal magnitude is equal to the local noise (also at 25 kHz) is given by a particular model as 2×10^{-13}. Thus, *in this model*, a total cosmic particle energy of some 5×10^{14} eV is needed to permit detection at a limit distance of 100 m. Other models yield somewhat different (or vastly different) values, depending on their assumptions. The conclusion is that several major problems in modeling remain to be solved:

- The basic physics of the conversion of cosmic particle energy into acoustic energy envisages the formation of a shock wave due to nearly instantaneous rise of heat deposition, yet modeling to date is based on linear acousatic theory of small amplitude wave motion.

- In all mathematical models the key parameter of time estimation appears explicitly, but the magnitudes of T_1 and T_2 to be assigned to the models are largely guessed at.

- Experiments conducted to date verify certain parameter dependencies which tend to verify particular models. These dependencies show that the acoustic pressure is proportional to the energy of the particles coming in from space, being proportional to the coefficient of thermal expansion of the medium, inversely proportional to the specific heat of the medium, and inversely proportional to the distance of the observation point (spherical spreading). In addition it is verified that the radiation is sharply pancake shaped normal to the axis of the cascade. Still unknown however is the basic mechanism of energy conversion, the modeling to date being purely phenomenological.

INTRODUCTION

Processing of Signals From the Separate Sources

A continuous bombardment of cosmic particles strikes every unit area of the earth's surface. Those that strike the sea penetrate into the water and generate a number of showers of secondary particles along their tracks. These showers create acoustic noise. An illustration of the process of noise generation is shown in Fig. 1a. Here cosmic particles A_1, A_2, etc. are distributed randomly along the track A_T, and radiate acoustic shock waves at time of birth.

As will be seen later the acoustic signal patterns S_{A1}, S_{A2}, etc. are sharply normal to the track. In view of this sharpness of pattern one can reproduce the scene as a space and time random distribution of showers, (Fig. 1b). An omnidirectional hydrophone H will then record the acoustic pulses (or spikes) due to contributing showers say 1, 2, 3, 4, etc. distributed in time (Fig. 1c). A directional (or searchlight) hydrophone will record only the acoustic spikes directly in line with the beam, say spikes 2 and 5 (Fig. 1d). The goal of acoustic analysis is to determine the directionality and statistical properties of the noise made by these sources.

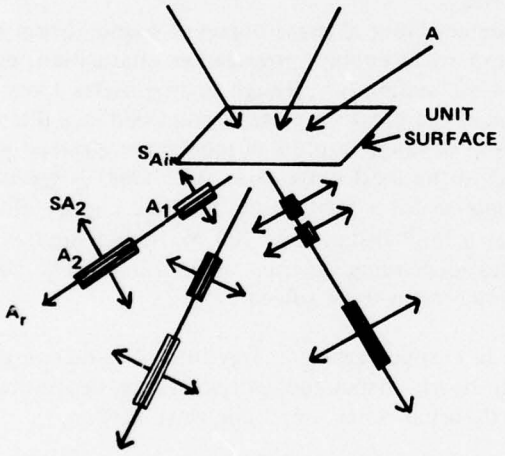

Fig. 1a – Schematic of noise generation by cosmic particles

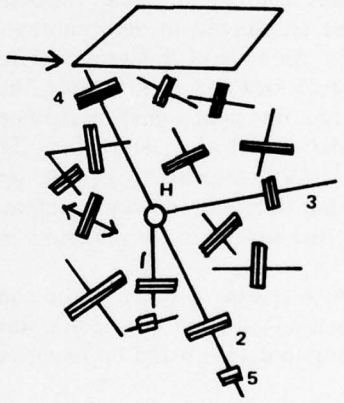

Fig. 1b – Space and time random distribution of showers

Fig. 1c – Schematic of voltage response of an omnidirectional hydrophone

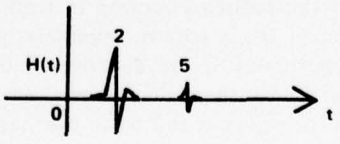

Fig. 1d – Schematic of voltage response of a directional hydrophone

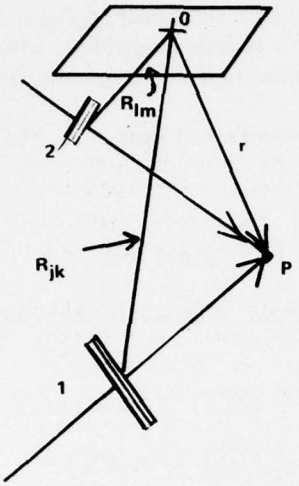

Fig. 2 – Addition of random noise from two showers

One must first construct an acoustic model of one shower. This is covered in the main body of the report. Secondly one must find a way to add sources together. In view of the random nature of the showers these effects must be added on a probabilistic basis. A schematic way of doing this is as follows. Figure 2 shows two contributing showers radiating noise to point **r**. Shower 1 is the jth random shower of the kth random high-energy particle, and shower 2 is the lth random shower of the mth random high-energy particle. Many more such showers contribute. The total time record of reception at **r** from all contributing showers is a simple sum of time-delayed elementary pulses:

$$P(\mathbf{r},t) = \sum_j \sum_k p_{jk} \left\{ t - \frac{|\mathbf{r} - \mathbf{R}_{jk}(t_k)|}{c} \right\}.$$

Since P is a random function of space and time, we will attempt to construct its autocorrelation. First, let exactly K contributing particles arrive in the time interval $0,T$, and let exactly J contributing showers of these particles occur in spatial volume V. Then the total pressure due to these showers is

$$P_{JK}(\mathbf{r},t) = \sum_{j=1}^{J} \sum_{k=1}^{K} p_{jk} \left\{ t - \frac{|\mathbf{r} - \mathbf{R}_{jk}(t_k)|}{c} \right\}.$$

Now let $g(J)$, and $g(K)$ be the probabilities that exactly J contributing showers will occur in volume V and exactly K contributing particles will occur in the time interval $0,T$. The autocorrelation ψ of the received time-pressure record at point **r** is then

$$\psi(\mathbf{l},\tau) = \sum_{J=0}^{\infty} \sum_{K=0}^{\infty} g(J)g(K) \left\langle \overline{P_{JK}(\mathbf{r},t)\, P_{JK}(\mathbf{r}+\mathbf{l},t+\tau)} \right\rangle ,$$

in which the overbar indicates the time average and the brackets indicate the ensemble average.

The probability distributions are not known. It is plausible however to assume that particles and showers constitute a shot effect and that $g(J)$ and $g(K)$ are Poisson distributions:

$$g(X) = \frac{(NQ)^X}{X!} e^{-NQ},$$

in which $g(X)$ is the probability that exactly X events will occur in the interval $0,Q$ and N is the average number of events per *unit* interval. It is further plausible to assume that space and time probabilities are statistically independent. Following Rice [2], we conclude that

$$\left\langle \overline{\psi(\mathbf{l},\tau)} \right\rangle = N_j N_k \int_{-\infty}^{\infty} \int_{-\infty}^{\infty} p(\mathbf{r},t)p(\mathbf{r}+\mathbf{l},t+\tau)\, d\mathbf{r}dt + \left\langle \overline{P(\mathbf{r},t)} \right\rangle^2$$

where

$$\left\langle \overline{P(\mathbf{r},t)} \right\rangle^2 = N_j N_k \int \int_{-\infty}^{\infty} p(\mathbf{r},t)\, d\mathbf{r}dt.$$

The space and time averaged power spectrum $W(\mathbf{K},\omega)$ is then obtained by Fourier transformation of ψ:

$$\left\langle \overline{W(\mathbf{K},\omega)} \right\rangle = 4 \int_{-\infty}^{\infty} d\tau \int_{-\infty}^{\infty} d\mathbf{l} \left\langle \overline{\psi(\mathbf{l},\tau)} \right\rangle \cos \omega\tau \cos \mathbf{K} \cdot \mathbf{l}$$

$$= 4\, N_j N_k |S(\mathbf{K},\omega)|^2 + 4 \left\langle \overline{P(\mathbf{r},t)} \right\rangle^2 \delta(\mathbf{K},\omega),$$

in which

$$S(K,\omega) = \int \int_{-\infty}^{\infty} p(\mathbf{r},t) e^{i(\mathbf{K}\cdot\mathbf{r}-\omega t)}\, d\mathbf{r}dt.$$

This means that one can obtain the *power* spectrum of the acoustic noise by first obtaining the space-time spectrum S of the transient pressure p and the space-time average of the total pressure and then adding them with the coefficients as shown. Other signal-processing schemes can be used to obtain further information on total effects in the ocean.

Models of the Separate Sources

The subject of this report is the development of acoustic models of the individual showers generated by a high-energy particle. In the process of this development we will bring out the important property of directionality of the acoustic signal which is a prime goal of analysis.

High energy atomic particles are decelerated upon passing through sufficient thicknesses of solid or liquid materials, losing kinetic energy as they do work on adjacent molecules of the medium. The energy loss is assumed to take place in the following steps: A fast moving particle strips off an electron at high energy, and then this electron strips off further electrons in the atoms along its path, the process continuing in a buildup of a multitude of fast-moving ionized atoms and electrons. These collision products distribute their energies among other molecules of the medium by additional successive collisions. Each loss of energy reappears ultimitely as heat in the absorbing medium or as a change in the medium's momentum or local chemical state. The energy transfer occurs quickly and is thought to be the origin of experimentally observed acoustic transients.

There are several origins of high-energy particles. Man-made sources are nuclear reactors, particle accelerators, atomic collisions, etc. In the natural world it is known that cosmic particles pervade the entire universe. Those that find their way into the earth's atmosphere, oceans, and crust are thought to originate from distant galaxies, supernovas, and the sun. Their detection is of scientific and military interest. Several schemes of detection have been

proposed, depending on the nature of the particles. If the particles are charged, one can detect them in cloud or bubble chambers in the presence of magnetic fields, or by Cerenkov radiation. If the particles are not charged (say neutrinos), their interaction with other matter may induce formation of secondary particles which then can be detected. Finally, it has been proposed that high-energy particles generate acoustic pulses in media and that these pulses are sufficiently intense to be detected, the models of this acoustic pulse generation being the subject of this report.

Several theoretical models have been proposed to explain the mechanisms of acoustic pulse formation by cosmic particles. The dominant models are thermoelastic models; in these models kinetic energy is converted into heat, which raises the temperature of the medium thereby altering the medium density on a short time scale which causes a pressure shock wave to radiate outward. Three distinct heat models have achieved prominence among scientists who have examined the problem [1]. These are the heated-rod model, the heated-spot model, and the heated-filament model.

In the heated-rod model the cosmic particle is thought to generate a cascade of ionization products that instantly heat a cylindrical rod in the medium of length L and diameter d (the numerical values of L and d depending on the energy of the particle) to a fractional degree above ambient (the temperature rise also depending on particle energy). Typical numbers are $L = 5$ to 10 m, $d = 1$ to 12 cm, and temperature rise $= 1\ \mu K$ for the case of a 10^{16} eV neutrino. The heated cylinder expands in 10 to 0.01 μs, radiating outward a transient shock wave with an efficiency of energy conversion of about 10^{-11} to 10^{-10}. The radiation along the entire length L is coherent over the range of the bandwidth frequencies of the transient and is directional with angle of detection.

In the heated-spot model the kinetic energy of the particle is converted explosively into a *concentrated* heat source (the hot spot), with the heat then diffusing outward in finite (but rapid) time. This thermal shock results in an elastic stress wave which radiates outward as a shock wave with a speed initially greater than, but eventually equalling, the speed of sound in the medium. The pressure pulse of these waves exhibit compression only and the spectral frequencies of the transient propagate independent of angle.

In the heated-filament model the heating is confined to narrow filaments (say 1 μm in diameter), there being showers of them. The temperature rise in a filament (like that of the hot-spot model) is 100 to 10,000 times higher than that in a rod. Each filament radiates a separate acoustic transient, and it is assumed that all the filaments in a shower radiate coherently. The heated-filament model (as well as the heated-spot model) predicts acoustic transients several orders of magnitude larger than the heated-rod model because of the confinement of heating to small volumes (with consequent greater temperature rise) and because of the much shorter time of heat deposition.

In addition to these three thermoelastic models, another model, not readily calculable but of equal importance, is the microbubble model. Here the concentrated heat of a secondary product particle quickly boils the liquid into a vapor bubble. The growth and collapse of this bubble radiates sound in the form of shock waves.

Thus the complexity of cosmic particle showers makes acoustic modeling highly uncertain. The most satisfactory approach is to simplify the final acoustic radiator to a collection of

recognizable (and computable) acoustic shapes. In this survey we will develop in detail cylinder, sphere, and vapor-bubble models, with the cylinder and sphere models being thermoelastic models. These models will be used to make numerical calculations.

Cosmic-Particle Showers in the Atmosphere [3]

The dominant high-energy particle arriving from outer space is the proton. Approximately 10^{10} arrive per sec on a 1-km^2 area at the top of the atmosphere with energies equal to or greater than 10^9 eV. Only the higher energy protons will reach sea level. The energy flux spectrum of these high energy protons on the top at the top of the atmosphere is extensively measured. A few entries are:

Energy (eV)	Flux ($s^{-1} \cdot km^{-2}$)
10^{15}	10
10^{17}	10^{-3}
10^{19}	10^{-7}

Upon entering the atmosphere the proton collides with air molecules about once every 7 to 8% of atmosphere thickness. Protons with energy of $\simeq 10^{12}$ eV create about 10 pi mesons at collision, and those with energy of $\simeq 10^{14}$ eV about 20 pi mesons. A proton survives each collision with about half its initial energy. Pi mesons themselves undergo collisions, creating additional pi mesons in the same numbers as proton collisions. Thus a cascade of pi mesons is created by each initial proton collision, the number sequence being one proton, then $\sim$ 10 pi mesons, $\sim$ 100 pi mesons, $\sim$ 1000 pi mesons, etc. Since the atmosphere is relatively thick, most of the proton energy that goes into creating pi mesons is absorbed before sea level is reached. However the newly created pi mesons are unstable and immediately decay. The plus- and minus-charged pi mesons decay into plus- and minus-charged muons and neutrinos. The neutral pi meson decays into two gamma rays. Decay products then interact with the atmosphere to produce a cascade of electrons and protons. Muons do not interact strongly as do pi mesons and protons, so they penetrate to sea level and below. Neutrinos have even weaker probability of interaction with the atmosphere. They too penetrate into the ocean.

If a high energy neutrino (say 10^{14} eV) does interact with the atmosphere, about half the initial energy goes into a hadronic cascade (a cascade of "hard" particles possessing significant mass), the other half going into the creation of muons or electrons. The hadronic cascade has the following history: The neutrino creates pi mesons. Of the total population of charged mesons within 50 cm along the interaction path about 10 generate (say) 10 more, resulting in a shower of mesons. Pi mesons with zero charge create a positron-electron cascade spatially distributed in a cone estimated to be 5 to 10 cm across and 5-10 m long. The number of particles in this cone exceeds 10^4.

If a high-energy muon (say 10^{13} eV) interacts with the atmosphere, it creates a particle shower approximately every 100 m. These showers may begin as gamma rays, positron-electron pairs, or pi mesons. The energy in a shower is about 10^{11} eV, there being about 100 particles in a cone a few meters long and about 10 cm wide. If the high-energy muon has 10 times the preceding energy ($\sim 10^{14}$ eV), it will also generate showers every 100 m but which will be 10 times more energetic with 10 times more particles. Along each 100-m segment of the shower path there is a regular ionization loss of 2×10^6 eV per cm, or 2×10^{10} eV. This is roughly 1% of the initial muon energy and can be assigned as a 1% energy feed into each shower.

Statistics of Particle Showers Reaching Sea Level

A useful model of an air shower reaching sea level is a thick rod of area 10 m by 10 m, one rod occurring per square kilometer. The flux of particles in this rod is a random quantity but can be modeled as follows:

- In every 100 s there will occur a shower of 10^7 particles. Of these some 99% are positrons or electrons, which are stopped in approximately 10 m of water. About 1% are muons, which penetrate deeper.

- In every 3 hours there will occur a shower of 10^8 particles.

- In every couple of months there will occur a shower of 10^{10} particles. Of these some 10^8 are muons, 10^4 of which have enough energy to penetrate 5 km into the ocean.

Each particle has a mean energy of 10^9 eV. The particles which penetrate into the ocean deep enough to be of significance in this survey are the neutrinos and the muons. The flux-and-energy statistics for the neutrinos are briefly as follows:

- One per year interacts in 1 km^3 of water with an energy of 10^{15} eV,

- 100 per year interact in 1 km^3 of 10^{14} eV, and

- 10^4 per year water with an energy of 10^{13} eV.

The flux-and-energy statistics for the muons are briefly as follows:

- 300 per second arrive on 1 km^2 of ocean at 10^{12} eV, each accompanied by 100 muons at 10^9 eV,

- One per second arrives on 1 km^2 of ocean at 10^{13} eV, accompanied by $\sim$ 1000 mesons at 10^9 to 10^{10} eV.

- One per 100 s arrives on 1 km^2 of water at 10^{14} eV.

THERMOELASTIC MODELS

Sound Sources and Their Governing Equations

The generation of sound by cosmic particles in the ocean may be investigated theoretically by adopting a reasonable model. Since the mechanism of energy deposition and acoustic conversion is not known with certainty, it will be useful to review various potential models.

A first approach to modeling is to state the equation of state for liquid pressure p in which small deviations from the ambient (or equilibrium) pressure p_o are dependent on changes in density $\Delta\rho$ and in extropy ΔS:

$$p = p_o + \left(\frac{\partial p}{\partial \rho}\right)_S \Delta\rho + \frac{1}{2}\left(\frac{\partial^2 p}{\partial \rho^2}\right)_{SS} (\Delta p)^2 + \cdots$$
$$+ \left(\frac{\partial p}{\partial S}\right)_\rho \Delta S + \frac{1}{2}\left(\frac{\partial^2 p}{\partial S^2}\right)_{\rho\rho} (\Delta S)^2 + \cdots .$$

For a heat-conducting viscous fluid the excess pressure (acoustic pressure) is

$$p' = c^2\rho' + \frac{1}{2}\left(\frac{\partial c^2}{\partial \rho}\right)_S \rho'^2 - \left[\frac{4}{3}\eta + \eta' + \chi\left(\frac{1}{C_V} - \frac{1}{C_p}\right)\right]\text{div } \mathbf{v} + \cdots$$

in which c is the speed of sound, η and η' are viscosity coefficients, χ is the thermal conductivity (units: $N/K \cdot s$), C_p and C_V are specific heats at constant pressure and constants volume (units: $m^2/K \cdot s^2$), and $\mathbf{v}$ is the vector fluid velocity. The simplest model of acoustic pressure generation is the one-term statement

$$p' = c^2\rho' .$$

This is the case of a linear nonviscous fluid in which the conduction of heat is negligible and the mechanism of sound generation is exclusively a function of change in density. However, the generation of sound pulses by cosmic particles is a complicated phenomenon. Hence a more complicated model will be needed.

We require various more complex mechanisms for changing density in liquids. These mechanisms are customarily listed as "sources" in writing the general linear equation of the propagation of sound [4, p.324]:

$$\nabla^2 p - \rho\kappa \frac{\partial^2 p}{\partial t^2} \simeq -f(\mathbf{r}, t) + \text{div } \mathbf{F} - \nabla \cdot T \cdot \nabla + \cdots ,$$

in which thermal and viscous terms have been omitted on the left-hand side but are included on the right-hand side as potential sources. Here $f(\mathbf{r}, t)$ is the sum of all monopole sources, div $\mathbf{F}$ represents the dipole source terms, and $\nabla \cdot T \cdot \nabla$ is the quadrupole source. Our interest will be focused on the monopole term. The general formula for the monopole sources is given by Eq. 7.1.22 of Ref. 4:

$$f(\mathbf{r}, t) = \frac{\partial}{\partial t}(\rho q) + \frac{\alpha\gamma\rho\kappa}{C_p}\frac{\partial \epsilon}{\partial t} - \rho\left(\frac{\partial \kappa}{\partial t}\right)\left(\frac{\partial P}{\partial t} - \frac{\alpha\gamma\epsilon}{C_p}\right)$$
$$-\frac{\rho}{\gamma}\left[\kappa^2 + \left(\frac{\partial \kappa}{\partial P}\right)_T\right]\left(\frac{\partial P}{\partial t} - \frac{\alpha\gamma\epsilon}{C_p}\right)^2 .$$

Here q is the volume flow (units: $m^3/s \cdot m^3$) and P is the equilibrium pressure. Other symbols will be explained below. The first monopole term represents an introduction of new fluid into the medium, the second term represents an introduction of time varying heat, and the third and fourth terms are sources by virtue of the temporal and spatial nonuniformity the medium properties. Although other sources are possible, most modelists of the acoustic effects of cosmic particles in liquids consider the heat source as the most appropriate:

$$f(\mathbf{r}, t) = \alpha\gamma\kappa \frac{\partial}{\partial t}\left(\frac{\rho\epsilon}{C_p}\right),$$

in which

$$\alpha = \left(\frac{\partial P}{\partial T}\right)_V, \left[\text{units: } \frac{\text{N}}{m^2 \cdot K}\right]; \quad \gamma\kappa = -\frac{1}{V}\left(\frac{\partial V}{\partial P}\right)_S \text{ (units: } \text{m}^2/\text{N}); \quad \gamma = \frac{C_p}{C_V}.$$

Since ϵ is the heat added per unit mass per unit time, the factor $\rho\epsilon$ is the heat added per unit volume per unit time. The factor ϵ/C_p is the temperature change due to the addition of heat. Introducing the coefficient of thermal expansion β (units: K^{-1}), one can write

$$\alpha\gamma\kappa = -\frac{1}{\rho}\left(\frac{\partial \rho}{\partial T}\right)_P = \beta.$$

Thus, by regrouping all factors, one arrives at a more significant expression for the monopole source directly attributable to heat:

$$f(\mathbf{r}, t) = \frac{\beta}{C_p}\frac{\partial H}{\partial t}, \quad H = \rho\epsilon \quad \left[\text{units: } \frac{\text{N} \cdot \text{m}}{m^3 \cdot s}\right].$$

The physical significance of the source is this: The addition of heat results in a change in temperature, which in turn causes an expansion of fluid, thus altering density; and the change in density generates an acoustic pressure, as indicated by the first equation of this section. The equation of propagation of the acoustic pressure is therefore

$$\nabla^2 p - \frac{1}{c^2}\frac{\partial^2 p}{\partial t^2} = \frac{-\beta}{C_p}\frac{\partial H}{\partial t}, \quad H = H(\mathbf{r}, t).$$

The negative sign appears on the right-hand side to insure a positive-sign source when the temperature increases (β being negative).

It will be useful to picture the acoustic phenomenon described by this equation. In analogy with a siren which ejects puffs of air by chopping a steady air stream, the equation describes a "heat siren" which ejects puffs of heat by chopping a steady deposition of heat. The heat stream is H (calories/s per unit volume), and the chopping action is $\partial/\partial t$. If the chopping is steady state, one sets $\partial/\partial t \rightarrow -i\omega$. A "one-shot" siren generates a transient heat puff. These heat puffs in turn generate density-temperature puffs (through multiplication by C_p^{-1}), and the latter are converted to pressure (density) puffs by β. The intensity of the sound generated will be directly proportional to the magnitude of the steady heat *flux* (= H) and to the rapidity of chopping ($= \partial/\partial t$).

This picture is common to all thermoelastic models. As we shall see, a different model is constructed for each description of H and $\partial/\partial t$. Actually H is specified as the calories per second *per unit volume*, making the developed pressure obtainable only by integrating over the effective volume which carries the heat. The heat in question is of course not directly deposited by the cosmic particle, which carries kinetic energy only. However for making estimates the magnitudes of kinetic energy and the developed heat are made equal.

We will now survey several useful models and will provide development of details when it is judged useful to an understanding of the limits of validity.

Heat Models Based on $\nabla^2 p - (1/c^2)(\partial^2 \rho/\partial t^2) = -(\beta/C_p)(\partial H/\partial t)$

We first enquire into the nature of H. Let the initial energy of a cosmic particle be E_o (units: N/m). We assume that when the particle enters the ocean, the heating effect on the water becomes volumetric. We can represent this effect as $\Delta E_o^*/\Delta V_o$, where E_o^* is the statement of the energy disturbance upon the water, as distinct from the particle energy E_o. Next we assume that at any particular point $\mathbf{r}_o$ along the track the water is at first quiescent, then responds to the heat disturbance, and then is quiescent again. The heat description is

$$\Delta H = \text{pulse} \times \frac{\Delta E_o^*}{\Delta V_o}$$

(units: $Nm/s \cdot m^3$). Three specific forms of this function will illuminate the meaning of the symbols.

For a point (or delta) deposition in space and time, the form is

$$\Delta H = \text{pulse} \times \frac{\Delta E_o^*}{\Delta V_o} = E_o\, \delta(\mathbf{r}_o)\, \delta(t_o).$$

For a deposition that is delta in time and uniform in cross-sectional area S, the form is

$$\Delta H = \frac{1}{S} \frac{dE(z_o)}{dz_o} \delta(t_o)$$

$$\Delta H = \frac{1}{S} \frac{dE(z_o)}{dZ_o} \delta(t_o),$$

which, if $E_o(z_o) = E_o\, e^{-\alpha z}$, becomes

$$\Delta H = \alpha \left(\frac{E_o}{S}\right) e^{-\alpha z}\, \gamma(t_o) \qquad \text{(case I)}$$

and, if $E_o(z_o)$ is Gaussian over volume V_o, becomes

$$\Delta H = \frac{E_o}{V_o} \exp\left[-\frac{(z_o - L/2)^2\, 8}{L^2}\right] \delta(t_o). \qquad \text{(case II)}$$

For a deposition that is delta in time and varies with z_o and with $S(r_\perp)$, $r_\perp = \sqrt{x^2 + y^2}$, the form is

$$\Delta H = \frac{dE_o}{dV_o}(r_\perp, z)\, \delta(t_o),$$

which, if the variation with r is parabolic, becomes

$$\Delta H = \frac{dE(z_o)}{S_o\, dz_o}\left[1 - \left(\frac{r}{r_o}\right)^2\right] \delta(t_o) \qquad \text{(case III)}$$

and, if the variation with r is Gaussian, becomes

$$\Delta H = \frac{dE(z_o)}{S_o\, dz_o} \exp\left[-\frac{\left(r - \frac{r_o}{2}\right)^2 \cdot 8}{r_o^2}\right] \delta(t_o). \qquad \text{(case IV)}$$

In these three forms the pulse nature of ΔH is written as $\delta(t_o)$. Other pulse expressions may be more appropriate. Writing "pulse" as $h(t)$ (units: s^{-1}), we list a few pertinent forms:

$$h_1(t) = \text{rect } (0, T) \text{ or rect } (-T/2, T/2),$$
$$h_2(t) = \text{triangle } (0, T) \text{ or triangle } (-T/2, T/2),$$
$$h_3(t) = \cos \Omega t \text{ rect } (-T/2, T/2).$$

Each pulse function has a Fourier spectrum of frequencies. Letting u and s be Fourier pairs, we have

$$\text{rect } u \rightarrow \text{sinc } s,$$
$$\text{triangle } u \rightarrow \text{sinc}^2 s,$$
$$\cos \pi u \text{ rect } u \rightarrow \frac{1}{2} \text{sinc} \left[s + \frac{1}{2} \right] + \frac{1}{2} \text{sinc} \left[s - \frac{1}{2} \right].$$

Since time is the analog of u and frequency is the analog of s, pulse descriptions and frequency descriptions are interchangeable by means of Fourier transformation. It will be convenient in the following analysis to consider both temporal and frequency descriptions. In all cases where the steady state solution $p(\mathbf{r}|\omega)$ of the pressure has been calculated, the temporal solution will be the standard one,

$$p(\mathbf{r}, t) = \int_{-\infty}^{\infty} p(\mathbf{r}|\omega)\, h(\omega)\, e^{-i\omega t} \frac{d\omega}{2\pi},$$

in which $h(\omega)$ is the Fourier transform of the pulse h(t).

We will now survey useful models.

Let the initial flux of particles entering the ocean be a beam of intensity I_o (units: $Nm \cdot s^{-1} \cdot m^{-2}$). The word initial means that we know I_o at some particular field point before additional absorption takes place. We assume that the rate of absorption with distance is exponential of form $e^{-\alpha z}$, where α (units: m^{-1}) is the absorption coefficient. This space rate of absorption is precisely H, namely,

$$H = \frac{-d}{dz} (I_o e^{-\alpha z}) = \alpha I_o e^{-\alpha z}.$$

The time variation of H is as yet unspecified. Initially we resolve the time variation into harmonic components. Thus the complete specification of the energy deposition in the fluid becomes

$$H = \alpha I_o e^{-\alpha z - i\omega t}.$$

Next we must assume a geometrical description of the space in which the acoustic field will be generated. For our first model, which we call heat model I, the space is assumed to be infinite in all directions. We will develop this model in detail.

Heat Model Ia (in Unbounded Space) [Westervelt-Larsen-Hanish]

The transient problem to be solved is

$$\nabla^2 p(\mathbf{r}, t) - \frac{1}{c^2} \frac{\partial^2 p(\mathbf{r}, t)}{\partial t^2} = -q(\mathbf{r}_o, t_0), \quad q = \frac{\partial H}{\partial t} \frac{\beta}{C_p}.$$

The solution of

$$\nabla^2 p - \frac{1}{c^2}\frac{\partial^2 p}{\partial t^2} = -4\pi q^*, \quad q^* = q/4\pi,$$

is known to be

$$4\pi p(\mathbf{r}, t) = 4\pi \int_0^{t^+} dt_o \int dV_o \, G(\mathbf{r}, \mathbf{r}_o | t, t_o) q^*(r_o, t),$$

where G is the Green's function of the scalar wave equation [5, p. 834]. For unbounded space

$$G = \frac{\delta[R/c - (t - t_o)]}{R},$$

where

$$R = |\mathbf{r} - \mathbf{r}_o|$$

and

$$R^2 = (x - x_o)^2 + (y - y_o)^2 + (z - z_o)^2.$$

Thus the solution of the transient problem is

$$p(\mathbf{r}, t) = \frac{\beta}{C_p 4\pi} \int_0^{t^+} dt_o \int dV \frac{\delta[R/C - (t - t_o)]}{R} \frac{\partial H(\mathbf{r}_o, t_o)}{dt}$$

$$= \frac{\beta}{4\pi C_p} \int dV_o \frac{H'(\mathbf{r}_o, t - R/c)}{R},$$

in which the prime signifies differentiation with respect to the argument of H (namely $t - R/C$). Let the volume of integration be a cylinder of area S, length l. Then, substituting the previously derived form of H in which the transient state, is replaced by the steady state we arrive at

$$p(\mathbf{r}, \omega) = -\frac{i\omega \alpha I_o S \beta}{4\pi C_p} \int_0^l \frac{dz_o \, e^{-\alpha z_o} e^{-i\omega(t - R/c)}}{R}.$$

In the far field

$$R \simeq |\mathbf{r}| - z_o \cos\theta,$$

where $|\mathbf{r}|$ is the distance from the origin to the field point. After a certain length $l^* = \alpha^{-1}$ the function $e^{-\alpha z_o} = e^{-1}$ is effectively negligible in its contributions to the value of the integral. By making $l > l^*$, one can extend l to infinity and thus approximate the integral to read

$$p(\mathbf{r}, \omega) = \frac{-\omega\alpha I_o S \beta}{4\pi C_p |\mathbf{r}|} e^{ik|\mathbf{r}|} \frac{e^{-i\omega t}}{d + ik\cos\theta}, \quad k = \frac{\omega}{c}.$$

The magnitude of pressure has a directivity $F(\theta)$, where

$$|p| = \frac{\omega I_o S \beta}{4\pi C_p |\mathbf{r}|} F(\theta), \quad F(\theta) = \frac{1}{\sqrt{1 + k^2 l^{*2} \cos^2\theta}}.$$

The maximum occurs at broadside ($\theta = 90°$). (See Ref. 6 additional details.) Although the exponential heat depostion is plausible, other types of track-dependent deposition are equally so.

An example is the Gaussian dependence on penetration length ($= z_o$), which earlier was labeled case II. Thus we use the earlier equation

$$\Delta H = \frac{E_o}{V_o} \exp\left[- \frac{(z_o - L/2)^2 8}{L^2} \right] \delta(t_o)$$

and consider only a single frequency. Defining the intensity flux as $I_o(r_\perp)$ (energy flux per unit cross sectional area), we write

$$\Delta H = \frac{I_o(r_\perp)}{L} \exp\left[- \frac{z_o - L/2)^2 8}{L^2} \right] e^{-i\omega t}.$$

This implies that the "Gaussian length" of deposition is L, that deposition is a maximum at $L/2$, and that the standard deviation of deposition is $\sigma = \sqrt{(1/2)\ (L^2/8)} = L/4$. The radiated acoustic pressure is

$$p(\mathbf{r}, \omega) = \frac{-i\omega\ \beta}{4\pi L\ C_p} \int_{V_o} \frac{\exp\left\{ - \frac{(z_o - L/2)^2 8}{L^2} \right\} \exp^{-i\omega(t - R/c)}}{R} I_o(r_\perp)\ dV_o$$

For simplicity we take $I_o(r_\perp)$ to be a constant independent of the cross sectional area variable $r_\perp$. Thus, $dV = dz_o\ dS(r_o)$, and

$$p(\mathbf{r}, \omega) = \frac{-i\omega\ \beta\ I_o\ S}{4\pi\ L\ C_p} e^{-i\omega t} \int_0^L \frac{\exp\left\{ - \frac{(z_o - L/2)^2 8}{L/2} \right\} e^{ikR}}{R} dz_o, \quad k = \omega/c.$$

In the far field

$$R \simeq |\mathbf{r}| - z_o \cos\theta,$$

where θ is the angle of the observation vector with the z (or track) axis. Let $y = z_o - L/2$, $dy = dz_o$; then, extending the limit of integration to infinity,

$$p(\mathbf{r}, \omega) = \frac{-i\omega\ \beta\ I_o\ S}{4\pi\ L\ C_p\ |\mathbf{r}|} e^{ik|\mathbf{r}|}\ e^{-i(k/2)L\cos\theta} \int_0^\infty e^{-y^2 8/L^2}\ e^{-iky\cos\theta}\ dy.$$

Let $8/L^2 = \alpha$ and $ik\cos\theta = \beta$. Then the integral reduces to

$$\int_0^\infty e^{-\alpha[y^2 + (\beta/\alpha)y]}\ dy = e^{\alpha(\beta/\alpha)^2} \int_0^\infty e^{-\alpha(y + \beta/2\alpha)^2}\ d\left[y + \frac{\beta}{2\alpha} \right]$$

$$= e^{\alpha(\beta/2\alpha)^2} \frac{\sqrt{\pi}}{2\sqrt{\alpha}}$$

$$= \frac{L}{4} \sqrt{\frac{\pi}{2}}\ e^{-k^2 L^2 \cos^2\theta/32}.$$

From this the magnitude of pressure is

$$|p(\mathbf{r}, \omega)| = \frac{\omega\ I_o\ S\beta}{16\ \sqrt{2\pi}\ C_p\ |\mathbf{r}|} e^{-\pi^2 L^2 \cos^2\theta/8\lambda^2}, \quad \lambda = \frac{c}{2\pi\omega}.$$

In most cases $L/\lambda >> 1$, so that the directionality of the pressure is sharp in the broadside direction ($\theta \simeq 90°$). The quantity $I_o S$ is again equal to E_o/T_1, the "time" T_1 being an estimate.

A second example of a spatial deposition of energy which is other than exponential is the uniform deposition in which dE_o/dz is constant. Thus

$$\Delta H = \frac{1}{S}\frac{dE_o}{dz_o}\,\delta(t_o) \rightarrow \frac{1}{T_1 S}\frac{dE_o}{dz_o}\,e^{-i\omega t_o},$$

so that

$$p(\mathbf{r}, \omega) = \frac{-i\omega\beta}{4\pi C_p}\frac{1}{T_1}\frac{dE}{dz_o}\int_0^L \frac{e^{ikR}}{R}\,dz_o.$$

In the far field

$$|p| = \frac{\omega\beta}{4\pi C_p}\frac{(dE_o/dz)}{T_1}\frac{1}{|\mathbf{r}|}\left|\int_0^L e^{ik\cos\theta z_o}\,dz_o\right|$$

or

$$|p| = \frac{\omega\beta\,(dE_o/dz)}{4\pi C_p T_1 |\mathbf{r}|}\,L\,\frac{\sin\left[\frac{\pi L}{\lambda}\cos\theta\right]}{\frac{\pi L}{\lambda}\cos\theta}.$$

Here again T_1 is unknown. The radiation pattern is sharp at broadside, just as in the case of the Gaussian deposition.

Heat Model Ib (in Unbounded Space)

When the heat deposition is transient and there are no preferred frequencies, we replace $e^{-i\omega t}$ by "pulse" $h(t)$. The solution is

$$p(\mathbf{r}, t) = \frac{\beta}{4\pi C_p}\int \frac{dV_o\,\alpha\, e^{-\alpha z_o}\,h'(t - R/c)}{R}.$$

Since all physically compatible transients $h(t)$ start and end in finite time, the time derivative will have both positive and negative values ($h' = dh/d(t - R/c)$). Hence the sound radiated will exhibit both compression and rarefaction.

A simple application of this formula is to assume the heat deposition is a delta function in space and time:

$$H(\mathbf{r}_o, t_o) = E_o\,\delta(t_o)\,\delta(\mathbf{r}_o) \quad \left[\text{units: } \frac{\text{N}\cdot\text{m}}{\text{s}\cdot\text{m}^3}\right].$$

Then the radiated transient is

$$p(\mathbf{r}, t) = \frac{\beta E_o}{4\pi C_p}\int_0^{t'} dt_o \int dV_o\,\frac{\delta\left[\frac{R}{c} - (t - t_o)\right]}{R}\,\delta'(t_o)\,\delta(\mathbf{r}_o)$$

$$= \frac{E_o\beta}{4\pi C_p}\,\frac{\delta'\left[\frac{|\mathbf{r}|}{c} - t\right]}{|\mathbf{r}|}.$$

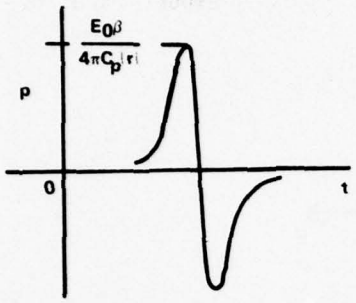

Fig. 3a – A double impulse of pressure

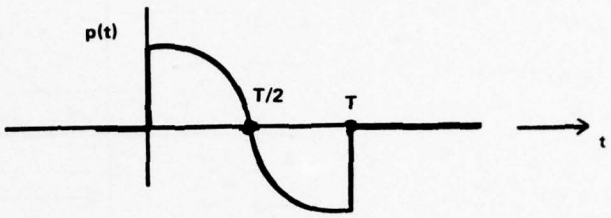

Fig. 3b – Pressure impulse

This pressure history exhibits a *double* impulse at point $|\mathbf{r}|$ (Fig. 3a). The first or compressure pulse is physically due to the shock of expanding heated fluid acting against the inertia of the stationary non-heated fluid; the second or rarifaction pulse is due to the "vacuum wave" created by the sudden cessation of expansion of the heated fluid while the inertia of the non-heated fluid continues its outward motion (Ref. 7,8). As a second example we assume a *time* history of deposition to be a sinusoidal pulse:

$$h(t) = (\sin \Omega t)\sqcap\left[\frac{t - T/2}{T}\right].$$

Here $\sqcap$ is a rectangle function of unit height and of base T s centered at $T/2$ s, which is zero outside the range 0 to T. The radiated pressure for exponential deposition of heat is

$$p(\mathbf{r}, t) = \frac{\beta I_o}{4\pi C_p}\int dV_o \frac{\alpha e^{-\alpha z_o}}{R}\left\{\Omega \cos \Omega (t - R/c)\sqcap\left[\frac{(t - R/c) - T/2}{T}\right]\right.$$
$$\left. + \sin \Omega (t - R/c)\sqcap'\left[\frac{(t - R/c) - T/2}{T}\right]\right\}.$$

The second term on the right-hand side represents a pair of impulses generated by the step functions appearing in $\sqcap$. We shall neglect them here, but will consider them later. Setting the limits of integration to infinity, we find the pressure at distance $R >> l^2/\lambda$ to be

$$p(\mathbf{r}, t) = \frac{\beta \Omega \alpha I_o S}{4\pi C_p (\alpha^2 + K^2 \cos^2\theta)|\mathbf{r}|}\left\{\alpha \cos \Omega\left[t - \frac{|\mathbf{r}|}{c}\right] - K \cos\theta \sin \Omega\left[t - \frac{|\mathbf{r}|}{c}\right]\right\}$$
$$\times\sqcap\left[\frac{(t - R/c) - T/2}{T}\right], \quad K = \frac{\Omega}{c}.$$

At $\theta = 90°$ the shape of the impulse pressure is shown in Fig. 3b. We see again that the pressure is a maximum at $\theta = 90°$ (broadside). This model is analogous to a "one-shot" siren. It will be used in a later section on numerical calculations.

Heat Model II (in Semi-Infinite Space)

In heat model II one again assumes that the cylindrical shower in the liquid due to the interaction products of a cosmic particle is caused by an external beam of the same cross-sectional area. This time however the beam enters a semi-infinite space ($z > 0$) from a

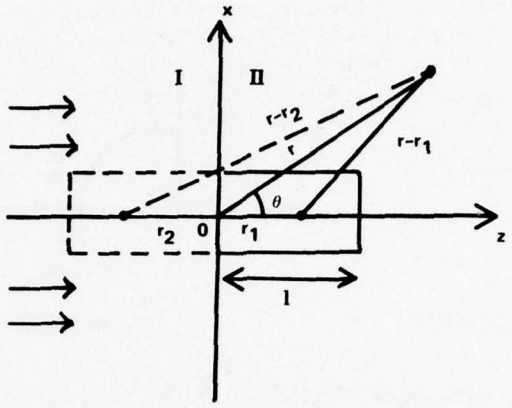

Fig. 4 – Laser beam entering an absorbing half space

nonabsorbing medium (region I) into an absorbing medium (region II) (Fig. 4). The energy deposition rate is again taken as

$$H = \alpha I_o e^{-\alpha z - i\omega t},$$

in which the units of H are again N · m/m^3 · s and the units of I_o are N · m/m^2 · s. Each point in region II along the centerline of the beam is an elementary point source of spherical waves. Corresponding to it is an image point source in region I. The sum of these two waves integrated over the length of the real beam gives the field pressure at **r**. Using the basic equations of model 1, one finds the solution to be

$$p(\mathbf{r}) = \frac{-\beta \alpha I_o S i \omega}{4\pi C_p} \int e^{-\alpha z} \left\{ \frac{e^{ik|\mathbf{r}-\mathbf{r}_1|}}{|\mathbf{r}-\mathbf{r}_1|} \pm \frac{e^{ik|\mathbf{r}-\mathbf{r}_2|}}{|\mathbf{r}-\mathbf{r}_2|} \right\} dz.$$

For an acoustically soft interface one chooses the negative sign. In the far field, where $R >> l^2/\lambda$ (l being the length of the beam, taken as α^{-1}), one can write

$$|\mathbf{r} - \mathbf{r}_1| \simeq R - z\cos\theta \text{ and } |\mathbf{r} - \mathbf{r}_2| \simeq R + z\cos\theta.$$

To simplify the analysis, the integral over z is extended to infinity. Thus

$$p = \frac{-\omega \beta \alpha I_o S}{4\pi C_p} \frac{e^{ikR - i\omega t}}{R} \int_0^\infty e^{-\alpha z} [e^{-kz\cos\theta} - e^{ikz\cos\theta}] dz$$

or

$$p = \frac{-\omega \beta I_o S}{4\pi C_p} \frac{e^{ikR - i\omega t}}{R} \frac{2kl\cos\theta}{1 + k^2 l^2 \cos^2\theta}.$$

(Kozyaev and Naugol' nykh ref. 7). The amplitude of radiated pressure is then

$$|p| = \frac{\omega \beta I_o S}{4\pi C_p R} F(\theta), \quad F(\theta) = \frac{2kl\cos\theta}{1 + (kl)^2 \cos^2\theta}.$$

The significance of this result is now examined. First, the amplitude depends directly on the power of the beam $I_o S$, where S is the cross-sectional area. This is actually the energy deposition rate in units of $N \cdot m/s$. Second, the amplitude depends on the frequency ω, which, in the

time domain, represents $\partial/\partial t$. This is the rate at which the energy, once deposited, is released to the medium. Third, the amplitude varies inversely as R, showing that the far-field radiation is spherical. Although the beam itself is a cylinder and the near field is cylindrical, the finite length of the radiation eventually appears as a point source to a distant observer. Fourth, the pattern function is a strong function of angle θ: at $\theta = 90°$, (in the plane $z = 0$) $F(90°) = 0$, as required for a pressure-release interface. The pressure reaches a maximum at an angle θ such that

$$\cos\theta = \frac{1}{kl}, \quad or \quad \theta = \cos^{-1}(\alpha/k).$$

If kl is large ($l/\lambda > > 1$), the angle θ lies near 90°:

$$\theta \rightarrow \frac{\pi}{2} - \frac{1}{kl}.$$

Thus the maximum radiation occurs *near* 90° (horizontal direction). At 90° the radiation vanishes. The amplitude of pressure in the direction of the maximum is independent of kl. In contrast, along the beam in the direction of the z axis the pattern amplitude is

$$F(0) = \frac{2kl}{1 + (kl)^2} \rightarrow \frac{2}{kl} = \frac{2\alpha}{k},$$

showing that the pressure amplitude for $l/\lambda > > 1$ is determined by the absorption α.

A parameter of importance in the detection of cosmic-particle noise is the total power radiated (an integrated effect):

$$W = 2\pi R^2 \int_0^{\pi} \frac{p^2(\theta)}{2\rho C} \sin\theta \, d\theta$$

$$= \frac{1}{8\pi\rho C}\left[\frac{\omega \beta I_o S}{C_p}\right]^2 \frac{1}{kl}\left[\arctan kl - \frac{kl}{1 + (kl)^2}\right].$$

Again if $l/\lambda > > 1$, this reduces to the simple form

$$W = \frac{\beta^2 (I_o S)^2}{16 \rho C_p^2} \omega \alpha.$$

The halfwidth of the main lobe of field intensity is then

$$\Delta\theta = \frac{2}{kl} = \frac{2\alpha}{k}.$$

Until this point one has assumed that the incident beam's effective cross-sectional diameter is small in comparison with the acoustic wavelength generated. If the two are comparable, there is an additional directivity arising from diffraction. Thus in place of $F(\theta)$ one has

$$F(\theta,\phi) = F(\theta)\,\phi(\theta),$$

where

$$\phi(\theta) = \frac{2 J_1(ka \sin\theta)}{ka \sin\theta}.$$

The maximum value of this function is unity (at $\theta = 0$). Hence the diffraction due to large beam diameters reduces the amplitude in all other directions.

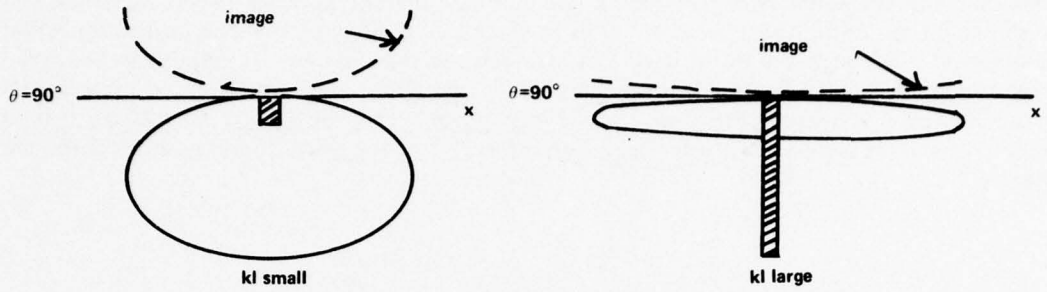

Fig. 5 – Pressure patterns of a laser beam in an absorbing half space

A sketch of $F(\theta)$ (no diameter — diffraction effects) is shown in Fig. 5 for kl small and kl large. The directionality closely resembles a dipole in which the beamwidths depend on kl.

It is instructive to compare these results with the steady state model I. The average intensity of sound generated over one period $2\pi/\omega$ of model I is

$$I_{av} = \frac{1}{(2\pi/\omega)} \int_0^{2\pi/\omega} \frac{p^2(\mathbf{r},t)}{2\rho c}\, dt = \frac{1}{2\rho c}\left(\frac{\omega \beta I_o S}{4\pi R C_p}\right)^2 \frac{\alpha^2}{\alpha^2 + k^2 \cos^2\theta}.$$

Assume the effective depth of penetration is $l = \alpha^{-1}$; then the directivity factor $F(\theta)$ becomes

$$F(\theta) = \frac{1}{1 + k^2 l^2 \cos\theta}.$$

The maximum intensity of sound occurs at $\theta = 90°$ (broadside). The angle at which the intensity is reduced to 1/2 of its maximum is

$$\theta_{1/2} = \frac{\pi}{2} + \frac{\alpha}{k}.$$

The total power generated is

$$W = \frac{\alpha \omega \beta^2 I_o^2 S_o^2}{16\pi\rho C_p^2} [\arctan kl - \arctan(-kl)],$$

in which for $kl >> 1$ $(l/\lambda >> 1)$ the bracket has value π, so that

$$W = \frac{\alpha \omega \beta^2 (I_o S)^2}{16 \rho C_p^2}.$$

A sketch of $F(\theta)$ for the two cases kl small and kl large is shown in Fig. 6.

Heat Model III (Heated-Rod Model)

In heat model III the entire shower of interaction products from one cosmic particle is considered to be an elastic rod L cm long and a cm in radius. A mathematical model of such a rod may be constructed as follows: The equation to be solved is

$$\nabla^2 p - \frac{1}{c^2}\frac{\partial^2 p}{\partial t^2} = -q(\mathbf{r}_o, t_o)4\pi, \quad q = \frac{\partial \hat{Q}}{\partial t}\frac{\beta}{C_p}\frac{1}{4\pi},$$

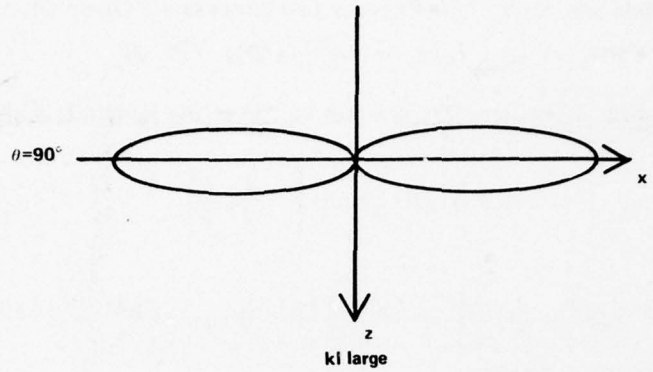

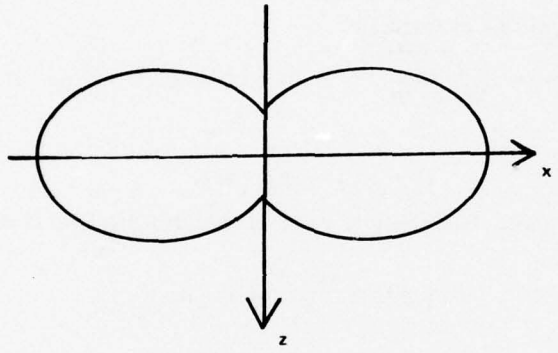

Fig. 6 – Intensity patterns of a laser beam in infinite space

in which $\hat{Q}$ is the heat flux (units: $N \cdot m/s \cdot m^3$), with the symbol $\hat{Q}$ replacing H of the previous sections to avoid confusion with the symbol $H_o^{(1)}$ for Hankel functions. We shall be interested in time harmonic solutions $q(\mathbf{r}_o, t_o) = q(r_o)e^{-i\omega t_o}$, so that the above equation reduces to the inhomogeneous Helmholtz equation:

$$\nabla^2 p + k^2 p = -4\pi q(r_o), \quad q(\mathbf{r}_o) = -\frac{i\omega_2 \hat{Q}\beta}{4\pi C_p}.$$

The solution is easily obtained by use of the appropriate Green's function G:

$$p_\omega(\mathbf{r}) = \int_{V_o} q(\mathbf{r}_o) G_\omega(\mathbf{r}|\mathbf{r}_o)\, dV_o,$$

in which V_o is the volume of the source. Because we will employ cylindrical coordinates, it is convenient to replace both p and G by their Fourier transforms, $p(r_\perp, n)$ and $F\{G\}$,

$$\int_{-\infty}^{\infty} p(r_\perp,\eta)e^{i\eta z}\frac{d\eta}{2\pi} = \int_{V_o} q(\mathbf{r}_o)\int_{-\infty}^{\infty} i\pi H_o^{(1)}(k^* P)e^{i\eta(z-z_o)}\frac{d\eta}{2\pi}\, dV_o,$$

$$P = |\mathbf{r}_\perp - \mathbf{r}_{o\perp}| = \sqrt{(x-x_o)^2 + (y-y_o)^2}, \quad \mathbf{r} = (r_\perp, z),$$

$$k^* = \sqrt{k^2 - \eta^2}, \quad \eta = k\sin\theta.$$

Here, $\theta = 0$ is broadside and $i\pi H_o^{(1)}(k^*P)$ is the two-dimensional Green's function. Thus

$$p(r_\perp,\eta) = \int_{V_o} q(\mathbf{r}_o) i\pi H_o^{(1)}(k^*P) e^{-i\eta z_o} dV_o.$$

We next assume the heat deposition $\hat{Q}$ is uniform in z over the length L of the rod and zero outside:

$$q(\mathbf{r}_o) = Q(r_{o\perp}) \operatorname{rect}\left[-\frac{L}{2}, \frac{L}{2}\right].$$

Now

$$\int_{-L/2}^{L/2} e^{-i\eta z_o} \operatorname{rect}\left[-\frac{L}{2}, \frac{L}{2}\right] = \frac{L \sin W(\eta)}{W(\eta)}, \quad W(\eta) = \frac{\eta L}{z} = \frac{kL \sin\theta}{2}.$$

We must next evaluate the expression,

$$\int_S H_o^{(1)}(k^*P) Q(r_{o\perp}) dS(r_{o\perp}).$$

Only the asymptotic field will be of interest.

$$\lim_{k^*P \to \infty} H_o^{(1)}(k^*P) = \sqrt{\frac{2}{\pi k^*P}} e^{ik^*P} e^{-i\pi/4}, k^* = \sqrt{k^2 - \eta^2} \text{ and } P = |\mathbf{r}_\perp - r_{o\perp}|.$$

In the far field

$$P \to |\mathbf{r}_\perp| - \mathbf{r}_{o\perp} \cos\phi,$$

where ϕ is an azimuthal angle. The absolute value of the pressure field is then

$$p(r_\perp,\eta) = \frac{\sin W}{W} LA(r_\perp,k^*),$$

where

$$A(r_\perp,k^*) = \pi \sqrt{\frac{2}{\pi k^* r_\perp}} \left| \int e^{-ik^* r_{o\perp}\cos\phi} Q(r_{o\perp}) dS(r_{o\perp}) \right|.$$

We next recover the field in z by taking the inverse transform in z:

$$p(r_\perp,z) = \int_{-\infty}^{\infty} \frac{\sin W}{W} LA(r_\perp,k^*) e^{i\eta z} \frac{d\eta}{2\pi}.$$

Since the first zeros of $\sin W/W$ are $\eta = \pm 2\pi/L$, we simplify by taking A to be constant between these limits with a value of $A(r_\perp, k)$ (i.e. $\eta = 0$); thus

$$p(r_\perp,0) = \int_{-2\pi/L}^{2\pi/L} LA(r_\perp,k) \frac{d\eta}{2\pi} = 2A(r_\perp,k),$$

$$A(r_\perp,k) = \pi \sqrt{\frac{2}{\pi k r_\perp}} \left| \int e^{-ikr_{o\perp}\cos\phi} Q(r_{o\perp}) dS(r_{o\perp}) \right|.$$

Noting that $Q(r_{o\perp})$ is constant across the endcap areas of the cylinder, we approximate the integral (and the absolute value of it) by QS. From the definition of Q we then multiply p by L/L to obtain

$$Q = \frac{\omega_2 \hat{Q}\beta}{4\pi C_p} \text{ and } QSL = \frac{\omega_2 \hat{Q} SL\beta}{4\pi C_p} = \frac{\omega_2 E \omega_1 \beta}{4\pi C_p}, \quad k = \frac{2\pi}{\lambda},$$

so that

$$p(r_\perp, 0) = \frac{1}{2\pi}\sqrt{\frac{\lambda}{r_\perp}}\,\frac{\omega_2 E \omega_1 \beta}{C_p L} .$$

The choice of λ is somewhat arbitrary. Let us restrict attention to frequencies 25 kHz and less, so that the smallest wavelength $\lambda = 1.5\times 10^3/25\times 10^3 \simeq 0.06$ m. Since the length L of the shower is about 10 m, it is seen that $\lambda \simeq L/160$. This choice is equivalent to stating that the radius of the first Fesnal zone at a distance equal to L is taken to be $R_F = (\lambda L)^{1/2} = L/4\pi$, or $\lambda = L/16\pi^2$. Thus the field will be measured in the Fesnel diffraction zone. Hence

$$p(r_\perp, o) = \frac{1}{2\pi}\sqrt{\frac{L}{16\pi^2 r_\perp}}\,\frac{\omega_2 E_1 \omega_1 \beta}{C_p L} = \frac{1}{2}\,\frac{f_2 E f_1 \beta}{C_p\sqrt{L r_\perp}} .$$

Finally,

$$p(r_\perp, \eta) = \frac{f_2 \beta E f_1}{2\, C_p \sqrt{L r_\perp}}\,\frac{\sin W}{W} .$$

In the DUMAND Proceedings [1] Dolgeshein took $f_1 = f_2$ and ascribed this form of the radiated pressure to Askarian. It is called the Dolgeshein-Askarian formula. From its derivation it is seen to be valid only when $kr_\perp > > 1$ or $r_\perp > > L/32\pi^3$. Although $\sin W/W$ is a Faunhofer pattern, the factor $\sqrt{L r_\perp}$ is added as a Fesnel (or near-field) correction.

Heat Model IV (Heated-Spot, or "Spike" Model)

Let a particular volume V_0 in infinite space suddenly receive a quantity of heat which then flows outward at the rate $H = \rho C_p V_f$, where the units of H are calories per unit volume per unit time ($N \cdot m/m^3 \cdot s$), ρ is the density of the medium ($N \cdot s/m^4$), C_p is the specific heat ($m^2 \cdot s/K$), and U_f is the flux of temperature (K/s). The equation of heat conduction to be solved is then

$$\frac{\partial T}{\partial t} = D\,\nabla^2 T + U_f$$

or

$$\nabla^2 T - \frac{1}{D}\,\frac{\partial T}{\partial t} = -\frac{U_f}{D} = -\frac{H}{\rho C_p D},$$

in which D is the diffusivity constant (units: m^2/s) and T is the temperature (K). To solve this equation, one uses an appropriate Green's function G_D which is the solution of the auxiliary equation

$$\nabla^2 G_D - \frac{1}{D}\,\frac{\partial G_D}{\partial t} = -4\pi\delta(\mathbf{r}-\mathbf{r}_o)\,\delta(t-t_o).$$

Thus the solution of the inhomogeneous temperature equation is

$$T = \frac{1}{4\pi}\,\frac{1}{\rho C_p D}\int_0^{t^+} dt_o \int G_D(\mathbf{r}, \mathbf{r}_o | t, t_o)\, H(\mathbf{r}_o, t_o)\, dV_o(\mathbf{r}_o) .$$

Now [9]

$$G_D(R, \tau) = \frac{1}{2}\,\frac{D}{\sqrt{\pi}}\,\frac{1}{(D\tau)^{3/2}}\, e^{-R^2/4DT},\ R = |\mathbf{r}-\mathbf{r}_o| \text{ and } \tau = t - t_o .$$

Thus

$$T = \frac{1}{8\pi^{3/2}} \frac{1}{\rho C_P} \int_0^{t^+} dt_o \int \frac{1}{(D\tau)^{3/2}} e^{-R^2/4D\tau} H(r_o, t_o) dV_o.$$

In conformity with the model we choose H to have the special form of a point source in shape and time,

$$H(\mathbf{r}_o, t_o) = E_o \delta(\mathbf{r} - \mathbf{r}_o)\delta(t - t_o),$$

in which the units of E_o are calories, i.e. (N·m), and we take $\mathbf{r}_o$, t_o to be at the origin. Then the history of the temperature distribution at space point $r(=|\mathbf{r}|)$ and time t is

$$T(r, t) = \frac{E_o}{\rho C_p} \frac{e^{-r^2/4Dt}}{(4\pi Dt)^{3/2}}.$$

We now turn to the propagation of a thermoelastic wave. In the immediate vicinity of the origin the temperature rise due to H causes an expansion of the medium in the amount βT (units of β:m/m·K). This expansion propagates away as the thermoelastic potential Φ (units: m^2), governed by the equation

$$\nabla^2\Phi - \frac{1}{c^2} \frac{\partial^2\Phi}{\partial t^2} = -4\pi\beta T^*, \quad T^* = T/4\pi.$$

This is a *small amplitude* linear equation of motion in which c is the speed of propagation of the disturbance. Since the Green's function of the scalar wave equation is well known, the solution is easily derived to be

$$\Phi = \frac{1}{4\pi} \int dt_o \int dV_o \frac{\delta\{R/c - (t - t_o)\}}{R} \beta T(\mathbf{r}_o, t_o)$$

$$\Phi = \frac{\beta}{4\pi} \int dV_o \frac{T(\mathbf{r}_o, t - R/c)}{R},$$

or

$$\Phi(\mathbf{r}, t) = \frac{\beta E_o}{4\pi\rho c_p} \int dV_o \frac{e^{-R^2/4D(t - R/C)}}{R[4\pi D(t - R/C)]^{3/2}}, \quad R = |\mathbf{r} - \mathbf{r}_o|.$$

The integral is taken over a volume of radius $R = ct$, with center at $\mathbf{r}$.

As it stands the form is difficult to evaluate. Nowacki [10] has circumvented these difficulties by solving the problem in a different way. He begins with the thermoelastic equation of motion,

$$\mu \nabla^2\mathbf{u} + (\lambda + \mu)\nabla(\text{div}\mathbf{u}) - \gamma\nabla T = \rho\ddot{u}$$

(units of each term, N/m^3), in which u is the displacement (m), μ is the second Lame' constant for an isotropic elastic continuum (units: N/m^2), λ is the first Lame' constant, γ is the thermoelastic constant (N/Km^2), and ρ is the medium density. He then seeks solutions of two scalar potentials Φ, and ψ such that

$$\mathbf{u} = \nabla\Phi + \text{curl}\psi.$$

Substitution leads to an equation for Φ:

$$(\lambda + 2\mu)\nabla(\nabla^2\Phi) - \gamma\nabla T = \rho \frac{\partial^2}{\partial t^2} \nabla\Phi,$$

or

$$\Box_1^2 \Phi = mT,$$

where

$$\Box_1^2 = \nabla^2 - \frac{1}{c^2}\frac{\partial^2}{\partial t^2}, \; c^2 = \frac{\lambda + 2\mu}{\rho}, \text{ and } m = \frac{\gamma}{\lambda + 2\mu}.$$

Since the heat-conduction equation for T is

$$\Box_3^2 T = \frac{-U_f}{D}, \quad \Box_3^2 = \nabla^2 - \frac{1}{D}\frac{\partial}{\partial t},$$

it is seen that

$$\Box_3^2 \Box_1^2 \Phi = -\frac{mU_f}{D}.$$

Formally this can be written as

$$\left(\Box_1^2 - \Box_3^2\right)\Phi = -\frac{m}{D}\left(\frac{1}{\Box_3^2} - \frac{1}{\Box_1^2}\right) U_f = m(T - S),$$

where

$$T = -\frac{U_f}{D}\frac{1}{\Box_3^2} \quad \text{and} \quad S = -\frac{U_f}{D}\frac{1}{\Box_1^2}.$$

Hence

$$\left(\frac{1}{D}\frac{\partial}{\partial t} - \frac{1}{c^2}\frac{\partial^2}{\partial t^2}\right)\Phi = m(T - S).$$

Assuming the thermoelastic continuum was free of all strains and stress for $t \leqslant 0$, one can take the Laplace transform (written with an overhead bar) and obtain

$$\left(\frac{s}{D} - \frac{s^2}{c^2}\right)\bar{\Phi} = m(\bar{T} - \bar{S}).$$

Since $\Box_1^2 = \nabla^2 - (1/c^2)\,\partial^2/\partial t^2$ and $\Box_3^2 = \nabla^2 - (1/D)\,\partial/\partial t$, the Laplace transform of S can be obtained from the Laplace transform of T by replacing s/D in the latter with s^2/c^2:

$$\bar{T} = \frac{Q^+}{4\pi DR} e^{-R\sqrt{s/D}},$$

so that

$$\bar{S} = \frac{Q^+}{4\pi DR} e^{-Rs/c}, \quad Q^+ = \frac{E_o}{\rho C_p} (\text{units: m}^3 \cdot \text{K}).$$

Thus

$$\bar{\Phi} = \frac{m\,Q^+}{4\pi R} - \frac{e^{-R\sqrt{s/D}} - e^{-\frac{R}{c}s}}{s - \frac{s^2}{C^2}D}.$$

Laplace inversion leads to

$$\Phi = \frac{m Q^+}{4\pi R}\left\{ f_1 (R,t) + \begin{bmatrix} 0, t < R/c \\ f_2 (R,t), t > R/c \end{bmatrix} \right\}.$$

Here, $f_1 (R,t)$ describes the heat diffusional effect in producing displacement potential, and $f_2 (R,t)$ describes the wave propagation effect (time scale much faster than f_1). Using f_2 only, one can directly show that the displacement potential of elastic waves produced by heat is

$$\Phi_{\text{wave}} = \frac{m Q^+}{4\pi R}\left[e^{-(t-R/c)c^2/D} - 1 \right], \quad t \geqslant \frac{R}{C}.$$

The pressure wave (shock wave) due to this potential is

$$p = \rho \frac{\partial^2 \Phi}{\partial t^2} = \frac{\rho m Q^+}{4\pi R} e^{\frac{C^2}{D}(R/C)} \frac{C^4}{D^2} e^{-C^2 t/D}, \quad t \geqslant R/C.$$

Since this is a transient, it will be convenient to form first the pressure impulse (units: $\text{N} \cdot \text{s/m}^2$) and then divide by some average time $\Delta\tau$ to obtain the time-average pressure, p_{av}. Thus

$$\int_0^\infty p(t)dt = \frac{\rho m Q^+}{4\pi R} e^{C^2/D(R/c)} \frac{C^4}{D^2} \int_0^\infty e^{-C^2 t/D}\, dt$$

$$= \frac{\rho m Q^+ C^2}{4\pi R D}.$$

Since $m = \lambda/(\gamma + 2\mu)$, and λ has the units $\text{N/m}^2/\cdot \text{K}$, m has the units of K^{-1}; that is, m is identical to β, the coefficient of thermal expansion. Similarly, since $Q^+ = E_o/\rho C_p$, one can write

$$\int_0^\infty p(t)\, dt = \frac{\beta E_o c^2}{4\pi C_p D R}.$$

Thus the time-average pressure will be

$$p_{av} = \frac{\beta E_o c^2}{4\pi C_p DR \Delta\tau}.$$

The crucial parameter in this model is $\Delta\tau$, the duration of the transient. A discussion of $\Delta\tau$ is reserved for the section on numerical calculations.

The preceding model was originally derived by Bowen [1], and is called the Bowen "hot-spot" model.

In a later paper (ref.11) Bowen reexamined his basic formulation in the light of contradicting experiments on received acoustic waveforms which displayed "bipolar transients" (namely plus and minus spikes) rather than a mono polar transient (or plus spike only). He concluded that the particular solution $I_p (= \Phi)$ already given by him above must be extended to a more general solution containing *complementary* solutions (called ψ^+) i.e.

$$\Phi_{total} = \Phi_p (r,t) + \frac{\psi^+}{r}(r - ct) + \frac{\psi^-(r + ct)}{r}$$

in which ψ^+ is an outgoing wave, and ψ^- is an ingoing wave. The solution is subject to the boundary condition that at the origin ($r = 0$) the displacement potential Φ_{total} must vanish for all time $t \geq r/c$, viz.

$$\psi_p(o,t) + \psi^+(0 - ct)\,|_{t \geq r/c} + \psi^-(0 + ct)|_{t \geq r/c} = 0$$

in which $\Phi_p = (K/r)\,\psi_p$. In addition the solution must satisfy a set of initial conditions,

$$\Phi_{tot}(r,0)\,|_{t \leq r/c} = 0; \quad \frac{\partial \Phi}{\partial t}(r,0)\,|_{t \leq r/c} = 0.$$

By use of this formulation Bowen made several improvements to his earlier theory: (1) the infinity at $r = 0$ in the particular solution $\Phi = \Phi_p$ was removed (2) the discontinuity at $r = ct$ in Φ_p (or in its derivatives) was removed (3) the *radiated* pressure impulse $I(r,t)$ ($\equiv \int_0^t p(r,t')\,dt' = \rho\,\partial\Phi/\partial t$) became $I(r,t) = \dfrac{E_o\,\beta\,c^2}{4\,\pi\,c_p\,dR}\,[F(ct - r,0)]$

$$F \equiv \frac{1}{2}\left[\exp\frac{c}{D}\,[c(b) + (ct - r)]\right].\left[erf\frac{(ct - r) + 2c(b + t)}{[4D\,(b + t)]^{1/2}}\right]$$

in which b is the "initial time" (not zero) related to the initial size $< r^2 >_{t=0}$ of the heated sphere by the formula $< r^2 >_{t=0} = 6Db$. When $c(b/D)^{1/2} >> 1$ it can be shown that the time variation of $I(r,t)$ is Gaussian,

$$F \propto \exp[-(ct - r)^2/4Db].$$

As a result, the acoustic pressure is bipolar, i.e.

$$p \equiv \frac{\partial I}{\partial t} \propto \frac{\partial F}{\partial t} = -\frac{2c(ct - r)}{4Db}\,F.$$

This result agrees with experiment. The first moment of the radiated pulse, namely

$$J \equiv \rho t'\,p(r,t')dt = \int t'\frac{\partial F}{\partial t}(t')\,dt'$$

can be shown to reduce to the value

$$J \simeq -\frac{E_o\,\beta}{4\pi C_p r}$$

if (again) $C(b/D)^{1/2} >> 1$. This agrees with the magnitude of the generalized Westervelt-Larson-Hanish model explained below.

These improvements by Bowen move his model in the direction of the generalized model used in the calculations noted above. Bowen notes again that the pressure itself because of its ultrashort time duration is essentially undetectable directly if a single hot-spot is in question. However J itself (as defined above) is finite, and certainly the superposition of many hotspots is detectable if E_o is large enough.

Far-Field Patterns of Pressure Radiation

It was shown in the section on heat model III that the far-field angular distribution of pressure $p(\theta)$ is proportional to the Fourier transform of the spatial distribution of heat deposition (designated here $h(z)$); that is,

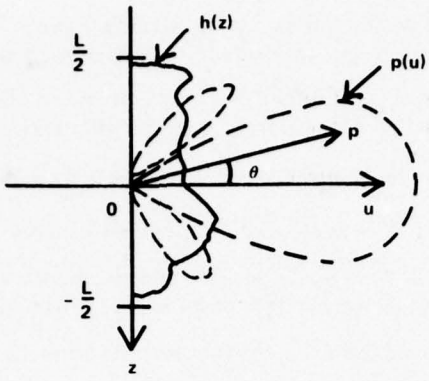

Fig. 7 – Definitions of aperture function and far field pressure pattern

$$p(u) \sim \int h(z)\, e^{-ikzu}\, dz, \quad k = 2\pi/\lambda, \text{ and } u = \sin\theta.$$

The angle θ is defined in Fig. 7.

Several distributions $h(z)$ may be pertinent to this survey. We list them here, together with facts on sidelobes of the developed patterns. In each case we take the length of the deposition track to be L and choose the center of the pattern to be at $z = 0$. Patterns other than the following can similarly be constructed as needed to conform to experimental result, or to additional modeling.

Exponential Heat Deposition

Let $h(z)$ be proportional to $e^{-\alpha z}$, and for ease of computation shift the line $z = 0$ to $z = L/2$; that is, take $h(z) = e^{-\alpha z}$, $z \geq 0$. Then, as sketched in Fig. 8 the normalized radiation pattern is

$$p(u) = \frac{1}{1 + i\dfrac{k}{\alpha}\sin\theta}.$$

This pattern has no zero crossing.

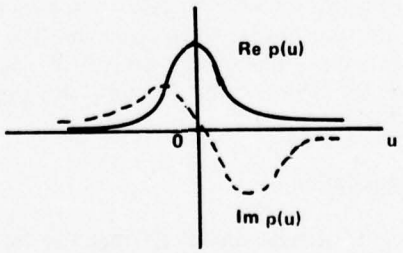

Fig. 8 – Radiation pattern caused by exponential heat deposition

Uniform Heat Deposition

Let $h(z) = \text{rect } L$, having unit amplitude between $-L/2$ and $+L/2$ and being zero elsewhere. Then, as sketched in Fig. 9, the normalzied radiation pattern is

$$p(u) = \frac{\sin(\pi Lu/\lambda)}{\pi Lu/\lambda}.$$

The first zero crossing is at $u = \lambda/L$, and the first sidelobe is at $u = 3\lambda/2L$. The 3 dB beamwidth is $0.88\ \lambda/L$, and the first sidelobe is -13.4 dB down. This is the case of heat model III.

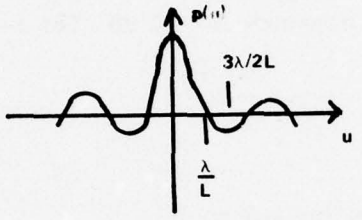

Fig. 9 – Radiation pattern caused by *uniform heat deposition*

Cosine Heat Deposition

Let $h(z) = \cos\frac{\pi z}{L}\ \text{rect}\ L$, for $\frac{L}{2} \leqslant z \leqslant \frac{L}{2}$, with $h(z)$ being zero elsewhere. Then, as sketched in Fig. 10, the normalized radiation pattern is

$$p(u) = \frac{\pi}{4}\left[\frac{\sin W}{W} + \frac{\sin Y}{Y}\right],$$

where

$$W = \frac{\pi L}{\lambda}\left[u - \frac{\lambda}{2L}\right] \text{ and } Y = \frac{\pi L}{\lambda}\left[u + \frac{\lambda}{2L}\right].$$

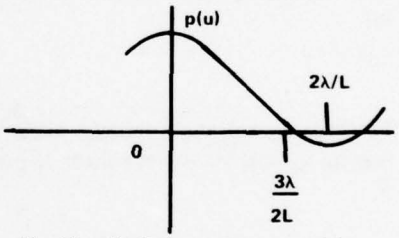

Fig. 10 – Radiation pattern caused by cosine heat deposition

The first zero crossing is at $u = \frac{3\lambda}{2L}$, and the first sidelobe is at $u = \frac{2\lambda}{L}$ and has a magnitude of -23.5 dB.

Gaussian Heat Deposition

Let $h(z) = e^{-2z^2/L^2}$, and assume no limits in z. Then, as sketched in Fig. 11, the normalized pattern is

$$p(u) = e^{-\pi^2 L^2 u^2/2\lambda^2}$$
$$= e^{-u^2/2\sigma_1^2},$$

in which σ_1 is its standard deviation, namely $\sigma_1 = \lambda/\pi L$. There are no zero crossings.

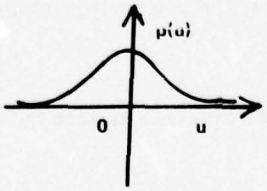

Fig. 11 – Radiation pattern caused by gaussian heat deposition

Parabolic Heat Deposition

Let $h(z) = \left[1 - (2z/L)^2\right]$ rect L, $-\frac{L}{2} \leqslant z \leqslant \frac{L}{2}$.

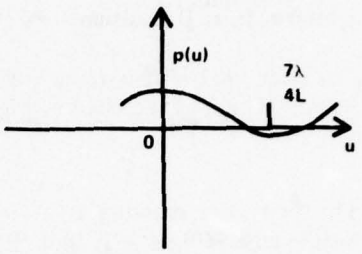

Fig. 12 – Radiation pattern caused by parabolic heat deposition

Then, as sketched in Fig. 12, the normalized beam pattern is

$$p(u) = \frac{3}{\psi^2}\left[\frac{\sin\psi}{\psi} - \cos\psi\right], \psi = \frac{kLu}{2}.$$

The first sidelobe occurs at $u = \frac{7\lambda}{4L}$, and its magnitude is -22 dB. The 3-dB beamwidth is $1.16\ \lambda/L$.

Impulse Response

As was noted earlier, the transient acoustic pressure given by

$$p(\mathbf{r},t) = \int_{-\infty}^{\infty} p(\mathbf{r},\omega)\, h(\omega)\, e^{-i\omega t}\, \frac{d\omega}{2\pi}.$$

The steady-state pressure is a directional function of the spatial coordinates. A discussion of spatial dependence has just been presented. We are interested now in the temporal aspect and omit details of spatial distribution by assuming the radial pressure to be spherically symmetrical:

$$p(r,\omega) = A\,\frac{e^{ikr}}{r}.$$

To find A, we shall specify some radial surface velocity of a fictitious sphere (radius a). Let this be v_r and let the medium of propagation be homogeneous and isotropic. Then

$$v_r = \frac{iA}{k\rho cr^2}\left[1 - ikr\right] e^{ikr},\ k = \omega/c,$$

and on the surface of the sphere

$$A(a,\omega) = \frac{v_r(a,\omega)\,k\rho ca^2}{i(1 - ika)}\, e^{-ika}.$$

Hence, the acoustic pressure anywhere is

$$p(r,\omega) = \frac{k\rho ca^2}{i(1 - ika)}\,\frac{e^{ik(r-a)}}{r}\, v_r(a,\omega).$$

If we choose a surface radial velocity $v_r(a,t)$ then

$$v_r(a,\omega) = \int v_r(a,t)\, e^{i\omega t}\, dt.$$

Thus the transient acoustic pressure radiated into the far field is

$$p(r,t) = \int_{-\infty}^{\infty} \frac{k\rho ca^2}{i(1 - ika)}\,\frac{e^{ik(r-a)}}{r}\left[\int v_r(a,t) e^{i\omega t}\, dt\right] e^{-i\omega t}\,\frac{d\omega}{2\pi}.$$

As an example, let the impulse of heat deposition be a rectangle:

$$\left.\begin{aligned} v_r(t) &= V_o, \\ &= 0 \end{aligned}\right\} \quad \begin{aligned} &0 < t < T_o, \\ &\text{elsewhere.} \end{aligned}$$

The Fourier spectrum is known to be

$$v_r(a,\omega) = \frac{i V_o}{\omega}\left[1 - e^{i\omega T_o}\right]$$

By direct integration one obtains the transient radiated pressure to be

$$\begin{aligned} p(r,t) &= 0, \qquad t < r - a/c, \\ &= \rho c V_o \frac{a}{r} e^{(-c/a)[t-(r-a)/c]}, \quad \frac{r-a}{c} < t < \frac{r-a}{c} + T_0, \\ &= \rho c V_o \frac{a}{r}\left[e^{-(c/a)[t-(r-a)/c]} - e^{-(c/a)[t-(r-a)/c + T_o]}\right], \quad t > \frac{r-a}{c} + T_o. \end{aligned}$$

Clearly the nature of the response will depend on the ratio $T_o/(a/c)$. Three conditions of this ratio, and the consequent pressure plots are shown in Fig. 13. In Fig. 13a the signal p travels a distance cT_o much greater than the radius of the sphere; both positive and negative impulses are widely separated in time and are therefore equal. In Fig. 13b the signal p travels a distance cT_o which is approximately the same as radius a. The positive impulse overrides the negative impulse, reducing the latter. In Fig. 13c the travel distance cT_o is smaller than a. This corresponds to a spherical radiation suddenly increasing in size from small to large. The negative pulse is due to the fluid inertia (moving radially outward) at the time of cessation of expansion. It is much larger than the positive pulse, because the larger sphere is a more effective radiator.

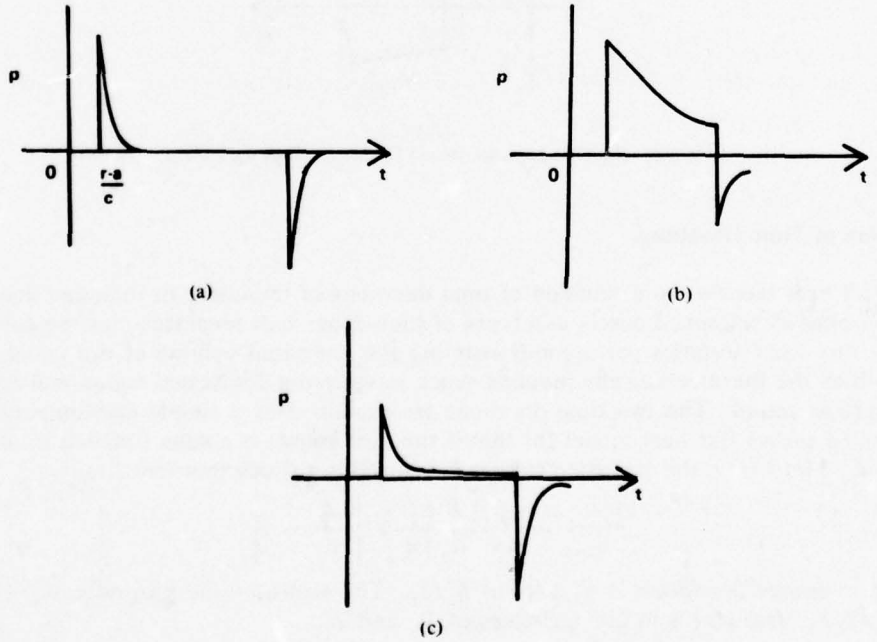

Fig. 13 – Impulse response caused by rectangular heat deposition

Another time impulse is the triangle

$$v(t) = mt, \; 0 < t < \frac{T_o}{2}.$$

$$= -mt + 2V_o, \; \frac{T_o}{2} < t < T_o,$$

$$= 0 \qquad : \text{elsewhere.}$$

The radiated transient appears as sketched in Fig. 14. (Reference [12] gives additional details.)

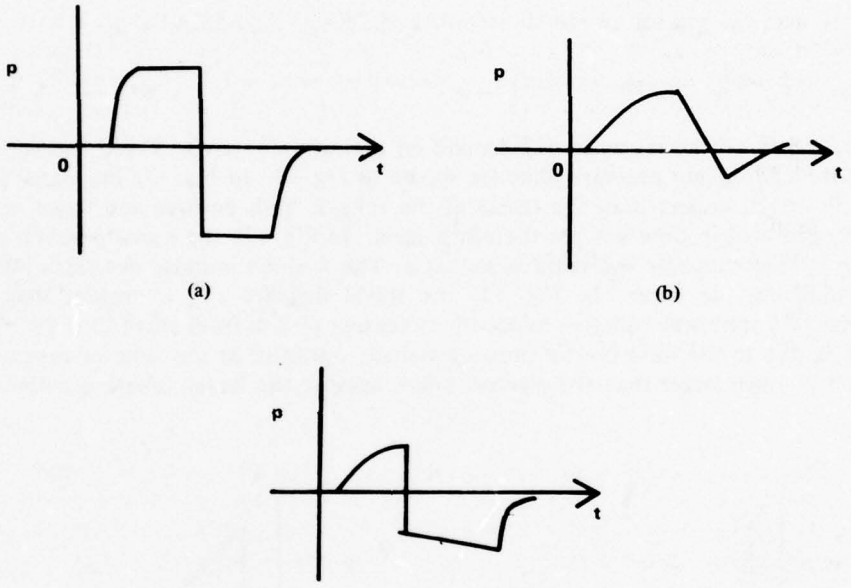

Fig. 14 – Impulse response caused by triangle heat deposition.

Estimation of Time Durations

In all heat models the estimation of time durations of impulsive heating and acoustic radiation is most important. Loosely two types of time-dependent processes must be considered: the heat flux itself (calories per second) entering the energized volume of the liquid and the rate at which the thermoelastically induced shock waves cross the heated region and are radiated outward as sound. The two time durations are explained by a simple mathematical model. It was noted earlier (for heat model Ib) that if the heat source is a delta function in space and time i.e. $E_o \, \delta(t) \, \delta(r)$), the acoustic pressure developed is a shock transient:

$$p(r,t) = \frac{1}{4\pi} \frac{\beta \, E_o}{C_p \, |r|} \, \delta' \left[\frac{|r|}{c} - t \right].$$

The rate of energy deposition is $E_o \, \delta(t)$ or E_o/T_1. The acoustic time history is $\partial/\partial t \, [E_o \, \delta(t)]$ or $\simeq E_o/T_1 \, T_2$. Our goal is to find estimates of T_1, and T_2.

It is simplest to estimate the "acoustic time" characteristic of the radiation process. Let d be a characteristic dimension of the heated volume (e.g. diameter of a cylinder or sphere). By analogy with traveling waves in a parallel-plate duct we seek a cutoff frequency of such waves, that is, the frequency associated with a mode which just fails to propagate down the duct. If l is the width of the duct, the first transverse mode (defined as reinforcement of incident and reflected waves one wavelength λ apart) travels at an angle θ such that $2l \cos \theta = \lambda$ (or such that $\lambda \leqslant 2l$). Each λ is associated with a particular θ. The largest wavelength for the first transverse mode is $\lambda = 2l$ at $\theta = 0°$, which means the wavefront is parallel to the duct wall and forms a standing wave, bouncing back and forth between walls at one wavelength reinforcement and not propagating down the duct. The cutoff frequency is then $f_m = \frac{c}{\lambda_m} = \frac{c}{2l}$. In a similar way acoustic reinforcement in a heated volume at one wavelength separation occurs when $\lambda = 2d$, and the cutoff frequency is $f_m = c/2d$. The choice $\lambda = 2d$ is equivalent to the wavenumber-diameter product $kd = \pi$ (or $k = 2\pi/\lambda$). In acoustic theory of radiating surfaces this product is favorable to radiation of wavelength λ (favorable in that the normalized radiation resistance is near unity and the reactance is low). Alternatively expressed, it is favorable to radiation of wave numbers near π/d.

The cutoff frequency may be taken as the bandwidth Δf of the radiated acoustic power spectrum. The time duration of the associated transient is $\Delta t \simeq (\Delta f)^{-1}$. Thus, roughly, $T_2 \simeq f_m^{-1}$. The estimation of T_1 is uncertain, the varying values put forth being the principal difference between models. All models in which heating of the fluid is the source of sound can be reduced to the schematic formula

$$|p| = \frac{\beta E_o}{4\pi C_p |r|} \left[\frac{1}{T_1^*} \frac{1}{T_2^*} \right],$$

in which the subscript 1 refers to heat deposition time and the subscript 2 refers to acoustic transient time. We assume $T_2^* = f_2^{-1} \simeq f_m^{-1}$. Thus T_2 is fixed by the speed of sound in the liquid and the characteristic dimension ($= d$) of the model. The value to be assigned to T_1^* depends on the model. Four models and their assigned values are as follows:

- *Heat model Ia* (infinite with space, steady state), with

$$|p| = \frac{\beta E_o}{4\pi C_p |r|} \left[\frac{2\pi}{T_1} f_2 \right],$$

so that

$$T_1^* = \frac{T_1}{2\pi}, \text{ where } T_1 \text{ is unknown;}$$

- *Heat model Ib* (infinite space, transient), with

$$|p| = \frac{\beta E_o}{4\pi C_p |r|} \left[\frac{\Omega}{T_1} \right], \quad \Omega T_2 = \pi,$$

so that

$$T_1^* = \frac{T_1}{\pi}, \text{ where } T_1 \text{ is unknown;}$$

- *Heat model III* (Dolgeshein-Askarian, or heated rod, model), with

$$|p| = \frac{\beta E_o}{4\pi C_p |r_\perp|}\left[\frac{2\pi f_1 f_2}{\sqrt{L/r_\perp}}\right], \quad f_1 = f_2,$$

so that

$$T_1^* = \frac{T_2\sqrt{L/r_\perp}}{2\pi},$$

- *Heat model IV* (Bowen, or heated-spot, model), with

$$|p| = \frac{\beta E_o}{4\pi C_p R}\left[\frac{C^2}{DT_2}\right], \quad T_2 = \Delta\tau,$$

so that

$$T_1^* = \frac{D}{C^2}.$$

Thus in both the Dolgeshein-Askarian model and the Bowen model the value of T_1^* *can be interpreted* as being assigned. For the other models we can estimate T_1 in the following (somewhat arbitrary) way: We assume that the cosmic particle on entering the liquid is decelerated at a constant rate from a maximum velocity v to zero, making the average velocity v/2. The time required to complete the transit over a length l of the shower is therefore

$$T_1 = \frac{2l}{\mathrm{v}}.$$

For a relativistic particle of energy E and rest mass $m_o c_L^2$, c_L being the speed of light, the velocity is

$$\mathrm{v} = c_L\sqrt{1 - \left[\frac{m_o c^2}{E}\right]^2}.$$

A typical application is for muons, for which $m_o c^2 \simeq 1 \times 10^8$ eV. Since cosmic particles of the heavy nuclei type have energies that exceed cosmic-ray protons ($E \simeq 2.5 \times 10^9$ eV), the speed of muons is approximately the speed of light. Thus

$$T_1 \simeq \frac{2l}{c_L}.$$

In each model in which T_1 is not assigned we choose some characteristic length l to estimate T_1 by this formula.

The arbitrariness of this estimate is apparent. From tentative experiments [1] and other models [7] it seems more plausible to take T_1, to be about $1\mu s$, which is some 2 or 3 orders of magnitude larger than the values predicted above. This estimate is sharply different from what is predicted from bubble models, from which, as discussed latter in this report, T_1 appears to be of the order 10^{-11}s.

Numerical Calculations

The models listed above will now be numerically evaluated. In each case we will present the absolute magnitude of the pressure field in the direction in which it is a maximum, at a

nominal distance of 1 m from the origin (or radiation center), and per unit energy input (in electron-volts). When, as discussed in the preceding subsection, the deposition time is not assigned, we will assume the interaction shower to be a cylinder a cm in radius and L m long, the values of a and L being assumed in particular cases.

Model Ia

In model Ia

$$|p| = \frac{\omega I_o S \beta}{4\pi C_p |\mathbf{r}|} \frac{1}{\sqrt{1 + k^2 l^2 \cos^2 \theta}}.$$

We take $I_o S = W = E_o/T_1$, and $\omega = 2\pi f_2$, where $f_2 = T_2^{-1}$, and we calculate the maximum at broadside, which is at $\theta = 90°$. To calculate T_1, we assume the shower length L to be 10 m [1]. Thus

$$T_1 \simeq \frac{2L}{c_L} = \frac{2 \times 10 \text{ m}}{0.3 \times 10^9 \text{ m/s}} = 67 \text{ ns}.$$

To estimate T_2, we will take $f_2 = c/2d$, where d is the diameter of the cylinder. The diameter depends on the energy and is estimated to be between 1 and 12 cm. Let us assume $d = 3$ cm, so that

$$f_2 = \frac{1.5 \times 10^5 \text{ cm/s}}{2 \times 3 \text{ cm}} = 25 \text{ kHz}$$

and

$$T_2 = f_2^{-1} = 40 \mu\text{s}.$$

Thus at 1 m

$$\frac{|p|}{E_o} = \frac{\beta}{4\pi C_p} \frac{1}{T_1 T_2 |\mathbf{r}|}$$

$$= \frac{1.4 \times 10^{-4} \text{ K}^{-1} \times 1.6 \times 10^{-19} \text{ J/eV}}{4\pi \times 4.18 \times 10^3 \text{ (m}^2/\text{s}^2 \text{ K)} \times 40 \times 10^{-6} \text{ s} \times 1 \text{ m} \times 67 \times 10^{-9} \text{ s}}$$

$$= 1.6 \times 10^{-16} \text{ N/m}^2 \cdot \text{eV} = 1.6 \times 10^{-15} \text{ dynes/cm}^2 \cdot \text{eV}.$$

Hence for Model Ia

$\|p\|/E_o = 1.6 \times 10^{-16}$ Pa/eV rms at 1 m from the axis of a rod 10 m long and 3 cm in diameter, for steady-state conditions at 25 kHz, with $T_1 = 67$ ns.

The total power radiated in the case $kl > > 1$ is

$$W_{\text{acoustic}} = \frac{\alpha \omega \beta^2 (I_o S)^2}{16 \rho C_p^2}.$$

Setting $I_o S = E_o/T_1$, $\alpha^{-1} = L$, we estimate

$$\frac{W_{\text{acoustic}}}{(E_o/T_1)^2} = \frac{2\pi f_2 \beta^2}{L 16 \rho C_p^2} = \frac{2\pi \times 2.5 \times 10^4 \times (1.4 \times 10^{-4})^2}{10 \times 16 \times 10^3 \times (4.18 \times 10^3)^2} = 1.10 \times 10^{-15}.$$

Hence for model Ia the total radiated power is

$W_{\text{acoustic}} = 1.10 \times 10^{-15} (E_o/T_1^2)$ W rms from a rod 10 meters long at 25 kHz.

Model Ib (One-Shot Siren)

For model Ib the time history of the transient radiation is

$$p(\mathbf{r},t) = \frac{\beta\ \Omega\ \alpha\ (I_o\ S)}{4\pi\ C_p\ (\alpha^2 + K^2 \cos^2\theta)|\mathbf{r}|} \left[\alpha \cos\ \Omega \left\{t - \frac{|\mathbf{r}|}{c}\right\} - K \cos\theta \sin\ \Omega \left\{t - \frac{|\mathbf{r}|}{c}\right\}\right] \times \sqcap \left[\frac{(t - R/c) - T/2}{T}\right], \mathrm{K} = \Omega/c.$$

At broadside $\theta = 90°$; Hence the maximum amplitude is

$$|p| = \frac{\beta\ E_o}{4\pi\ C_p |r|} \frac{\Omega}{T_1}.$$

As before we take $\Omega\ T_2 = \pi$, so that

$$|p| = \frac{\beta\ E_o}{4\ C_p\ |r|} \left[\frac{1}{T_1}\ \frac{1}{T_2}\right].$$

This is π times larger than model Ia; that is, for model Ib

$p_{\max} = 5.03 \times 10^{-16}$ Pa/eV at 1 m from the axis of a rod 10 m long and 3 cm in diameter, for transient conditions at center frequency of 25 kHz, with $T_1 = 67$ ns.

Model III

In the Dolgeshein-Askarian model

$$p\ (r_\perp, \eta) = \frac{f_1\ \beta\ E_o\ f_2}{2\ C_p\ \sqrt{L r_\perp}} \frac{\sin\ W}{W}.$$

On the axis at broadside $\sin\ W/W = 1$. Taking $f_1 = f_2$, and $T_1 = T_2$, one arrives at

$$\frac{|p|}{E_o} = \frac{\beta}{2\ C_p\ \sqrt{L r_\perp}} \left[\frac{1}{T_2 T_2}\right].$$

In the near field, at $r_\perp = 1$ m,

$$\frac{|p|}{E_o} = \frac{1.4 \times 10^{-4}\ (\mathrm{K})^{-1} \times 1.6 \times 10^{-19}\ \mathrm{J/eV}}{2 \times 4.18 \times 10^3\ (\mathrm{m}^2/\mathrm{s}^2 \cdot \mathrm{K})\ (10 \times 1)^{1/2}\ \mathrm{m}\ (4 \times 10^{-5})^2\ \mathrm{s}^2}.$$

Hence for model III

$|p|/E_o = 5.2 \times 10^{-19}$ Pa/eV rms at 1 m on the axis of a rod 10 m long for steady-state conditions at 25 kHz.

Model IV

In the Bowen model the average pressure radiated is

$$p_{av} = \frac{\beta E_o c^2}{4\pi C_p DR\Delta\tau}.$$

Thus

$$\frac{p_{av}}{E_o} = \frac{\beta}{4\pi C_p T_1 T_2 R}, \quad T_1 = \frac{D}{C_2} \text{ and } T_2 = \Delta\tau.$$

The effective deposit time is given by

$$T_1 = \frac{D}{C^2} = \frac{1.43 \times 10^{-7}\ \text{m/s}^2}{(1.5 \times 10^3)^2\ \text{m/s}^2} = 6.35 \times 10^{-14}\ \text{s},$$

and the interval between compression and rarefaction is

$$T_2 = 4 \times 10^{-5}\ \text{s}.$$

Hence

$$\frac{p_{av}}{E_o} = \frac{1.4 \times 10^{-4}\ \text{K}^{-1} \times 1.6 \times 10^{-19}\ \text{J/eV}}{4\pi \times 4.18 \times 10^3\ (\text{m}^2/\text{s}^2 \cdot \text{K}) \times 6.35 \times 10^{-14}\ \text{s} \times (4 \times 10^{-5})\ \text{s} \times 1\ m}$$

$$= 1.67 \times 10^{-10}\ N/m^2 \cdot eV.$$

Thus for the Bowen model

$p_{av}/E_o = 1.67 \times 10^{-10}$ Pa/eV at 1 m from the origin of a spike, averaged over 40μs, corresponding to 25 kHz.

Ambient Noise and Molecular Agitation Noise

Below 35 kHz the noise in the ocean at the lowest measured level is the ambient noise, in distinction to molecular agitation noise. The lowest limit of prevailing (ambient) noise has been compiled for all the oceans by Wenz [ref. 13]. Table 1 is a brief listing of sound-pressure spectrum level in a 1 Hz band in various units taken from this reference. Above 35 kHz the noise L_t (units: dB) due to molecular agitation is predominant. It can be calculated from an empirical formula at frequency f (units: Hz),

$$L_t \simeq -75 + 20 \log_{10} f, \text{ dB re } 1\ \mu\text{Pa}$$

[14]. At 25 kHz

$$L_t \simeq -75 + 20 \log_{10} 25{,}000 = 13 \text{ dB re } 1\ \mu\text{Pa.} = -87\text{dB re } \mu\text{bar}.$$

This is 5 dB less than ambient (Table 1). In making our calculations we will use the (rough) noise figure of 7.9×10^{-6} Pa in a 1 Hz band.

To process the acoustic transients in their entirety, one must arrange to have sufficient bandwidth in the receiver circuit. We noted earlier that the smallest time intervals to be recorded are of the order of 40 μs. Roughly we take the required bandwidth to be 10^4 Hz

Table 1 – Ambient-Noise Sound Pressure Spectrum Level in a 1-Hz Band

f (Hz)	μ Pa	dB re 20 μ Pa	dB re 1 μ bar
1	28,300	63	-11
10	1,120	35	-40
100	100.2	14	-60
1,000	22.4	1	-73
10,000	10	- 6	-80
25,000	7.9	- 8	-82
30,000	6.3	-10	-84

Hence the total noise spectrum level against which the signal spectrum level to be detected is (again roughly) $7.9 \times 10^{-6} \times \sqrt{10^4} = 7.9 \times 10^{-4}$ Pa at 25 kHz (say approximately 10^{-3} Pa). Here the spectrum level is assumed flat over the band. However, if we do not desire to know the entire signature of the transient radiation, the receiver bandwidth can be much smaller. The theory of signal detection in noise allows the choice of receiver bandwidth to optimize the probability of detection against the probability of false alarms relative to a threshold. Thus the bandwidth is fixed only to the extent that probabilities and thresholds are selected subject to the goals of the signal processing itself. We continue the analysis on the arbitrary basis of a 1-Hz band and a flat 10^4-Hz band.

Limits of Detection Range

Local noise (ambient or molecular) limits the detection of a distant signal to certain ranges. We choose a criterion that a signal is detectable if its absolute level is equal to or is above the sound pressure spectrum level of local noise over the bandwidth of the receiver. In practice the threshold is set higher than the local noise level, but here we are seeking orders of magnitude. Applying our criterion, we see that the limit range of detection (R_{limit}) in units of meters per eV may be obtained from the previous numerical calculations by use of the formula

$$R^n_{limit} \times BW^{1/2} = \frac{|p/E_o|_{R=1}}{\left(\frac{p_{\text{noise}}}{Hz^{1/2}}\right)},$$

in which n depends on the model and BW is the bandwidth of the receiver in hertz (relative to power). We choose the local noise to be in a 1-Hz band at 25 kHz: 7.9×10^{-6} Pa/(Hz)$^{1/2}$. Applying the formula to selected models we have the following. In these calculations we assume attentuation is due only to spherical spreading and neglect absorption.

Model Ia

In model Ia, $n = 1$ and $|p/E_o|_{R=1} = 1.6 \times 10^{-16}$ Pa/eV. Thus

$$R_{limit} \times BW^{1/2} = \frac{1.6 \times 10^{-16}\ \text{Pa/eV} \times 1\ \text{m}}{7.9 \times 10^{-6}\ \text{Pa/Hz}^{1/2}}$$

$$= 2.03 \times 10^{-11}\ \frac{\text{m (Hz)}^{1/2}}{\text{eV}},$$

from which we obtain

$$R_{limit} = 2.03 \times 10^{-11} \frac{\text{m}}{\text{eV}} \text{ for } BW = 1 \text{ Hz}$$

and

$$R_{limit} = 2.03 \times 10^{-13} \frac{\text{m}}{\text{eV}} \text{ for BW} = 10^4 \text{ Hz}.$$

Model Ib

In this model Ib $n = 1$ and the maximum amplitude of transient pressure measured at 25 kHz is 5.03×10^{-16} Pa/eV. The range limit is therefore

$$R_{limit} \times BW^{1/2} = \frac{5.03 \times 10^{-16}\ \text{Pa/eV} \times 1\text{m}}{7.9 \times 10^{-6}\ \text{Pa/Hz}^{1/2}}$$

$$= 6.37 \times 10^{-11}\ \frac{\text{m Hz}^{1/2}}{\text{eV}},$$

from which we obtain

$$R_{limit} = 6.37 \times 10^{-11} \text{ m/eV for } BW = 1 \text{ Hz}$$

and

$$R_{limit} = 6.37 \times 10^{-13} \text{ m/eV for } BW = 10^4 \text{ Hz}.$$

Model III

In model III, $n = \frac{1}{2}$ and $|p/E_o| = 5.2 \times 10^{-19}$ Pa/eV $\times$ m$^{1/2}$. The range limit is

$$r_{\perp limit}^{1/2} \times BW^{1/2} = \frac{5.2 \times 10^{-19}\ \text{Pa/eV} \times \text{m}^{1/2}}{7.9 \times 10^{-6}\ \text{Pa/Hz}^{1/2}}$$

$$= 6.58 \times 10^{-14}\ \text{m}^{1/2} \cdot \text{Hz}^{1/2}/\text{eV},$$

from which, for points of observation in the near field,

$$r_{\perp limit}^{1/2} = 6.58 \times 10^{-14}\ \frac{\text{m}^{1/2}}{\text{eV}} \text{ for } BW = 1 \text{ Hz}$$

and

$$r_{\perp limit}^{1/2} = 6.58 \times 10^{-16}\ \frac{\text{m}^{1/2}}{\text{eV}} \text{ for } BW = 10^4 \text{ Hz}.$$

In the far field $r_\perp$ replaces $r_\perp^{1/2}$.

Model IV

In model IV, $n = 1$, and $p_{av}/E_o = 1.67 \times 10^{-10}$ Pa/eV $\times$ 1 m. The range limit is

$$R_{limit} \times BW^{1/2} = \frac{1.67 \times 10^{-10} \text{ dynes/cm}^2\text{/eV} \times 1 \text{ m}}{7.9 \times 10^{-6} \text{ Pa/Hz}^{1/2}}$$
$$= 2.11 \times 10^{-5} \text{ m} \cdot \text{Hz}^{1/2}\text{/eV},$$

From which

$$R_{limit} = 2.11 \times 10^{-5} \text{ m/eV for } BW = 1 \text{ Hz}$$

and

$$R_{limit} = 2.11 \times 10^{-7} \text{ m/eV for } BW = 10 \text{ sup 4 Hz}.$$

MICROBUBBLE MODELS

The mechanism of the generation of sound by high-energy particles in water described in the preceding section is that of a thermal shock of an elastic medium. We consider next a different mechanism, in which sound is produced by formation and collapse of microbubbles. The theory of this process originated with Sette [15], who hypothesized that cavitation nuclei in liquids may be formed in part by irradiation by cosmic particles. In several subsequent articles Sette and Wanderlingh [16,17] elaborated on this hypothesis both with theory and experiment and applied it to explain the phenomena of bubble chambers. Although they did not discuss the connection between microbubble formation and collapse to acoustic noise generation, it is a direct matter to relate these two. We will make this connection later, but first we will review the theory of bubble nucleation to lay the basis for numerical calculation.

Bubble Nucleation

Historically the first significant paper on bubble nucleation by high-energy particles in liquids was that of Seitz [18] in connection with the theory of bubble chambers. He hypothesized that most of the bubbles are nucleated by energetic free electrons resulting from collisions of the particles with the molecules of the liquid medium in the bubble chamber. These electrons are decelerated with extreme rapidity, producing localized hot regions or "thermal spikes" which explode into bubbles of larger than critical size (that is, the minimum-size bubble is not in equilibrium with its surroundings, which permits growth by vaporization from its walls into in cavity at the temperature of the cavity). The time of bubble creation by explosion he calculated to be of the order of 0.1 to 0.01 ns. The bubble, after being created, is thought to expand by withdrawing heat from the immediate surrounding fluid. The maximum bubble size attained is limited by the initial energy of explosion, by heat diffusion away from the bubble, and by depletion of local permanent gas (air) in equilibrium with the surrounding medium.

The energy for growth of bubbles in the the bubble chamber is wholly supplied by the medium. In contrast to the theory of bubble chambers the production of microbubbles in ordinary liquids by high-energy particles requires that both creation and growth be energized by the kinetic energy of the particle; no energy is supplied by the medium. In bubble chambers

the temperature of the medium is locally near the boiling point. When a high-energy particle ionizes the medium, the particle supplies energy to create an embryo of critical size. Growth then proceeds by evaporation of the medium at the bubble wall, the heat being supplied by the medium to the embryo in an isothermal process. In contrast, when a high-energy particle enters an ordinary liquid whose temperature is well below the boiling point, there exist no embryos with critical radius. First a limited region of medium must be heated above the boiling point, and in it an embryo must be formed which has the critical size as determined by the initial temperature of explosion. Then, as the embryo expands, it draws heat from its heated surroundings, cooling down a local heat pocket ("spike") in the medium. As the temperature of the heated pocket falls, the *theoretical critical size* of a microbubble increases (Fig. 15) at the same time as the radius of the actual expanding bubble (of initial energy E_o) increases, the latter being larger, but the difference between them eventually growing smaller because of exhaustion of the original heat of deposition by heat transfer and gaseous diffusion At some lower temperature the bubble radius becomes critical, then growth ceases (point A). If E_o is large enough, the critical radius is not reached at any lower temperature: the bubble keeps on expanding (curve E_o) until stopped by exhaustion of the initial energy.

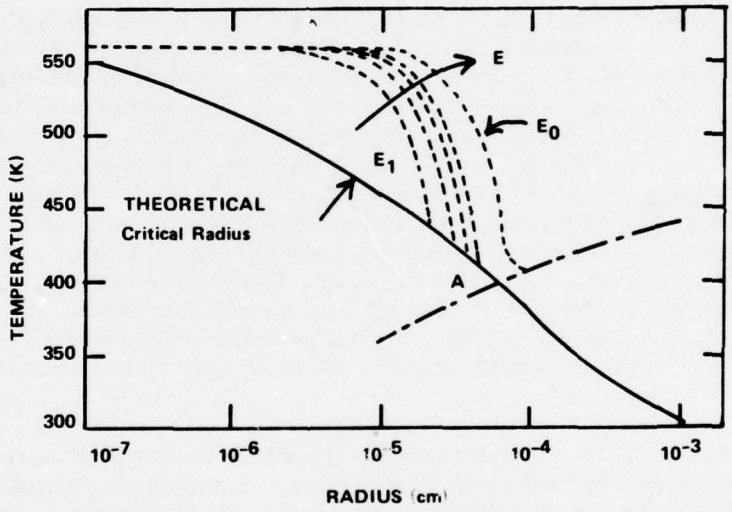

Fig. 15 – Theoretical critical radius vs temperature of medium
(Fig. 7 of Ref. 16)

A more intimate description of bubble nucleation has been developed by Sette and Wanderlingh [11]. From various experiments and thermodynamics they have constructed the following theory of the energy balance in bubble formation. The generation of a bubble of radius R requires an energy $E(R)$ which is the sum of two terms: the energy required to form an interface of given surface tension fixed by the temperture of the bubble and the energy required to evaporate water from the interface into the bubble. Thus

$$E(R) = 4\pi R^2 \sigma^* + m\,\Delta H,$$

in which σ^* is the surface energy density $\frac{J}{m^2}$, m is the mass of liquid (water) evaporated in grams and ΔH is the heat of vaporization in J/g. A calculation based on this equation shows

that hundreds of millions of electron-volts (1 eV $= 1.6 \times 10^{-19}$ J) are needed to produce bubbles of raduis 10^{-4} cm and larger and R is the radius in m. Experiments show that only 10 MeV (approximately) are needed, thus contradicting the calculation. The discrepacy is explained by noting that the role of dissolved gases has been neglected. Actually the heat ΔH is the sum of the heat associated with the transition of dissolved gases from the liquid into the bubble cavity and the heat of evaporation of water from the bubble wall. The first heat is negative (energy is released when gaseous air comes out of solution), and the second heat is positive. $E(R)$ is always positive and goes to zero at the critical point of the liquid. Below 450 K the gas diffusion predominates and ΔH is negative [Fig. 5 of Ref. 16]. The importance of this case requires additional comment. If one rewrites the energy balance in the form

$$E(R) = 4\pi R^2 \left\{ \sigma^* + \Delta H \left[(RP_0 + 2\sigma)/3RT \right] \right\}$$

in which the braces include the total surface energy, ΔH is the sum of gas and vapor heats, and $(RP_0 + 2\sigma)/3RT$ is the mass in grams, assuming a perfect gas (R being the gas constant), and if this equation is plotted as the expression in braces vs absolute temperature, it will be seen [Fig. 6 of Ref. 16] that the unit surface energy (the entity in braces) required to form a bubble of radius $R = 100\mu m$ is negative below 410 K and positive above it. This means that below 410 K the heat generated by the freeing of permanent gases from solution into the cavity is more than adequate to evaporate the medium at the wall and sustain surface tension of a $100\mu m$ bubble and above 410 K it is inadequate and energy must be supplied from the cosmic particle. Thus at 600 K, which is the threshold for the sure formation of a cavitation nucleus, an external source of energy will be required to form a $100\mu m$ bubble. In Ref. this energy is estimated to be 4 to 5 MeV for a $70\mu m$ bubble, both as to its initiation and its "indefinite" growth. Energies less than this create bubbles of lesser size whose growth ceases when a critical radius is reached. This phenomenon of bubble growth and cessation is vital enough to require additional comment. It can be pictured as follows (Fig. 16). A marble is pitched up the slope with an initial energy E_1, < 4 MeV. This brings the marble to radius R_1, where motion ceases (the bubble stops growing). If the energy is E_2, also less than 4 MeV, the marble stops at R_2. However, if the energy is 4 to 5 MeV the marble rolls over the threshold and continues on "indefinitely" (the bubble expands indefinitely by absorption of heat, if available from its surroundings).

The phenomenon of zero or negative energy required to form bubbles at particular temperatures may lead to the conclusion that there is no limit to the number of bubbles that can be formed. However each bubble formation is based on the availability of an embryo or nucleus. The probability of finding such a nucleus depends strictly on the initial temperature of the heated region. Above 600 K this probability is near unity (assuming atmospheric pressure), and below 600 K the probability becomes negligible [17]. Hence there must be enough energy to bring a sufficient volume of water to 600 K. Making the assumption that the water so heated is saturated leads to an initial water pressure (in a local area) of 12.2 MPa (1786.6 psi) abs (from steam tables). After expansion to ambient pressure (or below) the bubble reaches a final radius R_{max} whose value is determined by the initial energy of the interaction products.

The expansion to lower pressure occurs so rapidly it can be thought of as an explosion. It is pictured in this way: Water at room temperature is heated at nearly constant volume to 600 K (620°F), as if the water were in a tiny steel tank. The momentary existence of this tank is attributed to the high rate of deposition of the energy from the cosmic particle (or its interaction products). When sufficient heat is added to bring this tiny volume of water to satura-

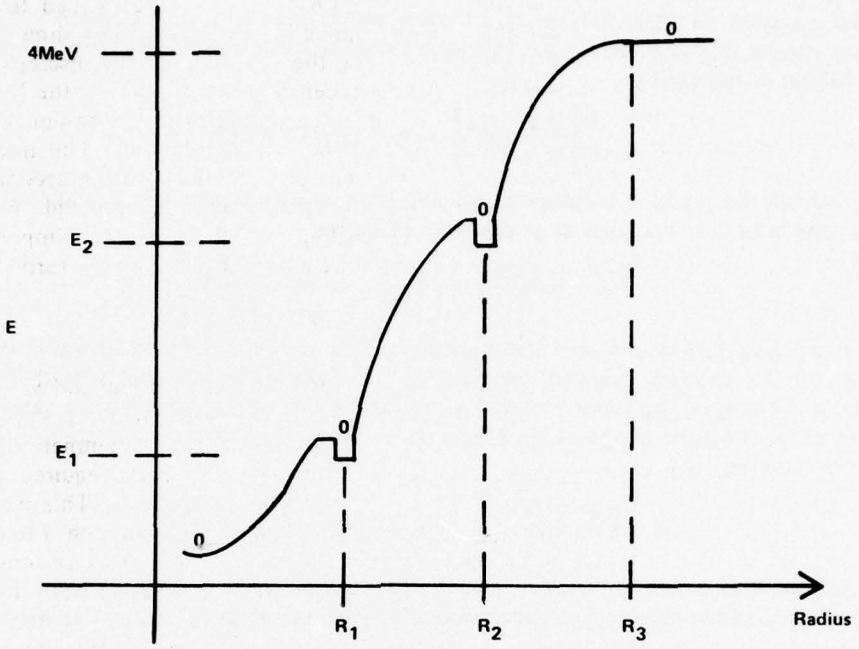

Fig. 16 – Illustrative analog of bubble growth and cessation

tion, the saturation pressure in the fictitious tank is 12.2 MPa, as noted above. At the instant of completion of deposition the tank explodes into a bubble which expands until the energy of deposition originally supplied is exhausted. The expansion is nearly isothermal as the bubble draws energy from the heated tank. Toward the end of the cycle, when no more heat is available, the bubble can continue to expand briefly in an adiabatic process down to ambient pressure or below, the driving force being the residual inertia of the water immediately surrounding the bubble.

Theory of Forster and Zuber

The preceding description of bubble formation and growth has yielded two important parameters: the driving initial temperature and the final (or maximum) radius. The driving temperature (here taken to be 600 K) initiates the explosion, and the initial input energy determines the final radius of the bubble. The time history $R(t)$ of the radial expansion is however not simple. Numerous authors have investigated this knotty problem. We will proceed here to sketch an approximate theory based on the work of Forster and Zuber [19], which has been selected because of the clarity with which it brings the intractable parts of the theory into focus.

The equation of radial motion of a bubble wall begins with an extended version of the early formulation of Rayleigh. To set this up we note that the rate of change of volume velocity of a bubble of radius R is

$$\frac{d}{dt}\left(\frac{d}{dt}\frac{4}{3}\pi R^3\right) = 4\pi\left(2R\dot{R}^2 + R^2\ddot{R}\right).$$

If one assumes the liquid is incompressible and then applies Bernoulli's law of the flow of an incompressible fluid, one arrives at an equation of motion

$$\frac{R^2\ddot{R} + 2R\dot{R}^2}{r} - \frac{R^4\dot{R}^2}{2r^4} = \frac{p_{int} - p_{ext}}{\rho_f},$$

in which r is any radius $\geqslant R$ and the right-hand side is the difference between the internal pressure and the external pressure (divided by ρ_f). Setting $r = R$ and writing the internal pressure as the sum of the vapor pressure p_v and the permanent gas pressure p_g and the external pressure as the sum of the surface-tension pressure p_σ and the hydrostatic pressure p_∞, one can then write

$$\rho_f\left(R\ddot{R} + \frac{3}{2}\dot{R}^2\right) = p_v + p_g - \left(p_\infty + \frac{2\sigma}{R}\right).$$

To simplify matters, one first neglects the internal gas pressure and then relates the quantity $\Delta p = p_v - p_\infty$ to the change in temperature ΔT by means of the Clausuis-Clapeyron equation

$$\Delta p = \frac{L}{T(v_g - v_f)}\Delta T$$

in which v_g and v_f denote the specific volume of the vapor and fluid respectively, L is the latent heat of vaporization, and ΔT is the rise in temperature above T. The temperature difference ΔT is determined by the solution of a problem involving heat conduction across a moving surface of evaporation (in spherical geometry). This solution may be found in Ref. [15]. If the heat input to the fluid is Q calories per unit volume per unit time, then for thermal diffusivity D

$$\Delta T(t) = \frac{-L\rho_g}{C_f(\pi D)^{1/2}\rho_f}J(t) + \Delta\tau + \frac{Qt}{\rho_f C_f}.$$

Here ρ_g and ρ_f are the densities of vapor and liquid respectively, D is the thermal diffusivity of the fluid, $J(r,\dot{r},t)$ is an integral functional arising from the solution of the heat-conduction equation noted in Ref. [20], $\Delta\tau$ is the superheat, and C_f is the specific heat of the liquid cal/gm K. Subsitituting all these expressions into the equation of motion, one obtains

$$R\ddot{R} + \frac{3}{2}\dot{R}^2 + \frac{\alpha}{R} - \beta + \gamma J(t) = Q^*t,$$

where

$$\alpha = \frac{2\sigma}{\rho_f}, \beta = \frac{L\Delta\tau}{\rho_f T(v_g - v_f)}, \gamma = \frac{L^2\rho_g}{\rho_f^2 T(v_g - v_f)(\pi D)^{1/2}C_f},$$

$$Q^* = \frac{QL}{\rho_f^2 C_f T(v_g - v_f)}.$$

This is an integral-differential equation in $R(t)$: $J(t)$ is a functional of $R(t)$. A more revealing equation can be obtained by introducing the concept of *critical radius*. This is done by noting that for superheat $\Delta\tau$ there is a corresponding pressure rise

$$\Delta p_s = \frac{L\Delta\tau}{T(v_g - v_f)} = \beta\rho_f.$$

The bubble radius corresponding to a surface tension σ at pressure Δp_s is called the critical radius

$$R_{crit} = \frac{2\sigma}{\Delta p_s} = \frac{2\sigma}{\beta\rho_f} = \frac{\alpha}{\beta}.$$

Dividing the equation of motion by R_{crit}^2, one has the more useful form,

$$r\ddot{r} + \frac{3}{2}\dot{r}^2 - \frac{A(r-1)}{r} + BJ = qt,$$

where

$$A = \frac{2\sigma}{\rho_f R_{crit}^3}, \; B = \frac{\gamma}{R_{crit}^2}, \; \frac{Q^*}{R_{crit}^2}, \; r = \frac{R}{R_{crit}}.$$

Because of the functional integral $J(t)$ the solution of this equation is intractable as it stands. Hence a general formula $r(t)$ for all time t is not available. Forster and Zuber demonstrate that for very small bubbles one can neglect the water inertia during growth. They then reduce the problem to the solution of an equation of the Volterra type,

$$\frac{r-1}{r} + q(t) = \frac{1}{C^* r}\int_0^t \frac{r'(t)\dot{r}(t')}{(t-t')}\,dt', \; C^* = \frac{A}{BR_{crit}},$$

in which $J(t)$ has been reduced by various arguments to the integral shown. Even this form is intractable. However an upper limit for $r(t)$ may be obtained by using the mean-value theorem to calculate the integral (which then becomes $2r\dot{r}t^{1/2}$). Using this approximation and assuming $q(t)$ is small relative to the other terms, one finally arrives at a solution for $r(t)$ implicitly given by

$$r + \ln\frac{r-1}{r_1 - 1} = C^* t^{1/2}, \; t > \left(\frac{r_1}{C^*}\right)^2.$$

The initial condition is $r = r_1$ for $t = r_1^2/C^{*2}$. To start the numerical calculation, one assumes r_1 is slightly greater than 1, say $r_1 = 1.01$. Since

$$C^* = \frac{A}{BR_{crit}} = \frac{2\sigma}{\rho_f R_{crit}^3}\,\frac{\rho_f^2 T(v_g - v_f)(\pi D)^{1/2} C_f R_{crit}^2}{L^2\rho_g R_{crit}}$$

$$= \frac{\rho_f \Delta T(\pi D)^{1/2} C_f}{R_{crit} L\rho_g},$$

we can interpret ΔT to be the initial superheat. Hence

$$C^* = \frac{\Delta\tau C_f(\pi D)^{1/2} v_g}{R_{crit} L v_f}.$$

This is a useful formula for estimating the numerical value of the right-hand side of the solution. To obtain a feeling for the magnitude of the terms and parameters involved we will calculate two cases as follows.

Case 1. The liquid (water) is superheated 5°C above boiling at atmospheric pressure. We desire to find R_{crit} and the time required to form a bubble of radius $R = 20\ \mu m$.

Solution to Case 1: The thermodynamic chart for water shows that at $T = 373 + 5 = 378°K$, $v_g = 27\ ft^3/lb$, $v_f = 0.02\ ft^3/lb$, $L = 974$ Btu/lb, $C_f = 4.18$ J/g/·K, and $D = 1.43 \times 10^{-3}\ cm^2/s$. Then

$$\beta = \frac{L\Delta\tau v_f}{T(v_g - v_f)} = \frac{(974 \times 2.32)\,(J/g) \times 5°K \times 0.02 \times 62.4\ cm^3/g}{378°K\,[(27 - 0.02) \times 62.4]\,cm^3/g}$$
$$= 2.3 \times 10^5 cm^2/s^2$$

and

$$\alpha = \frac{2\sigma}{\rho_f} = 2\sigma v_f = 2 \times 50 \times 0.02 \times 62.4 = 124.8 cm^3/s^2.$$

Therefore

$$R_{crit} = \frac{\alpha}{\beta} = \frac{124.8 cm^3/s^2}{2.3 \times 10^5 cm^2/s^2} = 5.6 \times 10^{-4}\ cm = 5.6\ \mu m.$$

From this

$$C^* = \frac{\Delta\tau\,(\pi D)^{1/2} C_f v_g}{R_{crit} L v_f}$$

$$C = \frac{5°K\,(\pi \times 1.43 \times 10^{-3})^{1/2} cm/s^{1/2} \times 4.18\ (J/g \cdot K) \times 27 \times 62.4 cm^3/g}{5.6 \times 10^{-4}\ cm \times 974 \times 2.32\ (J/g) \times 0.02 \times 6.24\ cm^3/g}$$
$$= 1494\ s^{-1/2}.$$

Since $r = R/R_{crit} = 20\ \mu m/5.6\ \mu m = 3.57$, we find

$$r + \ln\frac{r - 1}{r_1 - 1} = C^* t^{1/2}$$

or

$$3.57 + \ln\frac{2.57}{0.01} = 1494 t^{1/2}$$

or

$$t = 37\ \mu s.$$

This is approximately the result that Forster and Zuber show in their Fig. 1, where $R = 2 \times 10^{-3}$ cm corresponds to a formation time of about $30\mu s$. Note that t depends on C^* inversely; that is, the higher the superheat, the faster the time of formation of a bubble of specified size.

Case 2. We now calculate the case of a cosmic particle (or interaction product) with enough energy to form a 600-K spike. We desire to find the time required to expand an embryo to a radius of 70 μm.

Solution to Case 2. The superheat is 227°C. From steam tables, using vapor at 15 psi and 620°F, and fluid at 15 psi, 212°F, we have $v_g = 43.6\ ft^3/lb = 2.72 \times 10^3\ cm^3/g$, $v_f = 0.02\ ft^3/lb = 1.25\ cm^3/g$, latent heat of vaporization is $1345 - 180 = 1165$ Btu/lb $= 2.7 \times 10^{10}$ erg/g. The specific heat at constant pressure is 4.18×10^7 erg/g·K, and the diffusivity is $1.43 \times 10^{-13}\ cm^2/s$. Then

$$\beta = \frac{L\Delta\tau v_f}{T(v_g - v_f)} = \frac{2.7 \times 10^{10} \times 227 \times 1.25\,(\mathrm{cm}^3/\mathrm{g})}{600\,(2.7 \times 10^3\,\mathrm{cm}^3/\mathrm{g})} = 4.7 \times 10^6\,\mathrm{cm}^2/\mathrm{s}^2$$

and

$$\alpha = \frac{2\sigma}{\rho_f} = 2 \times 10 \times 1.25 = 25.$$

Therefore

$$R_{crit} = \frac{\alpha}{\beta} = \frac{25}{4.7 \times 10^6} = 5.3 \times 10^{-6}\,\mathrm{cm} = 53\mathrm{nm}.$$

From this,

$$C^* = \frac{\Delta\tau\,(\pi D)^{1/2} C_f v_g}{R_{crit} L v_f}$$

$$= \frac{227\,(\pi \times 1.43 \times 10^{-3})^{1/2} 4.18 \times 10^7 \times 2.72 \times 10^3}{5.3 \times 10^{-6} \times 2.7 \times 10^{10} \times 1.25}$$

$$= 9.7 \times 10^6\,\mathrm{s}^{-1/2}.$$

The time required to form a bubble of radius $R = 7 \times 10^{-5}\mathrm{cm}$ $\left(r = \frac{7 \times 10^{-5}}{5.3 \times 10^{-6}} = 13.2\right)$ is then

$$13.2 + \ln\frac{12.2}{0.01} = 9.7 \times 10^6 t^{1/2}$$

or

$$t = 4.38 \times 10^{-12}\,\mathrm{s}.$$

This is the same order of magnitude as that predicted by Seitz ($\simeq 10^{-11}\,\mathrm{s}$).

Clearly such small times must be treated with caution. The process is essentially an explosion, and the difficulty of treating an untractable integral-differential equation places a great strain upon the analyst to quantify the growth of a bubble in such short times. Although the work of Forster and Zuber allows one to construct a graph of $r(t)$ vs t and from it $\dot{r}(t)$ and $\ddot{r}(t)$ needed for estimating the radiated sound, the limited conditions of validity, negligible heat input, simplified heat conduction, mean value integration, etc.) make it unsatisfactory for small radius bubbles and short times. We adopt next a different approach.

Approximate Solution of Bubble Growth and Collapse Using Thermodynamic Charts

The formation and growth of a bubble will be traced on a temperature vs entropy (TS) chart for water (Fig. 17). We imagine the process to occur as follows: water at 77°F (room temperature), point A, is heated nearly at constant volume (as if in a tiny steel tank) to 620°F, point B; the heated spike then furnishes heat to an embryo along a constant temperature line BC, followed by a final expansion to ambient pressure along an unknown route CD. With such a picture in mind we perform the following calculations.

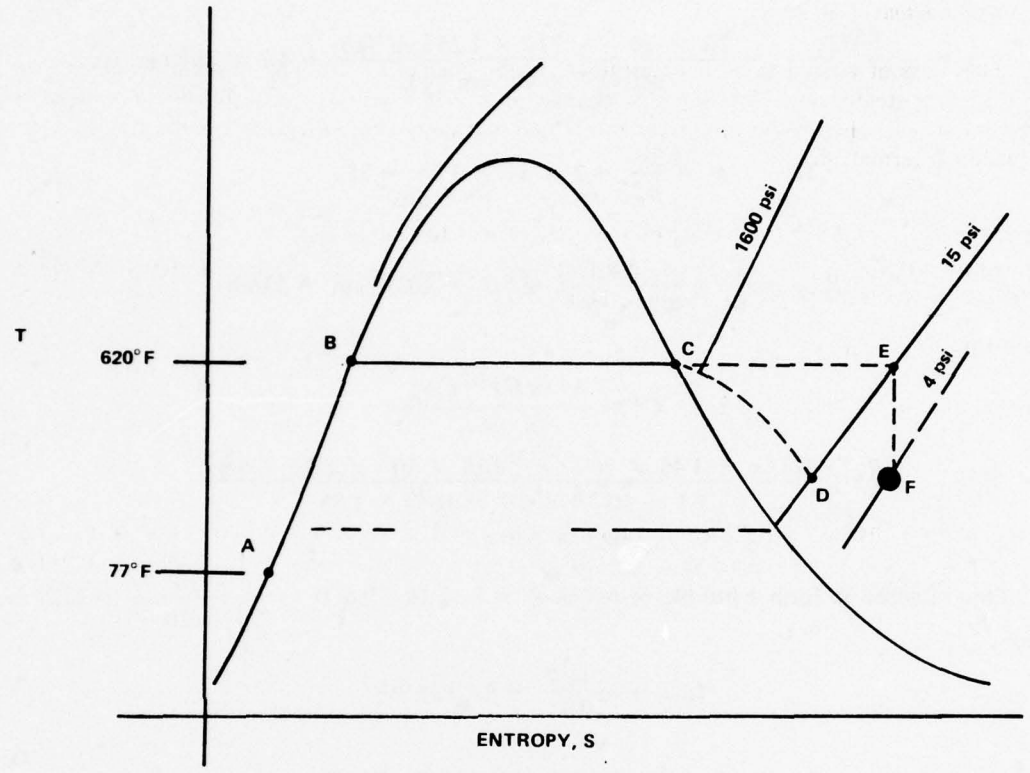

Fig. 17 – Temperature entropy chart for water

Embryo Bubble Radius (Critical Radius)

At the instant of explosion (point B on the TS chart) there is present an embryo (or initial bubble) in the heated spike. We wish to determine its size. The critical bubble size is obtained by momentarily balancing all pressures at the bubble wall:

$$p_v + p_g - \left[p_\infty + \frac{2\sigma}{R_{crit}}\right] = 0.$$

neglecting the vapor pressure due to permanent gases (p_g), we have

$$R_{crit} = \frac{2\sigma}{p_v(T) - p_\infty}.$$

Here σ is the surface tension; estimated from Ref. [21] to be 10 dyne/cm at $T = 600°K$. Taking p_∞ to be 15 psi, we calculate

$$R_{crit} = \frac{2 \times 10}{(1786 - 15)\, 6.895 \times 10^4} = 1.6 \times 10^{-7}\ \text{cm} = 1.6\ \text{nm}.$$

Mass and Volume of Water Heated

The mass of water heated is determined by the change in enthalpy in going from 77°F to 620°F. From steam tables we find this change to be 646.7 − 45 ≃ 600 Btu/lb. For reasons noted earlier, we choose the energy of the cosmic particle to be 4 Mev. Thus the mass of water heated (thermal spike) is

$$m_W = \frac{E}{\Delta h} = \frac{4 \times 10^6 \text{ eV} \times 1.6 \times 10^{-5} \text{ J/eV}}{600 \text{ (Btu/lb)} \times 2.32 \text{ (J/g)/(Btu/lb)}} = 4.6 \times 10^{-16} \text{ g}.$$

The volume V_w of heated water is found from the specific volume of water at 620°F, which is 0.0247 ft^3/lb ($\times$ 62.428 = 1.54 cm^3/g). Thus

$$V_w = 4.6 \times 10^{-16} \text{ g} \times 1.54 \frac{\text{cm}^3}{\text{g}} = 7.1 \times 10^{-16} \text{ cm}^3$$

whose radius is

$$R_w = \left[7.1 \times 10^{-16} \times \frac{3}{4\pi}\right]^{1/3} = 5.5 \times 10^{-6} \text{ cm} = 55 \text{ nm}.$$

In accord with the growth process pictured by Sette and Wanderlingh this volume of water is considered to be a heat source which contains a supply of heat (4 MeV) to expand the embryo (process BCD on the TS chart, Fig. 17).

Final Bubble Radius

From the heat balance equation we have

$$\Delta T = \frac{E}{mL}.$$

In infinitesimal form,

$$dT(t) = -\frac{1}{mL}\frac{\partial E(R)}{mL\,\partial R} = -\frac{\Delta T}{E}\frac{\partial E(R)}{\partial R}\,dR.$$

The minus sign means that an increase in radius of the bubble corresponds to a decrease in temperature. As before

$$E(R) = 4\pi R^2 \sigma^* + m_g \Delta H^v\,[T(R)].$$

To estimate the mass of vapor, we note that 4 MeV will bring 4.6 $\times$ 10^{-16} g water to 600°K. The same 4 MeV will expand an embryo to a radius of unknown value at point A on the TS chart, where the enthalpy is 1150 Btu/lb. Thus the mass of vapor is estimated to be

$$m_g = \frac{600}{1150 - 45} \times 4.6 \times 10^{-16} = 2.5 \times 10^{-16}\text{g}.$$

From Fig. 18 the value of ΔH^v of gassed water at 375 K is approximately −6.5 kJ/mole. Hence the energy required is

$$E(R) = 4\pi (7 \times 10^{-5})^2\, 140 - 6.5 \times 10^3 \left[\frac{10^7}{18}\right] (2.5 \times 10^{-16}) \text{ erg}$$

$$= 5 \text{ MeV},$$

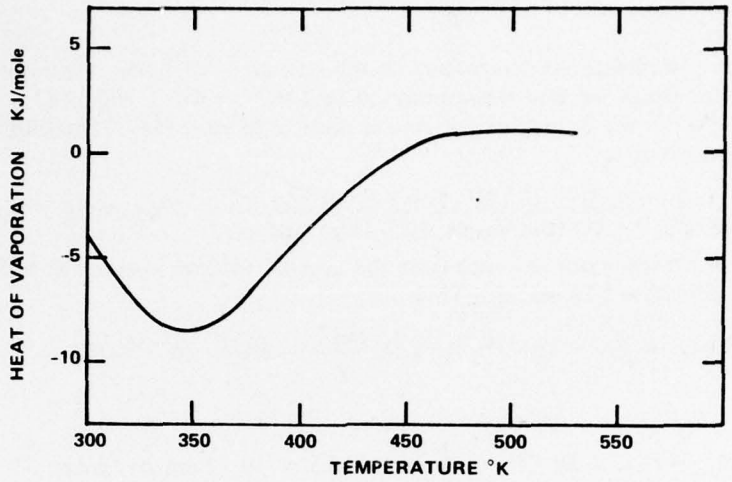

Fig. 18 – Heat of vaporization of water vs temperature

where $\sigma^* = 140$ in from Ref. [21]. Here the final temperature is taken to be 215°F. Since this energy is nearly the 4 MeV we have postulated, we will accept the 4 MeV as consistent with a mass m_g of 2.5×10^{-16} g vapor.

Let us specify the terminal thermodynamic point more carefully. The specific volume is

$$V_g = \frac{\frac{4}{3}\pi\ (7 \times 10^{-5})^3}{2.5 \times 10^{-16}} = 5.74 \times 10^3 \frac{\text{cm}^3}{\text{g}} = 92\ \text{ft}^3/\text{lb}.$$

Thus point D on the TS chart has $h = 1155$ Btu/lb, $s = 1.896$, $T = 215$°F (~375 K), and $p_v = 4.3$ psi.

If the water is not gassed, the latent heat ΔH^v and critical radius change. From a bubble at $R_{crit} = 7 \times 10^{-5}$ cm is at temperature of about 410 K (137°C or ~280°F), and from Fig. 18 (Ref. 17) ΔH^v is -4×10^3 J/mole. The total energy required is still about 4 MeV, and the mass of vapor is still 2.5×10^{-16} g. The specific volume is also the same, the enthalpy is 1185 Btu/lb, the entropy $S = 1.93$, and the vapor pressure is 4.8 psi.

Acoustic Radiation Based on Rayleigh's Formulas

Since the derivation of a history of wall expansion (namely $R(t)$) is fraught with difficulties, we will resort to a modified Rayleigh theory to calculate the acoustic effect of growing and collapsing bubbles. A convenient summary of this modified theory is found in Ref. [22].

We first simplify the picture and assume there is an average driving pressure throughout the growth period which performs work in expanding the bubble from $R \sim O$ to $R = 7 \times 10^{-5}$ cm. We neglect compression of the medium. Thus, for a volume change ΔV, and 100% heat-to-work efficiency,

$$p_{av}\,\Delta V = E_{\text{input}}$$

or

$$p_{av} = \frac{4 \times 10^{6} \times 1.6 \times 10^{-12}\ \text{erg}}{\frac{4}{3}\pi (70 \times 10^{-6})^{3}} = 4.45 \times 10^{6}\ \text{dyne/cm}^{2}.$$

Thus although the initial pressure is 1786 psi abs and the final pressure is about 4 psi, the average pressure is about 4-1/2 atmospheres (say 67 psi). The potential energy of the fully expanded bubble is then

$$P.E. = p_{av}\,\Delta V = 6.4 \times 10^{-6}\ \text{erg}.$$

According to Rayleigh's theory the wall velocity is approximately constant during most of the growth phase. Thus [23]

$$\dot{R} = \sqrt{\frac{2}{3}\frac{P_{av}}{\rho_f}} = \sqrt{\left[\frac{2}{3}\right]\frac{4.45 \times 10^{6}\text{dyne/cm}^{2} \cdot \text{cm}^{4}}{1\ \text{dyne} \cdot \text{s}^{2}}}$$

$$= 17\ \text{m/s}.$$

(Note that the density of the water is taken at room temperature.) Since this wall velocity is well below the velocity of sound (~1.5 km/s), compressibility effects can be neglected. The average time required to expand the bubble to its final radius is

$$t_{av} = \frac{0.7 \times 10^{-6}\text{m}}{17\ \text{m/s}} \simeq 0.04\ \mu\text{s}.$$

The *average* acoustic power radiated over the period of the growth phase is obtained by integrating over the square of the acceleration:

$$E_{ac} = \frac{\rho_f}{4\pi\, C_f} \int_0^t \ddot{R}^2(t)\, dt, \quad \ddot{R} = 4\pi (2R\dot{R}^2 + R^2\ddot{R}).$$

For constant velocity this reduces to [24]

$$\frac{E_{ac}}{P.E.} = \frac{8}{3}\sqrt{\frac{2p_{av}}{3\,\rho_f\, C_f^2}} = \frac{8}{3}\sqrt{\left[\frac{2}{3}\right]\frac{4.45 \times 10^{6}}{1\,(1.5 \times 10^{5})^{2}}} \simeq 0.03.$$

Thus only about 3% of the input energy is radiated as sound. For an input of 4 MeV, the acoustic power radiated in 0.04 μs is

$$E_{ac} = 0.03 \times 4\ \text{MeV} \times 0.16\ \text{pJ/MeV} = 0.02\ \text{pJ} = 2 \times 10^{-7}\ \text{erg}.$$

The average acoustic pressure at 1 m from the center of the bubble is

$$< p^2 >^{1/2} = \sqrt{\frac{E_{ac}\,\rho_f\, C_f}{\Delta t\, 4\pi\, R^2}} = \sqrt{\frac{2 \times 10^{-7} \times 1 \times 1.5 \times 10^{5}}{4 \times 10^{-8}\, 4\pi\, (10^{2})^{2}}}$$

or

p_{av} = 2.4 dynes/cm^2 at 1 m, transient, from one bubble due to 4-MeV cosmic-particle interaction product.

Resonant Frequency, Steady-State Radiation

The pressure calculated above is the average (shock wave) pressure transient over the period of bubble formation. Subsequent to formation the bubble will execute quasi-harmonic vibrations at the resonant frequency f_R, where [25]

$$f_R = \frac{1}{2\pi R_o} \sqrt{\frac{3\gamma P_{ext}}{\rho_f}}$$

in which R_o is the nominal bubble radius, $\gamma = C_p/C_v$ of the gaseous contents of the bubble, P_{ext} is the external pressure on the bubble, and ρ_f is the density of the water "at infinity." For air $C_p = 0.24$, $C_v = 0.17$, and $\gamma = 1.41$; for water $C_p \simeq 0.35$, $C_v \simeq 0.27$, $\gamma_{water\ vapor} \simeq 1.3$ at room temperature. For ease in computation we take $\gamma = 4/3$ for both gases in the cavity. The external pressure is

$$P_{ext} = P_\infty + \frac{2\sigma(T)}{R_o}.$$

Let us make this calculation on the assumption that the final bubble temperature is 410 K (137°C $\simeq$ 280°F); we then estimate $\sigma = 40$ dyne/cm [21]. Setting $P_\infty = 1$ atmosphere, we obtain for a 0.7μm bubble,

$$P_{ext} = 1.03 \times 10^6 + \frac{2 \times 40}{7 \times 10^{-5}} = 2.2 \times 10^6 \text{ dyne/cm}^2$$

Thus the resonant frequency of the bubble is

$$f_R = \frac{1}{2\pi \times 7 \times 10^{-5}} \sqrt{\frac{3\left[\frac{4}{3}\right] 2.2 \times 10^6}{1}}$$

$$\simeq 7 \text{ MHz}.$$

To calculate the acoustic radiation due to resonance of the bubble, we must account for energy losses. We assumed earlier that the potential energy of the bubble at radius $R = 0.7$ μm is exactly the energy of deposition (4 MeV). Now let y represent the fraction of energy input lost in shock-wave radiation *both* in the growth and collapse phase. Although we have not calculated the collapse phase, we assume it radiates the same as the growth phase. Thus the energy available for energizing bubble vibrations is $E_R = (1 - y)\, E_{input} = (1 - y)4$ MeV. We use this energy to determine the volume displaced in going from $R = R_o = R_{nominal}$ $= 0.7$ μm (say) to some minimum radius $R_o - a$ during vibration. The potential energy at minimum radius is seen to be

$$P.E._{\min} = 6\pi\gamma P_{ext} R_o a^2,$$

so that

$$a = \sqrt{\frac{E_R}{6\pi\gamma P_{ext} R_o}}.$$

where E_R is the potential energy *ar* radius R. From the previous calculation we estimate y to be 0.06, so that $E_R = 0.94 \times 4 \times 10^6 \times 1.6 \times 10^{-12} = 6 \times 10^{-6}$ erg. Hence

$$a = \sqrt{\frac{6 \times 10^{-6}}{6\pi \left[\frac{4}{3}\right] 2.2 \times 10^6 \times 7 \times 10^{-5}}} = 0.39\ \mu\text{m}.$$

If we assume sinusoidal radial motion during vibration, so that at the resonant frequency

$$R = R_o + a \sin 2\pi f_R t,$$

then

$$\dot{R} = 2\pi f_R a \cos 2\pi f_R t.$$

The volume velocity is then

$$S = (4\pi R_o^2) 2\pi f_R a \cos 2\pi f_R t.$$

Hence the steady-state amplitude of radiated (acoustic) pressure will be (at 1 m)

$$|p_{ac}| = \frac{\omega \rho_f}{4\pi R} (\omega S) = \frac{(2\pi \times 6.7 \times 10^6)^2 (1) (7 \times 10^{-5})^2 (3.9 \times 10^{-5})}{10^2}$$

or

$|p_{ac}|$ =3.4 dynes/cm^2, rms steady state (maximum) at 1 meter at resonant frequency f_R = 6.7 MHz from 1 bubble excited by 0.94 × 4 MeV.

Since the radiation has a finite band of frequencies because the radial motion is not exactly periodic, we will calculate the acoustic effect at 25 kHz. That is, roughly,

$$|p_{ac}| = 3.4 \times \left[\frac{2.5 \times 10^4}{6.7 \times 10^6}\right]^2 = 4.7 \times 10^{-5} \text{dynes/cm}^2$$

rms steady state at 25 kHz at 1 meter from 1 bubble excited by 0.94 × 4 MeV.

This result is based on acoustic pressure being proportional to radial acceleration of the bubble wall, hence proportional to (frequency)^2.

Extrapolation to Higher Energies

Let us assume that a single cosmic particle enters the ocean with an energy of 10^{14} eV. If every 4-MeV interaction collision generated one bubble, we could expect 2.5×10^{7} bubbles to form (at the maximum). Further, if all bubbles radiated coherently, then the steady-state acoustic pressure measured at 25 kHz would be

$$|p_{ac}| = 4.7 \times 10^{-5} \times 2.5 \times 10^{7} = 1.2 \times 10^{3} \text{ dynes/cm}^2 \text{ at 1 meter at 25 kHz due to a } 10^{14}\text{-eV particle (steady state).}$$

At 100 m this pressure reduces to

$$|p_{ac}| \simeq 12 \text{ dynes/cm}^2.$$

This is above ambient noise (at 25 kHz).

Collapse Pressure and Acoustic Radiation

The initial calculation made above was based on an isothermal expansion *BC* to a final state *B* at 280°F and about 4 psi, the last part of the expansion being unknown. To estimate collapse pressures, we require a more expicit statement of the final stage of expansion. From Ref. 17 it can be inferred (though it is not so stated by them) that the final expansion is adiabatic. Hence we hypothesize the path on the *TS* chart (Fig. 17) to be *ABCDEF*.

Let us calculate the final radius at point *E*. We calculated previously that 4.6×10^{-16} g of water are heated on the thermal spike to 620°F, requiring an input of 4 MeV. We now allow this heated spike to transfer heat to the embryo bubble, expanding it isothermally from *B* to *C* to *E*, the point *E* being at 620°F and atmospheric pressure, with a specific volume of 43.6 ft^3/lb ($\times 6.24 = 2.72 \times 10^{3}\ \text{cm}^3/\text{g}$), enthalpy of 1344 Btu/lb, and entropy of 1.982. We next imagine that the final expansion from *E* to *F* takes place at constant entropy to a temperature of 280°F. At this point the pressure p_v is 2.1 psi, the specific volume is 192 ft^3/lb, and the enthalpy is 1159 Btu/lb. To bring water to superheat at *E* requires an addition of $1344.5 - 45 \simeq$ 1300 Btu/lb. We estimate the number of grams of superheated vapor to be

$$m_s = \frac{600}{1300} \times 4.6 \times 10^{-16} = 2.12 \times 10^{-16} \text{ g}.$$

Since the specific volume is $192 \times 62.4 = 1.198 \times 10^{4}\ \text{cm}^3/\text{g}$, the volume of superheated vapor is

$$V_s = 2.12 \times 10^{-16} \text{ g} \times 1.198 \times 10^{4} \frac{\text{cm}^3}{\text{g}} = 2.54 \times 10^{-12} \text{ cm}^3,$$

whose radius is,

$$R_s = \left(2.54 \times 10^{-12} \times \frac{3}{4\pi}\right)^{1/3} = 0.846\ \mu\text{m}.$$

This is close, but not quite the assumed final value of 0.7 μm. To obtain a more consistent final point we require that the adiabatic expansion arrive at a radius of 0.7 μm, hence at a specific volume of

$$N_s = \frac{V_s}{m_s} = \frac{\frac{4}{3}\pi(7 \times 10^{-5})^3}{2.12 \times 10^{-16}} \frac{\text{cm}^3}{\text{g}} = 6.8 \times 10^3 \text{ cm}^3/\text{g}$$
$$= 108 \text{ ft}^3/\text{lb}.$$

The terminal point (from steam tables) is then 350°F, enthalpy is 1209 Btu/lb, entropy is 1.982, and pressure is 4.5 psi.

After expansion the forces acting on the maximum bubble are unbalanced. The net collapse pressure will now be calculated. This is

$$p_{net} = P_\infty + \frac{2\sigma}{R_{\max}} - p_v - p_g.$$

at $T = 350°\text{F}$ ($\simeq 175°\text{C}$) we estimate $\sigma = 35$ dyne/cm, so that

$$p_\sigma = \frac{2\sigma}{R_{\max}} = \frac{2 \times 35}{7 \times 10^{-5}} = 10^6 \text{ dyne/cm}^2.$$

Also, at a temperature of 350°F ($\simeq$458 K) we estimate the dissolved gases to have a pressure of 2.7×10^3 dynes/cm^2 (see below for this estimate). Since $p_v = 4.5$ psi ($\times 6.895 \times 10^4 = 3.1 \times 10^5$ dynes/cm^2), and since $P_\infty = 1$ atmosphere,

$$p_{net} = 1 \times 10^6 + 1 \times 10^6 - 3.1 \times 10^5 - 2.7 \times 10^3$$
$$= 1.69 \times 10^6 \text{ dynes/cm}^2.$$

Let us asume that during collapse the vapor is not instantly reabsorbed, so that it can act as a buffer to total disappearance of the cavity. Then the ratio of the net collapse pressure to the vapor pressure (called P/Q) is

$$\frac{p_{net}}{p_v} \equiv \frac{P}{Q} = \frac{1.69 \times 10^6}{3.1 \times 10^5} = 5.44, \quad \text{or} \quad \frac{Q}{P} = 0.18.$$

These ratios will enable us to calculate bubble dynamics on collapse. The minimum radius of collapse is obtained by setting [26]

$$R_{\min} = R_{\max}\left(\frac{Q}{P(\gamma - 1)}\right)^{1/3(\gamma-1)}\left(1 + \frac{Q}{P(\gamma - 1)}\right)^{-1/3(\gamma-1)}$$

This formula is due to Neppiras and Noltingk [27].

Assuming $\gamma = 4/3$, we obtain

$$\frac{R_{\min}}{R_{\max}} = \frac{0.18 \times 3}{1 + 0.18 \times 3} = 0.35 \left[\text{say } \frac{1}{3}\right].$$

This parameter, plus knowledge of P/Q, allows us to calculate the peak radiated shock wave on collapse. From Ref. [28] at 1 m

$$p^+_{\max} = \frac{P_{net}}{3}\frac{R_{\max}}{r}\left(\frac{R_{\max}}{R_{\min}}\right)^2\left[1 - 4\left(\frac{R_{\min}}{R_{\max}}\right)^3\right]$$
$$= \frac{1.69 \times 10^6 \text{ dyne/cm}^2}{3} \times \frac{7 \times 10^{-5}\text{cm}}{10^2}(3)^2\left[1 - 4\left(\frac{1}{3}\right)^3\right]$$

or

P^+_{max} $\simeq$ 3 dyne/cm^2 shock amplitude at 1 m during collapse of a 0.7 μ m bubble based on assuming the vapor acts as a buffer.

The shock power radiated is (roughly) given by [29]

$$\frac{E_{ac}}{P.E.} \simeq \frac{1}{3}\sqrt{\frac{2P_{net}}{3\rho_f C_f^2}}\left(\frac{R_{max}}{R_{min}}\right)^{3/2}$$

$$\simeq \frac{1}{3}\sqrt{\frac{2 \times 1.69 \times 10^6}{3 \times 1 \times (1.5 \times 10^5)^2}}\,(3)^{3/2}$$

$$= 0.012.$$

We estimated earlier that the acoustic output on collapse was about the same as upon growth (3% each). Here the figure on collape is 1%. Of course some of the vapor will be reabsorbed on collapse. Hence 1% is too pessimistic. If *all* the vapor returned to the liquid (water) upon collapse, and left only permanent gas pressure, then it is simple to calculate that the peak shock wave pressure will be $p^+_{max} = 1.5 \times 10^5$dynes/cm^2 at 1 m from one bubble. This is overly optimistic.

Calculation of Gas Pressure

The partial pressure of the permanent gases in the bubble is an essential parameter in calculating the shock-wave magnitude. However it is difficult to calculate it. The gas content of the ocean is reported in books on oceanography in the following way. First, whatever the location of the water volume, it is assumed that at some time it had been at the surface of the ocean and in equilibrium with the air [30]. Thus regardless of depth the water is assumed nearly saturated (at NTP = normal temperature and pressure). Hence gas content is reported in saturation values (say *ml/l*) in equilibrium with a normal dry atmosphere. From page 188 of Ref. [21] we see that at 0°C and 35% salinity the saturation volume of oxygen in seawater is about 8 *ml/l* and of nitrogen is about 14 *ml/l*. We next suppose this dissolved gas is in the microbubble described above, and we desire to calculate the partial pressure of the dissolved gases at the interface. According to Henry's law the concentration m of a gas in a liquid is related to the partial pressure of the gas as $m = C_s p$, where C_s is the coefficient of saturation. If m is expressed in units of milliliters per liter and p is expressed in torr (760 torr = 1 atmos = 1 $\times 10^6$ dynes/cm^2), then at 0°C (273 K) and 35% salinity the value of C_s is 38 for oxygen (O_2) and 14 for nitrogen (N_2) [Table 41, p. 191, Ref. [30]]. Thus the partial pressures are

$$O_2\colon p_{O_2} = \frac{m}{C_s} = \frac{8}{38} \times \frac{1 \times 10^6}{760} = 2.8 \times 10^2 \text{ dynes/cm}^2$$

and

$$N_2\colon p_{N_2} = \frac{14}{14} \times \frac{1 \times 10^6}{760} = 1.3 \times 10^3 \text{ dynes/cm}^2.$$

The total gas pressure is therefore about 1.6×10^3 at O°C. However the temperature of the bubble at maximum radius is taken to be 458 K. Hence the estimated gas pressure is 458/273 $\times$ $1.6 \times 10^3 = 2.6 \times 10^3$ dynes/cm^2.

Effect of Depth of Particle in the Ocean

Let us again consider a 4-MeV particle heating a mass of 4.6×10^{-16} g water in a thermal spike to 620°F, at which temperature the specific volume is 0.0247 ft^3/lb ($= 1.54\ cm^3/g$). As before this water acts as a heat source and feeds an embryo that expands (say) to ambient pressure. Let ambient be 1600 psi (say about 3500 ft, or 1 km, of water). At the end of expansion the pressure is so great that the specific volume is only 0.272 ft^3/lb ($\times\ 62.4 = 16.97\ cm^3/g$) the enthalpy is 1187 Btu/lb, and the entropy is 1.348. Since only 600 Btu/lb is available, the mass of the heated vapor is

$$m_g = \frac{600}{1187 - 45} \times 4.6 \times 10^{-16} = 2.4 \times 10^{-16}\ g.$$

Thus the volume of superheated vapor is

$$V_s = 2.4 \times 10^{-16}\ g \times 16.97 \frac{cm^3}{g} = 4.1 \times 10^{-15}\ cm^3,$$

whose radius is

$$R_s = \left[4.1 \times 10^{-15} \times \frac{3}{4\pi}\right]^{1/3} = 9.9 \times 10^{-6}\ cm\ (\text{say } 0.1\ \mu m).$$

We compare this expansion to 1600 psi with the earlier calculated expansion to 15 psi (at 620°F). At the latter point the specific volume is $2.72 \times 10^3\ cm^3/g$, from which the volume of heated vapor is

$$V_{s_{15psi}} = 2.4 \times 10^{-16}\ g \times 2.72 \times 10^3 \frac{cm^3}{g} = 6.5 \times 10^{-13}\ cm^3,$$

whose radius is

$$R_{s_{15psi}} = \left[6.5 \times 10^{-13} \times \frac{3}{4\pi}\right]^{1/3} = 5.4 \times 10^{-5}\ cm = 0.54\ \mu m.$$

Thus the resultant bubble at 1600 psi is about 5-1/2 times smaller than at 15 psi for the same energy. However it is larger than critical ($\simeq$ 1 nm); hence it can grow by further adiabatic expansion. But Sette and Wanderlingh show [Fig. 7] that the final expansion (after isothermal expansion) is small. We have calculated that in the case of adiabatic expansion from 620°F at 15 psi to 350°F at 4.5 psi the change in radis is about 2/7 or 30%. Thus we estimate the final radius at the depth of 1 km to be about 0.13 μm, still a factor of about 7 smaller than a bubble near the ocean surface. This smaller radius bubble will reduce the acoustic effect. For example the peak shock wave on collapse will be about 7 times smaller, assuming the ratio of R_{min}/R_{max} is about the same as in the earlier case. Greater depths will even have a more drastic effect, primarily due to reduction of the maximum bubble that can form with the given input energy. Of course, if higher energy particles participate in bubble formation, a larger acoustic output can be expected.

JET MODELS AND OTHER MODELS

Jet Models

After a cosmic particle creates a shower of interaction products in a liquid, the shower itself can be imagined to be the continuation of a jet of equal diameter entering the liquid from

the outside. This jet creates noise as it traverses the liquid. Several mechanisms may be considered. The principal mechanism is injection of mass of jet, hence monopole radiation is to be expected. However, if the flow of the jet meets obstacles (fluid molecules), the expected radiation is dipole. If the jet creates thermal (or velocity) turbulence, the radiation will be quadrupole. Our objective will be to calculate the noise power due to these three mechanisms.

By dimensional analysis one can establish relations between the parameters of jet noise. These are: the density ρ_j of the jet material, the speed V of the jet flow, the pertinent length L and the mach number $M = V/c$, where c is the speed of sound in the liquid. For jets of finite cross-sectional area S one chooses L such that $L^2 \simeq S$. The relations between the noise power W generated and these parameters are as follows:

monopole radiation: $W_m \propto \rho_f L^2 V^3 M$
dipole radiation: $W_d \propto \rho_f L^2 V^3 M^3$
quadrupole radiation: $W_q \propto \rho_f L^2 V^3 M^5$

The constants of proportionality depend on the process. Various estimates of their magnitude have been calculated. For example, if the mechanical stream of the jet has a kinetic power

$$W_{mech} = \frac{1}{2} m_j V^2 \quad \text{(units of } m_j\text{: kg/s)},$$

then the acoustic power generated is roughly

$$W_{ac} \simeq W_{mech} \frac{M^{5.5}}{1420}, \quad \frac{\rho_j}{\rho_f} = 10,$$

$$\simeq W_{mech} \frac{M^{5.5}}{10{,}830}, \quad \frac{\rho_j}{\rho_f} = 1,$$

$$\simeq W_{mech} \frac{M^{5.5}}{120{,}470}, \quad \frac{\rho_j}{\rho_f} = 0.01,$$

provided $W_{ac} < W_{mech}$ [Ref. 31]. Since $W_{mech} \equiv \rho_f SV = \rho_f L^2 V$, we see that

$W_m = W_{mech} M \simeq const.\ W_{ac} M^{-4}$,
$W_d = const.\ W_{ac} M^{-2}$,
$W_q = const.\ W_{ac}$.

The constant in each case matches the constant in the expression for W_{ac}.

The calculation of the effective mach number M of the fluid jet requires considerable care. Let the imagined cosmic-particle jet have a unit flux of energy (per cross-sectional area) of magnitude W_j. Upon interaction with the liquid the particle jet is converted to a liquid jet whose power is W_f. The interaction itself depends on the capture area presented by the fluid to the incident particle stream. The ratio of powers W_f to W_p is designated γ, where

$$\gamma = \frac{m_f V_f^2/2}{m_j V_j/2},$$

in which m_j and m_f represent mass flow. Assume next that the mass flows are proportional to mass density. Then

$$\gamma = \frac{\rho_f V_f^2}{\rho_j V_j^2} \text{ or } V_f = \left(\frac{\gamma \rho_j}{\rho_f}\right)^{1/2} V_j.$$

This is the initial velocity of the fluid. Thus the effective mach number of the jet is,

$$M_f = \frac{V_f}{C_f} = \frac{1}{C_f}\left[\frac{\gamma\rho_j}{\rho_f}\right]^{1/2} V_j.$$

Noting that $W_{mech} = \gamma W_j$, we see that the acoustic power generated is

$$\frac{W_{ac} = \gamma\ W_j \left[\left[\frac{\gamma\rho_j}{\rho_f}\right]^{1/2} \frac{V_j}{C_f}\right]^{5.5}}{K_1},$$

where

$$K_1 = 1420 \quad \frac{\rho_j}{\rho_f} = 10$$

$$K_1 = 10{,}830 \quad \frac{\rho_j}{\rho_f} = 1$$

$$K_1 = 120{,}470 \quad \frac{\rho_j}{\rho_f} = 0.1$$

The coefficient of momentum transfer γ is roughly the ratio of the scattering cross section of the incident particle to that of the fluid particle. The noise power generated is seen to be proportional to $\gamma^{3.75}$.

Transient Radiation From Sources in Motion

When a cosmic particle is decelerated by a liquid the liquid itself is accelerated. Such an acceleration constitutes an acoustic source, and an acoustic pressure (shock wave) is radiated outward. A simple theory constructed on this picture is as follows.

Let the volume flux of liquid set into motion be $S(m^3/s)$, and let the corresponding mass flux be $\rho_f S = q(t)$ (units: N · s/m). The motion of the cosmic particle is equavalent to the motion of $q(t)$. The latter constitues source distribution density $Q(\mathbf{r},t)$ (units: N · s/m^4) of form,

$$Q(\mathbf{r},t) = q(t)\ \delta(z - Vt)\ \delta(y)\delta(x),$$

which radiates shock waves according to the formula

$$\nabla^2 p - \frac{1}{c^2}\frac{\partial^2 p}{\partial t^2} = -\frac{\partial}{\partial t} q(t)\ \delta(z - Vt)\ \delta(y)\ \delta(x).$$

The solution of this equation is obtained by a coordinate transformation [4, pp. 721 ff]. When the velocity V of the equivalent source is supersonic (as we assume), the solution can be expressed as function of distances R^+, R^-, and angles θ^+, θ^-, explained below; thus

$$p(R,\theta,t) = \frac{-q'\left(t - \frac{R^+}{c}\right)}{4\pi R^+ (M\cos\theta^+ - 1)^2} + \frac{q'(t - R^-/c)}{4\pi R^- (m\cos\theta^- - 1)^2}$$
$$- \frac{q(t - R^+/c)\ (M - \cos\theta^+)V}{4\pi\ (R^+)^2\ (M\cos\theta^+ - 1)^3} + \frac{q(t - R^-/c)}{4\pi\ (R^-)^2\ (M\cos\theta^- - 1)^3}\frac{(M - \cos\theta^-)V}{},$$

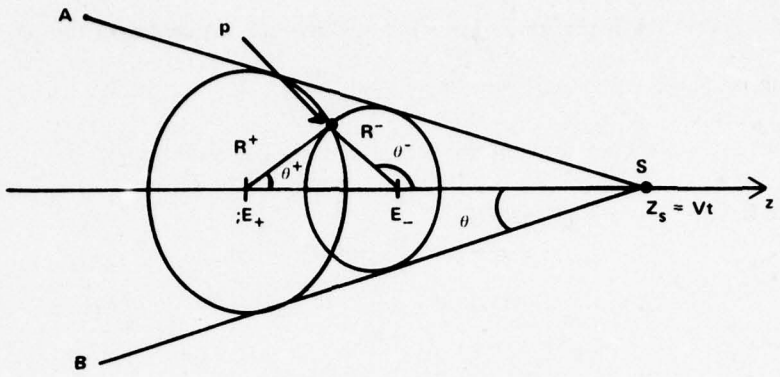

Fig. 19 – Transient radiation from a source in motion

in which q' is the derivative with respect to the argument. Distances and angles are given by Fig. 19. In this figure the source S is moving in the direction z with supersonic velocity V (mach number $M > 1$). It is the origin of a cone of shock waves (A, B). Any point P inside the cone will hear the pressure p given above at time t. This pressure will consist of radiation from two fictitious origins, E_+ and E_-, with E_+ at a distance R_+ from P, and E_- at distance R_- from P (E_- is in front of P and E_+ is behind). The distances are given by

$$R_{\pm} = \frac{M(Vt - z) \pm (Vt - z)\sqrt{1 - \dfrac{(M^2 - 1)r^2}{Vt - z)^2}}}{M^2 - 1}, \quad r^2 = y^2 + z^2.$$

The half angle of the cone is $\theta = \sin^{-1}(M^{-1})$. Outside the cone at time t there is silence. The directionality inherent in the formula for pressure p must be obtained by numerical evaluation. If the time dependence is harmonic, that is, $q'(t - R/c) = q_O\omega_o \cos \omega_o(t - R/c)$ then the fields due to E_+ and E_- interfere, so that the reserved sound pressure oscillates with time (beating phenomenon). The amplitude spectrum of the radiated pressure can be obtained by Fourier transformation:

$$p(R,\theta,\omega) = \int_{-\infty}^{\infty} e^{i\omega t}\, p(r,\theta,t)\, dt.$$

Another model of cosmic particles as travelling sources may have relevance to acoustic pulse formation. In this picture the interaction products bounce back and forth due to successive collisions. Thus the advance of the cosmic particle is imagined to be that of a *dipole* source travelling with supersonic speed. A formulation of the pressure field developed is presented for convenience.

The bouncing byproducts exert a force F_j (per unit volume) conceived to be

$$F_j = f_j(t)\, \delta(z - Vt)\, \delta(x)\, \delta(y),$$

in which $f_j(t)$ is an impulse force (units: N). To apply this force to the pressure equation, one lets $p = \text{div } \mathbf{A}$, and solves for $\mathbf{A}$; the governing equation is

$$\nabla^2 A_j - \frac{1}{c^2}\frac{\partial^2 A_j}{\partial t^2} = f_j(t)\,\delta(z - Vt)\,\delta(x)\,\delta(y),$$

whose solution is

$$A_j = -\frac{f_j(t - R^+/c)}{4\pi R_1^+} - \frac{f_j(t - R^-/c)}{4\pi R_1^-}.$$

Ultimately the field pressure is [4 page 721ff]

$$p(\mathbf{r},t) = -\frac{f_j'(t - R^+/c)\cos\theta^+}{4\pi R^+ c(M\cos\theta^+ - 1)^2} - \frac{f_j(t - R^+/c)(M - \cos\theta^+)}{4\pi (R^+)^2 (M\cos\theta^+ - 1)^3}$$
$$+ \frac{f_j'(t - R^-/c)\cos\theta^-}{4\pi R^- c\,(M\cos\theta^- - 1)} + \frac{f_j(t - R^-/c)\,(M - \cos\theta)}{4\pi\,(R^-)^2\,(M\cos\theta^- - 1)^3}.$$

This dipole case is conceptually related to the monopole travelling source: if one sets $q\,V = f$, so that the oscillating force is numerically equal to the monopole mass flux traveling at velocity V, it is then possible to interchange the formulas. In particular one sets $q' = f'/c$, and then the derivations of the formulas are identical.

CONCLUSION

The generation of sound by sources is well understood when the sources can be categorized as monopole, dipole, quadrupole, etc. In the particular case of the noise pulses generated by cosmic particles in the ocean the greatest emphasis in modeling to date is on monopole sources related to the time-varying application of heat. Two varieties of heat models have been surveyed and developed in this report: the thermoelastic model, in which a deposition of heat into the liquid results in an elastic expansion which radiates outward as a shock wave, and is the microbubble model, in which the deposition of heat "boils" the liquid locally, creating an expanding (and collapsing) bubble, which radiates sound as shock waves. Other models are possible, such as a jet noise model, a moving-source model, and an explosion model. The first two have been noted, but no detailed calculations given. An explosion model is discussed in Appendix A. Numerical calculations of several heat models have been made in the text and are further amplified in Appendixes B and C. As expected, they yield different (even radically different) answers for the same input parameters. These differences are attributed to different conceptions of what the precise physical event is in the liquid. It is concluded that further progress in modelling must await renewed effort in experiment work.

ACKNOWLEDGMENTS

The author acknowledges the aid given to him during many fruitful discussions of the subject matter of this survey by Dr. M.M. Shapiro, Dr. R. Silberberg, and Mr. N. Seaman of the NRL Laboratory for Cosmic Ray Physics and Dr. D. Palmer and Mr. A. Rudgers of the NRL Acoustics Division.

REFERENCES

1. A. Roberts, editor, DUMAND Proceedings of Summer Workshop, U. of Hawaii, Sept. 1976, Office of Publications of Fermi Nat. Accel. Lab, Batavia, Ill.
2. "Selected Papers on Noise", N. Wax Ed. Dover 1954.

3. Obtained in private conversations with R. Silberberg and N. Seeman of the NRL Laboratory for Cosmic Ray Physics.
4. P.M. Morse and U. Ingard *Theoretical Acoustics*, McGraw-Hill, 1968.
5. P.M. Morse and H. Feshbach *Methods of Mathematical Physics*, McGraw-Hill, 1953.
6. P.J. Westervelt and R.S. Larson, J. Acous. Soc. Amer. **54**, 121-122 (1973).
7. E.F. Kozyaev and K.A. Naugol'nykh, Sov. Phys. Acoust. **22**, 206 (1976).
8. L.M. Lyamshev, K.A. Naugol'nykh "Sound Gen. by Thermal Sources" Sov. Phys. Acoust. **22**, (4), 354 (1976). 206 (1976).
9. Ref. [5], p. 857
10. W. Nowacki, *Dynamics of Elastic Systems*, Wiley, 1963.
11. "Sonic Particle Detection", T. Bowen, 15 th Int. Conf. on Cosmic Rays, Plovdiv, Bulgaria.
12. W. Probst "Die Schallerzeugang durch eine expandieren Krigel" Acoustica, **27**, 299 (1972).
13. G. Wenz, J. Acoust. Soc. Am. **34**, 1936 (1962).
14. R.H. Mellen, J. Acoust. Soc. Am. **24**, 478 (1952).
15. D. Sette, 3rd ICA 1959, 330-333.
16. D. Sette and F. Wanderlingh, Phys. Rev. **125**, 409 (1962).
17. D. Sette and F. Wanderlingh, J. Acoust. Soc. Am. **41**, 1074 (1967).
18. F. Seitz, Phys. Fluids **1**, 2(1958).
19. H.K. Forster and N. Zuber, J. Appl. Phys. **25**, 474 (1954).
20. J. Carslaw, *Conduction of Heat in Solids*, Oxford U. Press, 1st edition, p. 216.
21. J.F. Lee and F.W. Sears, *Thermodynamics*, 2nd edition, Addison-Wesley 1955.
22. D. Ross, *Mechanics of Underwater Noise*, Pergamon Press 1976.
23. Ref. [22], Eq. 7.9
24. Ref. [22], Eq. 7.41
25. M. Minnaert, Phil. Mag. **16**, 235 (1933).
26. Ref. [22], Eq. 7.25
27. B.E. Noltingk and E.A. Neppiras, Proc. Phy. Soc. London **63B**, 674 (1950).
28. Ref. [22], Eq. 7.47
29. Ref. [22], Eq. 7.45
30. Sverdrup et al. *The Oceans.*
31. L. Beranck "Noise and Vibration Control"

A1. R. Cole "Underwater Explosions" Dover Publ. p. 241.
A2. "Seismic Energy Sources" Bendix Handbook 1968, United Geophysical Corporation.

A1a. R.H. Cole "Underwater Explosions" Dor. Pub. p. 241
A1b. Ref. [A1a], p. 231
A1c. Ref. [A1a], p. 241
A1d. Ref. [A1a], p. 242
A1e. Ref. [A1a], p. 239
A1f. Ref. [A1a], p. 240

Appendix A
RADIATION MODEL BASED ON THE THEORY OF EXPLOSIVE SOURCES

In the theory of explosive acoustic sources the potential energy of the explosion bubble (W_B) is only a small percentage of the intrinsic energy of the source (W_s), that is, $W_B = K\,W_s$, where K is 0.10 or less. In the well-known theory of Willis the initial radius of a bubble due to potential energy W_B at hydrostatic pressure P is

$$R_o = \left(\frac{3\,W_B}{4\pi P}\right)^{1/3} = \left(\frac{3KW_s}{4\pi P}\right)^{1/3},$$

and the first period of the bubble oscillation from the Willis-Rayleigh theory is

$$T_B = 2 \times 0.914 \left(\frac{3KW_s}{4\pi P}\right)^{1/3} \left(\frac{\rho_f}{P}\right)^{1/2}.$$

Two types of radiation propagate from the bubble: a shock wave, and then a wave due to bubble oscillation. The peak pressure developed by the shock wave has been empirically found to be

$$P_{\max} = k\left(\frac{W^{1/3}}{R}\right)^{\alpha},$$

in which W is the weight of explosive (its internal energy), R is the distance of measurement, and k, α are empirical constants. Many experiments show that α is approximately unity. Thus $P_{\max} \propto W^{1/3}$ [A1a]. To include the effect of the explosion pressure subsequent to the passage of the peak pressure, one uses the time integral of the pressure, called the impulse, defined as

$$I(t) = \int_0^t P(t)\,dt.$$

Empirically the impulse is given by [A1b]

$$I = I\,W^{1/3}\left(\frac{W^{1/3}}{R}\right)^{\beta},$$

where I and β are constants

A third characterization of the shock wave is the energy flux E_f per unit area of a fixed surface normal to the directions of propagation. This is given by [A1c]

$$E_f = m\,W^{1/3}\left(\frac{W^{1/3}}{R}\right)^{\gamma},$$

where m and γ are constants

To use these empirical formulas, one requires a knowledge of the constants. They will depend on the type of explosive and the units. For example, let the explosive be TNT (density 1.52) and the units be English: pressure in psi, distance in feet, weight in pounds (mass), and energy density in inch-pounds of force per square inch. Then [A1d]

$$P_{\max} = 2.16 \times 10^4 \left(\frac{W^{1/3}\ \text{lb}}{R\ \text{ft}}\right)^{1.13} \quad \text{(units: psi)},$$

$$I = 1.46\ W^{1/3} \left(\frac{W^{1/3}}{R}\right)^{0.89} \quad \text{(units: psi} \cdot \text{s)}$$

and

$$E = 2.41 \times 10^3\ W^{1/3} \left(\frac{W^{1/3}}{R}\right)^{2.05} \quad \text{(units: lb} - \text{in./in.}^2$$

Here the integration time is taken (somewhat arbitrarily) as 6.7θ, where θ is the time constant of the initial high-pressure region.

To use these formulas for the case of high-energy particles we must relate the particle energy to the weight of TNT that is energetically equivalent. Only approximations are possible, and these depend on experience factors. Since the energy release of TNT depends on depth, we will take 30 ft, or 9 m, to be the depth in the following calculation.

We assume from experience [A2, p. 17] that 1 lb of TNT will release roughly 1.5×10^6 ft-lb of energy. (Another convenient estimate is: 1 g of explosive liberates 1 kilocalorie = 4.18 kJ $= 2.61 \times 10^{22}$ eV, or 1.19×10^{25} eV/lb or 1.4×10^6 ft·lb.) Converting to more convenient units, we have for the conversion factor E_W

$$E_W = \frac{1.5 \times 10^6\ \text{ft. lb/lb} \times 1.3558\ \text{J/ft. lb}}{453.6\ \text{g/lb}\ 1.6 \times 10^{-19}\ \text{J/eV}}$$

$$= 2.802 \times 10^{22}\ \frac{\text{eV}}{\text{g}}, \text{ or } 1.271 \times 10^{25}\ \text{eV/lb}.$$

For example a high-energy particle with $E_o = 10^{16}$ eV is equivalent to

$$\frac{10^{16}\ \text{eV}}{1.27 \times 10^{25}\ \text{eV/lb}} = 7.87 \times 10^{-10}\ \text{lb of TNT}$$

or

$$\frac{10^{16}\ \text{eV}}{2.802 \times 10^{22}\ \text{eV/g}} = .0356\ \mu\text{g of TNT}.$$

In conformity with our calculations in the section on microbubbles, we apply the above formulas to the case of a 4-MeV particle. The equivalent weight of TNT of such a particle is

$$W = \frac{4 \times 10^6\ \text{eV}}{1.271 \times 10^{25}\ \text{eV/lb}} = 3.15 \times 10^{-19}\ \text{lb of TNT}.$$

We indicated in the main text that the conversion efficiency from particle power to acoustic power is roughly 3% on expansion of the bubble and 1% on contraction. Let us arbitrarily assume a 2% energy conversion. Thus the actual energy available to form a bubble is assumed to be

$$W = 3.15 \times 10^{-19} \times 0.02 = 6.3 \times 10^{-21}\ \text{lb of TNT}.$$

Thus, applying the formula for the peak shock pressure (at 1 m = 3.28 ft), we obtain

$$p_{max} = 2.16 \times 10^4 \left[\frac{(6.3 \times 10^{-21})^{1/3}}{3.28}\right]^{1.13} = 1.388 \times 10^{-4} \text{ psi}$$

$$= 9.58 \text{ dynes/cm}^2 \text{ (peak)}.$$

Similarly, we can calculate the impulse at 1 m:

$$I = 1.46 \times (6.3 \times 10^{-21})^{1/3} \left[\frac{(6.3 \times 10^{-21})^{1/3}}{3.28}\right]^{0.89}$$

$$= 9.52 \times 10^{-14} \text{ psi} \cdot \text{s or } 6.57 \times 10^{-9} \text{ dynes/cm}^2 \cdot \text{s}.$$

If the dominant frequency is 25 kHz, we assume the integration time to be 1/25,000 = 40μs. The *average* pressure radiated is then

$$p_{av} = \frac{I}{\Delta t} = \frac{6.57 \times 10^{-9} \text{ dynes/cm}^2 \cdot \text{s}}{40 \times 10^{-6} \text{ s}} = 1.64 \times 10^{-4} \frac{\text{dyne}}{\text{cm}^2} \text{ at 1 meter.}$$

We note that both p_{max} and p_{av} are of the same order or magnitude as previously calculated in the main text. However this choice of integration time is quite arbitrary. Cole [A1e, p. 239] takes the integration time to be $t = 6.7\theta$ where θ, is the time constant of exponential decay of the main shock pulse (as if the pulse had the form $p = p_m \exp(-t/\theta)$). A plot of reduced time constant $\theta/W^{1/3}$ vs $W^{1/3}/R$ [A1f, p. 240] is out of the range of our numerical work. However we can try an estimate. We note that $\theta/W^{1/3}$ rises 0.05 ms sec per falling decade of $W^{1/3}/R$. For a 4-MeV particle whose effective TNT equivalent is roughly 6.3×10^{-21} lb, the value of $W^{1/3}/R$ at $R = 1$ m is

$$\frac{(6.3 \times 10^{-21} \text{ lb})^{1/3}}{3.28 \text{ ft}} = \frac{1.8469 \times 10^{-7}}{3.28} = 5.6 \times 10^{-8}.$$

This is roughly 10^7 or 7 decades lower than $W^{1/3}/R = 1$. Hence by extrapolation

$$\frac{\theta}{W^{1/3}} = 0.05 \times 10^{-3} + (0.05 \times 10^{-3})\, 10^7 = 5 \times 10^2.$$

The time constant is therefore

$$\theta \simeq 5 \times 10^2\, W^{1/3} = 5 \times 10^2 \times (6.31 \times 10^{-21})^{1/3} = 92.3\ \mu\text{s}.$$

Our estimated integration time is

$$t = 6.7 \times \theta = 6.7 \times 92.3\ \mu\text{s} = 0.62 \text{ ms}.$$

The average pressure radiated in this time is estimated to be

$$p_{av} = \frac{I}{\Delta t} = \frac{6.57 \times 10^{-9} \text{ dynes/cm}^2 \cdot \text{s}}{0.62 \times 10^{-3} \text{ s}} = 1.06 \times 10^{-5} \text{ dynes/cm}^2.$$

The characteristic frequency of the transient is $(\Delta t)^{-1} \simeq 16$ kHz.

Appendix B
COMPARISON OF ENERGY DENSITY OF COSMIC PARTICLES AND ENERGY DENSITY OF AMBIENT NOISE IN THE OCEAN

Ambient noise in the ocean is reported in decibel units referenced to the intensity (or energy density) of a plane wave of unit amplitude in a 1-Hz band. Thus if E_N is the energy density actually measured and E_{ref} is the reference, then the number of measured decibels is

$$N = 10 \log_{10} \frac{E_N}{E_{ref}}.$$

Hence

$$E_N = E_{ref}\, 10^{N/10} \text{ (units: } erg/cm^3 \cdot \text{Hz)}.$$

For example at 25 kHz the *lowest* measured ambient noise is reported as $N = -82$ dB "re 1 dyne /cm^2." This means that

$$E_N = E_{ref}\, 10^{-8.2} = E_{ref} \times 6.3 \times 10^{-9}.$$

Now the energy density of a plane wave of unit amplitude is

$$E_{REF} = \frac{p^2}{\rho c^2} = \frac{(1)^2}{1 \times (1.5 \times 10^5)^2} = 4.44 \times 10^{-11} \frac{\text{erg}}{\text{cm}^3},$$

from which

$$E_N = 4.44 \times 10^{-11} \times 6.3 \times 10^{-9} = 2.8 \times 20^{-19} \frac{\text{erg}}{\text{cm}^3 \cdot \text{Hz}}.$$

Using the same procedure we construct the following table.

Freq. (Hz)	N (dB)	(E_N (erg/cm^3 · Hz)
1	-11	3.5×10^{-12}
10	-40	4.4×10^{-15}
100	-60	4.4×10^{-17}
1,000	-73	2.2×10^{-18}
10,000	-80	4.4×10^{-19}
25,000	-82	2.8×10^{-19}
30,000	-84	1.76×10^{-19}

Let us assume that for various reasons we are requied to use a 10-kHz band for underwater detection of these particles. The average noise energy density in a 1-Hz band between 10,000 and 25,000 Hz is $\sim 3.6 \times 10^{-19}$ (erg/cm^2 · Hz). Thus in a 10^4-Hz band the average energy density is

$$3.6 \times 10^{-19} \times 10^4 = 3.6 \times 10^{-15} \text{ erg/cm}^3.$$

We desire to compare this with the energy density of the cosmic-particle flux. To do this, we let I_{Ω} be the particle flux density per steradian and E_p be the average energy per particle.

Then the total energy flux (intensity) is obtained by integrating over the solid angle of incidence:

$$I_p = \int I_\Omega E_p \, d\Omega \text{ (units: erg/cm}^2 \cdot \text{s)}.$$

We next assume that the particle flux is a plane wave of light. We then estimate the energy density E to be

$$E_\mu = \frac{I_p}{c_L} = \frac{\int I_\Omega E_p \, d\Omega}{c_L} \text{ (units: erg/cm}^3\text{)},$$

in which c_L is the speed of light.

As an estimate we take the case of muons and choose $I_\Omega = 1.83 \times 10^{-2}/\text{cm}^2 \cdot \text{s} \cdot \text{sr} \times \cos^2\theta$ and $E_p = 2 \times 10^9 \text{ eV} = 2 \times 10^9 \times 1.6 \times 10^{-12} = 3.2 \times 10^{-3}$ erg/muon. Over the hemisphere of incidence

$$I_p = \frac{1.83 \times 10^{-2} \text{ muons}}{\text{cm}^2 \cdot \text{s} \cdot \text{sr}} \left(\frac{1}{2} \int_0^\pi \cos^2\theta \, 2\pi \sin\theta \, d\theta \right) 3.2 \times 10^{-3} \text{ erg/muon}$$

$$= 1.83 \times 10^{-2} \left(\frac{2\pi}{3} \right) 3.2 \times 10^{-3} = 1.23 \times 10^{-4} \text{ erg/cm}^2 \cdot \text{s}.$$

The energy density of the equivalent plane wave of "light" is

$$E_\mu = \frac{1.23 \times 10^{-4} \text{ erg/cm}^2 \text{ s}}{3 \times 10^{10} \text{ cm/s}} = 4.08 \times 10^{-15} \frac{\text{erg}}{\text{cm}^3}.$$

Thus, if we listen underwater over a 10-kHz band, the energy density of the muon flux is about the same as the energy density of noise in the ocean over the band of 10,000 Hz to 25,000 Hz. On the other hand, if we listen over a 1-Hz band, the noise due to the muous (of energy 10^9 eV) is about 10,000 times higher than the ambient noise due to all other causes. However the presence of a muon signal is a random event in space and time. The probability of detection is still to be calculated.

Appendix C
TOTAL NOISE OF MUONS

Assume that muons of energy 2 GeV penetrate the ocean with a total flux of $1.82 \times 10^{-2}/\text{cm}^2 \cdot s \cdot \text{sr}$. The angular distribution of particles varies as $\cos^2 \theta$, where θ is the angle of the muon track with the vertical. The rate of absorption is 2 MeV/cm, so that the effective range of the track is $L = 10$ m. We wish to calculate the total noise production of the muons and compare it with the noise of molecular agitation in the ocean. To do this, we use the formulas of model Ia. For kL large the total acoustic power generated by vertically incident particles is

$$W = \frac{\alpha\, \omega\, \beta^2\, (I_o\, S)^2}{16\, \rho\, C_p^2}.$$

First we assume that $\alpha = L^{-1} = (1/10)\ \text{m}^{-1}$. Then we must replace the uniform intensity I_o of vertically incident particles by an effective intensity to account for the $\cos^2 \theta$ dependency of arrival. As a simple approximation we take

$$I_{eff} = \frac{1}{2} \int_0^{\pi} I_o \cos^2 \theta\, 2\pi \sin \theta\, d\theta = \frac{2\pi}{3} I_o.$$

Next we calculate the input heat power W_1 to the water caused by one muon, which according to the model is to be based on the heat deposition time T_1:

$$W_1 = I_{av}\, S = \frac{2\pi}{3} I_o\, S = \frac{2\pi}{3} \frac{E_o}{T_1} \quad (\text{units: } N \cdot m/s).$$

To choose T_1 we assume first that the noise caused by muons is not greater than the measured ambient noise of the ocean at the selected frequency. As we shall see later, the smallest $T_1 \simeq$ 41 ns. Thus

$$W_1 = \frac{2\pi}{3} \times \frac{2\ \text{GeV} \times 1.6 \times 10^{-19}\ \text{N} \cdot \text{m/eV}}{0.41\ \text{ns}}$$
$$= 1.635 \times 10^{-2}\ \text{N} \cdot \text{m/s}.$$

The total acoustic power "radiated" by one muon at a frequency of 25 kHz (say) is therefore

$$W = \frac{1}{L} \frac{\omega\, \beta^2 (W_1)^2}{16\, \rho\, C_p^2}$$
$$= \frac{1}{10\ \text{m}} \times 2\pi \times 25 \times 10^3\ \text{s}^{-1} \times \frac{1}{16} \times \frac{1}{10^3\ N \cdot \text{s}^2/\text{m}^4}$$
$$\times \frac{(1.4 \times 10^{-4})^2}{\text{K}^2} \times (1.635 \times 10^{-2})^2 \frac{\text{N} \cdot \text{m}^2}{\text{s}^2} \times \frac{1\ \text{s}^4\ \text{K}^2}{(4.18 \times 10^3)^2\ \text{m}^4}$$
$$= 2.94 \times 10^{-19} \frac{\text{N} \cdot \text{m}}{\text{s muon}}.$$

We are given that there are 1.83×10^{-2} muons/s $\cdot$ cm^2; or 183 muons/s $\cdot$ m^2, so that the total power of N muons is

$$W_N = 2.94 \times 10^{-19} \frac{\text{N} \cdot \text{m}}{\text{s muon}} \times 183 \frac{\text{muons}}{\text{s} \cdot \text{m}^2}$$

$$= 5.39 \times 10^{-17} \left(\frac{\text{N} \cdot \text{m}}{\text{s}} \right) \times \left(\frac{1}{\text{m}^2 \cdot \text{s}} \right).$$

We interpret W_N as the acoustic power (watts) flowing through a spatially averaged 1 m^2 of ocean surface temporally averaged over 1 s. We will go one step farther and assume the acoustic power so generated belongs to a plane wave of sound arbitrarily oriented, the energy density of which is

$$E = \frac{W_N/S}{c}, \quad c = \text{speed of sound in water},$$

$$E = \frac{5.39 \times 10^{-17} \text{ N} \cdot m/\text{s} \cdot \text{m}^2}{1.5 \times 10^3 \text{ m/s}} = 3.59 \times 10^{-20} \frac{\text{N} \cdot \text{m}}{\text{m}^3}$$

$$= 3.59 \times 10^{-19} \text{ erg/cm}^3 \text{ (averaged over 1 s)}.$$

This is nearly the energy density of ambient noise (per herz) measured in the ocean between 15 and 25 kHz. The equality of muon noise and ambient noise was deliberately made to occur by choosing T_1 to be 41 ns. The energy density is calculated on a 1-s averaging basis as required by the specified incidence rate.

The input energy E_o is actually taken from the spectrum of measured energy versus incidence rate. It is an arbitrary selection. Similarly T_1, the time factor in the rate of deposition of heat, is taken to be a plausible estimate in the absence of concrete experimental fact. Previously for various reasons we adopted T_1 to be 1 ns. We will now make a calculation based on this choice.

For $T_1 = 1$ ns the heat deposition of a single muon is

$$W_1 = \frac{2\pi}{3} \times \frac{2 \times \text{GeV} \times 1.6 \times 10^{-19} \text{ N} \cdot \text{m/eV}}{1 \text{ ns}}$$

$$= 0.67 \text{ N} \cdot \text{m/s}.$$

The acoustic power at 25 kHz of one muon is therefore

$$W = \frac{1}{10 \text{ m}} \times 2\pi \times \frac{25 \times 10^3}{\text{s}} \times \frac{1}{16} \times \frac{1}{10^3 \text{ N} \cdot \text{s/m}^4} \frac{(1.4 \times 10^{-4})^2}{\text{K}^2}$$

$$\times (6.7 \times 10^{-1})^2 \frac{\text{N}^2 \cdot \text{m}^2}{\text{s}^2} \times \frac{1 \text{ s}^4 \cdot \text{K}^2}{(4.18 \times 10^3)^2 \text{ m}^4}$$

$$= 4.95 \times 10^{-16} \text{ N} \cdot \text{m/s}.$$

We multiply this by the incidence rate to obtain the unit areal power flux:

$$W_N = 4.95 \times 10^{-16} \frac{\text{N} \cdot \text{m}}{\text{s muon}} \times \frac{183 \text{ muons}}{\text{s} \cdot \text{m}^2}$$

$$= 9.05 \times 10^{-14} \frac{\text{N} \cdot \text{m}}{\text{s}} \times \left(\frac{1}{\text{m}^2 \cdot \text{s}} \right).$$

This is then divided by the speed of sound c to obtain the space-and time-averaged energy density of an equivalent plane wave:

$$E = 9.05 \times 10^{-14} \frac{\mathrm{N \cdot m}}{\mathrm{s}} \times \left(\frac{1}{\mathrm{m^2 \cdot s}}\right) \times \frac{1}{1.5 \times 10^3\ \mathrm{m/s}} = 6.04 \frac{\mathrm{N \cdot m}}{\mathrm{m^3}} \times \frac{10^{-17}}{\mathrm{s}}$$
$$= 6.04 \times 10^{-16}\ \mathrm{erg/cm^3}\ \text{(averaged over 1 s)}.$$

This is larger than the ambient noise in a 1-Hz band by a factor of $6.04 \times 10^{-16}/3.59 \times 10^{-19} = 1.7 \times 10^3$. It is seen to be 10 × smaller than the noise energy density in a 10-kHz band.

From this calculation shows that the prediction of noise generation from muons in the ocean is highly sensitive to the correct estimate of heat deposition rate. Since an upper limit of this noise (at 25 kHz) is the measured ambient noise, one can find T_1 for any choice of E_0 with the understanding that it is the smallest possible time in the limit that *all* the ambient noise is due to muons of this energy.

A final calculation based on the experimentally more plausible value of $T_1 \sim 1\ \mu s$ will serve to illustrate the wide divergence in predictions. Thus

$$W_1 = \frac{2\pi}{3} \times \frac{2\ \mathrm{GeV} \times 1.6 \times 10^{-19}\ \mathrm{N \cdot m/eV}}{1\ \mu s}$$
$$= 0.67 \times 10^{-3}\ \mathrm{N \cdot m/s}$$

Thus the "particle power" which is considered in this model to be the analog of the laser power of Westervelt-Larson is 0.67 mW. The total acoustic power radiated by one muon at 25 kHz is then

$$W = \frac{1}{10\ m} \times \frac{2\pi \times 2.5 \times 10^4}{\mathrm{s}} \times \frac{(1.4 \times 10^{-4})^2}{\mathrm{K^2}} \times (0.67 \times 10^{-3})^2 \frac{\mathrm{N^2 \cdot m^2}}{\mathrm{s^2}}$$
$$\times \frac{1}{16} \times \frac{1}{10^3}\ \mathrm{N \cdot s^2/m^4} \times \frac{1\ \mathrm{s^4\ K^2}}{(4.18 \times 10^3)^2\ \mathrm{m^4}}$$
$$= 4.94 \times 10^{-22}\ \mathrm{N \cdot m/s}.$$

For an incidence rate of 183 muons/s · $\mathrm{m^2}$ the power generated over 1 $\mathrm{m^2}$ in an averaging time of 1 s is

$$W_N = 4.94 \times 10^{-22}\ \mathrm{N \cdot m/s\ muon} \times 183\ \mathrm{muons}$$
$$= 9.04 \times 10^{-20}\ \text{watts of acoustic power.}$$

Considering again each square meter to be a unit area of a plane wave, we find the energy density to be

$$E_\mu = \frac{9.04 \times 10^{-20}\ \mathrm{N \cdot m/s \cdot m^2}}{1.5 \times 10^3\ \mathrm{m/s}} = 6.03 \times 10^{-23} \frac{\mathrm{N \cdot m}}{\mathrm{m^3}}$$
$$= 6.03 \times 10^{-22}\ \mathrm{erg/cm^3}.$$

The ratio of muon noise to ambient noise (in a 1 Hz band) is then

$$\frac{E\mu}{E_{ambient}} = \frac{6.03 \times 10^{-22}}{3.59 \times 10^{-19}} = 1.7 \times 10^{-4}.$$

The comparison with molecular agitation noise is different. According to Mellen [14] the thermal noise in the ocean is empirically given by

$$N_{th} = -175 + 20 \log_{10} f$$

in units of dB re 1 μbar of equivalent plane wave of unit amplitude, with f being given in hertz. In arithmetic units the energy density of thermal noise is therefore

$$E_{th} = E_{ref} \left(\frac{f}{5.623 \times 10^8} \right)^2 .$$

Here we take the reference energy density to be that of a plane wave of unit amplitude:

$$E_{ref} = \frac{p^2}{\rho c^2} = \frac{(1)^2 \ (\text{dyne/cm}^2)^2}{1 \ \frac{\text{dyne} \cdot s^2}{\text{cm}^4} \times (1.5 \times 10^5)^2 \ \frac{\text{cm}^2}{s^2}} = 4.44 \times 10^{-11} \ \frac{\text{erg}}{\text{cm}^3} .$$

Thus the thermal energy density is

$$E_{th} = 4.44 \times 10^{-11} \left(\frac{f}{5.623 \times 10^8} \right)^2 \frac{\text{erg}}{\text{cm}^3} .$$

At $f = 25$ kHz,

$$E_{th} = 4.44 \times 10^{-11} \left(\frac{2.5 \times 10^4}{5.623 \times 10^8} \right)^2 = 8.78 \times 10^{-20} \ \frac{\text{erg}}{\text{cm}^3} .$$

The ratio of acoustic energy density caused by muons to the noise energy density of molecular agitation depends on the bandwidth of listening and on the choice of deposition time T_1. Using the results just calculated, we can construct a ratio (Table C1). Thus, to detect muon noise above thermal noise, the bandwidth of the receiver must not be appreciably more than 1 Hz.

Table C1 — Ratio of $\mathcal{E}_\mu / \mathcal{E}_{th}$ at 25 kHz

Bandwidth (kHz)	$\mathcal{E}_\mu / \mathcal{E}_{th}$	
	$T_1 = 41$ μs	$T_1 = 1$ ns
1	$3.59 \times 10^{-19} / 8.78 \times 10^{-20} \approx 4$	$6.04 \times 10^{-16} / 8.78 \times 10^{-20} \approx 7 \times 10^3$
10	$3.59 \times 10^{-19} / 8.78 \times 10^{-16} \approx 4 \times 10^{-4}$	$6.04 \times 10^{-16} / 8.78 \times 10^{-16} \approx 0.7$

REMARKS I

The procedure used in the above calculation is to calculate the acoustic radiation from one muon and then use the statistics of muon incidence to calculate the power per unit of time per unit of area. The statistical basis of the muon count must not not be overlooked. Most likely, muon incidence corresponds to shot noise and has therefore a Poisson-type probability distribution in time. Over a long record (say many seconds, hours, days, etc.) the average of the distribution is taken, and this is the number used in the above calculation. Other probability moments can be of use in developing the statistics of acoustic radiation developed by the

muons. For example, by quoting the variance of the random incidence, we can find the variance of the power crossing a square meter of the ocean surface; hence we can find the variance of the acoustic energy density. This would be a valuable statistic in comparing the acoustic radiation developed by muons to the noise of molecular agitation in the ocean.

We have made our calculation on the basis of a component (25 kHz) of the power spectrum of the radiated acoustic noise, choosing a single muon particle as our basic model. When we deem N muons incident in 1 s (as averaged over many seconds of record), we have assumed incoherent summation by taking the total power to be N times the power of one muon. If the summation is coherent, there will be a *directional gain* in radiation, as if the volume of incidence were a volume array of sources. The energy density would then be higher in specific directions.

We can also treat the problem in the time domain rather than in the frequency domain. Thus we can calculate the transient power $W(t)$ per muon, find the average power

$$W_\Delta = \int_0^{\Delta t} W(t)\, dt/\Delta t$$

for the duration Δt of the transient, and then multiply by the statistically determined time and space rate of incidence N to find the total power for all frequencies per unit of time and area.

Finally we could proceed to calculate a long time record of power $W(t)$, taken over many seconds, and subject it to a probability analysis. This can be done by dividing the record into M records and making histograms of the average, the variance, etc. among the components of the set. An autocorrelation could then lead directly to the power spectrum.

REMARKS II

The total noise energy density generated by the flux of muons is an average over all space. The sharp directionality of vertically incident particles has been canceled in the averaging process. Although illustrative, the calculation of acoustic energy densities does not lend itself to experimental check directly. One must measure acoustic pressure and use it to calculate energy density according to some simplifying assumption, say plane waves. The significant directional power quantity is the acoustic intensity. From Model Ia in the main text this intensity is seen to depend on the angle θ as

$$\frac{1}{1 + (kL)^2 \cos^2 \theta},$$

in which θ is measured relative to the vertical. Actually muons arrive at all angles ξ (relative to the vertical). The sound radiated from a track at angle ξ in direction of angle ζ from ξ then depends on

$$\frac{\cos^2 \xi}{1 + (kL)^2 \cos^2 (\xi + \zeta)}.$$

Thus the greatest contributions to muon noise occur in the horizontal, from tracks near the vertical ($\xi \to 0$). A rough approximation to noise generation is to average $\cos^2 \xi$ in the numerator over a solid angle of hemisphere and to neglect ξ in the denominator.

REMARKS III: DIRECTIONALITY

The number of particles incident on a unit area is proportional to $\cos^2\theta$, where θ is the angle of the track of the particle relative to the vertical. Since the radiated sound from a track is sharp in a direction normal to the track, we assume that the directionality of all the tracks through a unit area is also proportional to $\cos^2\theta$, where θ is now taken relative to the horizontal. The 3-dB points of the *intensity* pattern of acoustic radiation occurs at θ values such that $\cos^2\theta = 1/2$, or $\cos\theta = 0.707$, or $\theta = \pm 45°$. Hence the 3-dB beamwidth of muon noise is 90° centered on the horizontal. We compare this directionality with that of ambient noise and of directional noise. Ambient noise at low frequencies (say less than 10 kHz) normally arrives in a wedge $\pm 20°$ centered on the horizontal [Ref. 22, p. 282]. High-frequency ambient noise originating in surface wave action arrives at a point in a vertical cone whose vertex angle depends on depth of the listening sensor. In the range of interest (25 kHz and above) high-frequency muon noise can be differentiated from ambient noise by the difference of angle of arrival: muon noise arrives horizontally, and surface noise arrives vertically. In contrast thermal or molecular-agitation noise dominates at high frequency and is omnidirectional.

REMARK IV: RELATION BETWEEN ENERGY DENSITY AND INTENSITY [4, p. 577]

We imagine the total acoustic effect of cosmic particles in the ocean to be analogous to the assemblage of randomly distributed standing plane waves in a room, each wave traveling in some direction ϕ, θ. Let each plane wave have amplitude $A(\mathbf{r}, \phi, \theta)$. The power incident on a unit area normal to ϕ, θ is the intenstiy I:

$$I(\mathbf{r}) = \frac{1}{\rho c}\int_0^{2\pi} d\phi \int_0^{\pi/2} |A(r, \phi, \theta)|^2 \cos\theta \sin\theta \, d\theta.$$

Similarly the energy density $w(\mathbf{r})$ is,

$$W(\mathbf{r}) = \frac{1}{\rho c^2}\int_0^{2\pi} d\phi \int_0^{\pi} |A(r, \phi, \theta)|^2 \sin\theta \, d\theta.$$

At high enough frequency we can take the sound field in the room to be isotropic, meaning that $A(r, \phi, \theta)$ is independent of r, ϕ, θ. This is the frequency range of geometrical acoustics. Upon integrating in this region, one obtains

$$I = \frac{A^2\pi}{\rho c}, \quad w = \frac{4\pi A^2}{\rho c^2}.$$

Hence the relation of I to w is,

$$w = \frac{4I}{c}.$$

In the above numerical calculation of muon noise we have omitted the factor 4 and written $w = I/c$. This omission was done because an integration over the hemisphere of particle incidence had already converted angular incidence to vetical incidence.

STATISTICS OF NOISE IN THE OCEAN

The power spectrum level of noise in the ocean has been complied by Wenz [13] and is reproduced as Fig. C1 for convenience. The ordinate of this chart represents the noise level (NL), defined as

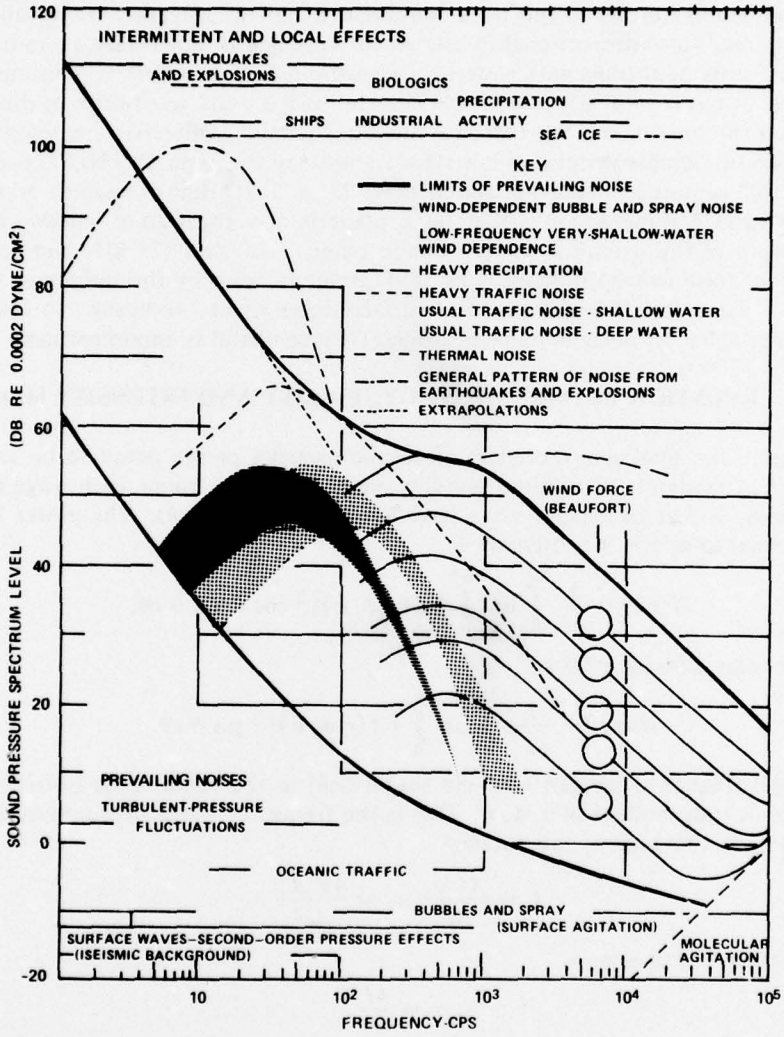

Fig. C1 – Wenz chart of noise in the ocean

$$NL = 10 \log_{10} \frac{p^2(f)}{p_{ref}^2(f)}, f = \text{frequency } (Hz)$$

in which the reference is the quantity p^2 of a plane wave of unit amplitude at the frequency f. All curves shown (except the one labeled molecular agitation) represent measured values of ambient noise. The curve for molecular agitation is a straight line extending to the right with the slope shown. All quantities are based on noise power in a 1-Hz band. The lower limit of ambient noise in the ocean at 25 kHz is $-8 \quad -74 = -82$ dB re 1 dyne/cm^2 (spectrum level), and the noise of molecular agitation is $-13 \quad -74 = -87$ dB re 1 dyne/ cm^2. By use of the Mellen formula [14] one can extend this latter curve upward as desired.

Signal Processing of Muon Noise When the Time of Arrival is Random

We form a conceptual analog: let the unit area of the ocean surface be likened to an anode in a vacuum tube, and let the cosmic particles incident on it be likened to electrons arriving randomly. Also let each particle generate the same heat source $h(\mathbf{r}, t)$ in the water and hence the same acoustic pressure $p(\mathbf{r}, t)$. Assume all effects of a unit area of incidence are additive, taking $\mathbf{r}$ the same for all. The total effect at time t due to all the particles of a small enough unit area is

$$p(\mathbf{r}, t) = \sum_{k=-\infty}^{\infty} p(\mathbf{r}, t - t_K).$$

Since the individual p occurs at random time the total P is a random function of time.

Choose an interval T and let exactly K cosmic particles arrive on the unit area in this interval at random times t_K. Then the contribution of these K particles to the total time history of acoustic pressure is called P_K, where

$$p_K(t) = \sum_{k=1}^{K} p(\mathbf{r}, t - t_k).$$

If $\mathbf{r}$ is dropped for convenience, the autocorrelation $\phi(\tau)$ of the total acoustic pressure will be

$$\psi(\tau) = \overline{P(t)\, p(t + \tau)} = \sum_{k=0}^{\infty} g(K)\, \overline{p_k(t)\, p_K(t + \tau)},$$

in which $g(K)$ is the probability that exactly K muons arrive in the interval 0, T. If one chooses $g(K)$ to be a Poisson distribution corresponding to shot (or impulse) noise, then one can show that

$$\psi(\tau) = N \int_{-\infty}^{\infty} p(t)\, p(t + \tau)\, dt + \overline{p(t)}^2,$$

in which N is the average number of muons arriving per second and $\bar{P}(t)$ is the average value of $P(t)$, namely,

$$\overline{p(t)} = N \int_{-\infty}^{\infty} p(t)\, dt.$$

The ensemble averaged power spectrum $\bar{w}(f)$ can now be calculated from the standard relation

$$\bar{w}(f) = 2 \int_{-\infty}^{\infty} \bar{\psi}(\tau) \cos 2\pi f \tau \, d\tau$$

$$= 2N |s(f)|^2 + 2 \overline{P(t)}^2 \delta(f)$$

in which

$$s(f) = \int_{-\infty}^{\infty} p(t)\, e^{-2\pi i f t}\, dt.$$

Thus, to find the power spectrum, one must Fourier transform the impulse acoustic pressure of one muon to obtain the amplitude spectrum $s(f)$. Then one must take $2N$ times the absolute value squared of $s(f)$ and finally add to it twice the square of the mean value of the total pressure $P(t)$ as a "DC" component.

When $\overline{w}(f)$ is available over the frequency range of interest, we can estimate the statistical behavior of $P(t)$. A convenient reference is S. O. Rice ("Mathematical Analysis of Random Noise," in *Seletected Papers on Noise,* N. Wax, editor, Dover Publications, 1954). As a special case we list the applicable formulas for narrowband noise, assuming the total muon noise $P(t)$ will be processed through a narrowband filter to obtain spectral information at (say) 25 kHz.

Thus assume the autocorrelation is of the for m $\psi(\tau) = A \cos \beta\tau$; then, if $P(t)$ and $\partial P/\partial t$ are both Gaussian, the expected number of zero crossings per second is

$$Z_N = \frac{1}{\pi}\left[-\frac{\ddot{\psi}(0)}{\psi(0)}\right]^{1/2} = 2\left[\frac{\int_0^{\infty} f^2\, w(f)\, df}{\int_0^{\infty} w(f)\, df}\right]^{1/2}$$

where

$$\psi''(0) = -4\pi^2 \int_0^{\infty} f^2 w(f)\, df.$$

The probability that the time interval between successive zeros lies between τ and $\tau + d\tau$ is approximately

$$\frac{d\tau}{2}\, \frac{a}{[1 + a^2(\tau - \tau_1)^2]^{3/2}}$$

where

$$a = \sqrt{3}\, \frac{(f_b + f_a)^2}{f_b - f_a} \text{ and } \tau_1 = \frac{1}{f_b + f_a},$$

in which $f_b - f_a$ is the passband.

Writing $P(t) = P_c \cos \omega_m t - P_s \sin \omega_m t$, where $\omega_m = 2\pi f_m$ is the midfrequency of the filter and P_c and P_s are quadrature components, we take P_c and P_s as normally distributed with the same standard deviation. The statistics of the pair P_c and P_s, and of the envelope $R(t) = \sqrt{P_c^2 + P_s^2}$ are the following:

- the probability that the point (P_c, P_s) lies in the elementary rectangle $dP_c\, dP_s$ is

$$\frac{dP_c\, dP_s}{2\pi\psi(0)} \exp\left[\frac{P_c^2 + P_s^2}{2\psi(0)}\right];$$

- the number of maxima of the envelope $R(t)$ expected in 1 s is $0.6\,(f_b - f_a)$;

- the probability that a maximum selected at random lies between R and $R + dR$, when the envelope $R > 2.5\sqrt{\psi(0)}$, is

$$1.13\,(y^2 - 1)\,e^{-y^2/2}\,\frac{dR}{\psi(0)^{1/2}}, \quad y = \frac{R}{\psi(0)^{1/2}};$$

- the expected number of maxima per second is

$$M_N = \left[\frac{\int_0^\infty f^4 w(f)\,df}{\int_0^\infty f^2 w(f)\,df}\right]^{1/2}$$

Appendix D
MAGNITUDE OF CONSTANTS USED IN THE NUMERICAL CALCULATIONS

$\beta = 1.4 \times 10^{-4} °K^{-1}$, coefficient of thermal expansion of water

$C_p = 4.18 \times 10^3 \frac{\text{joules}}{Kg\ °K}$ $\left[\text{or } \frac{M^2}{sec^2\ °K}\right]$, specific heat of water at constant pressure

$eV = 1.6 \times 10^{-19}$ joules $= 1.6 \times 10^{-12}$ erg, energy

$D = 1.43 \times 10^{-3} \frac{\text{cm}^3}{\text{sec}} = 1.43 \times 10^{-7} \frac{m^2}{\text{sec}}$, heat diffusion constant of water

$C = 1.5 \times 10^3 \frac{m}{\text{sec}}$, speed of sound in water

1 atmosphere $= 10^5 \frac{N}{m^2} = 10^6 \frac{\text{dynes}}{\text{cm}^2}$

reference pressure on dB scale:

(1) dB re 1 dyne/cm^2

(2) dB re 0.0002 dyne/cm^2, subtract 74 dB to convert to dB re 1 dyne/cm^2

(3) dB re 1 micropascal, subtract 100 dB to convert to dB re 1 dyne/cm^2

1 calorie $= 4.18$ joules $= 4.18 \times 10^7$ ergs $= 2.6 \times 10^{19}$ eV

U.S. GOVERNMENT PRINTING OFFICE: 1977 240-824/280 1-3